A GENERALIZED LUMINOSITY FUNCTION FOR EXTRAGALACTIC RADIO SOURCES

By

V.K. KULKARNI

Radio Astronomy Group

Tata Institute of Fundamental Research

Homi Bhabha Road, Bombay 400005.

A Thesis

Submitted for the Ph.D. degree

of the

University of Bombay

May 1979

DEDICATED

TO

ROSE

A GENERALIZED LUMINOSITY FUNCTION FOR EXTRAGALACTIC RADIO SOURCES

SYNOPSIS

In this thesis we have attempted to explain the observed radio source counts at different frequencies and also expected variations in spectral index distributions with flux density. It is shown that an evolutionary world model is required to explain the data. A Generalized Luminosity Function (GLF) has been derived for extragalactic radio sources by following a model-fitting procedure. This generalized luminosity function describes the comoving space density of extragalactic radio sources as a function of radio luminosity, redshift and spectral index. In this model, we have considered a correlation between radio luminosity and spectral index as well as different forms of cosmological evolution for flat- and steep-spectrum sources. The results are consistent with the observed source counts and spectral index distributions both at low and high frequencies.

The interpretation of the observed radio source counts in terms of evolutionary world models involves two steps. The first is the determination of the local luminosity function for which we require to know the distances of radio sources. Hence it is necessary to assume that all radio sources including quasars are at 'cosmological' distances as given by their redshifts. We have made an analysis of the observed magnitude-redshift relation for the brightest quasars and have shown that the results are consistent with the cosmological hypothesis.

The second step in the interpretation of the observed source counts is the determination of the evolution function.

Many schemes have been given in the literature for deriving the evolution function from the observed counts. A simple iterative method of solving for the evolution function, starting from a given local luminosity function, has been given by Robertson. An extension of this scheme that starts from the observed luminosity distribution rather than the derived local luminosity function is proposed and some results are presented.

Most of the previous attempts have been confined to derivation of suitable evolutionary models at a single frequency. However, well-defined source counts and spectral index distributions are now available at several different frequencies. The principal conclusions from these observations may be summarized as follows:

i) There is a significant deficit of sources at high flux densities at 408 MHz and 1400 MHz.

ii) The deficit is not so evident at 2700 MHz and 5000 MHz; however the observations are not inconsistent with a deficit similar to that observed at low frequencies.

iii) The form of radio source counts varies with frequency; the low frequency counts show rapid convergence at low flux densities but this convergence is not so rapid for the high frequencies counts.

iv) At high frequencies, pronounced variations are observed in spectral index distributions with flux density; for example, at the highest flux densities the fraction of flat-spectrum sources increases with decreasing flux density but for lower flux densities, there is a decrease in this fraction. At low frequencies such variations are much smaller.

It is important to be able to reconcile these results regarding the observed counts and spectral index distributions at several different frequencies within the framework of a single model. Some of these results can be explained by simply

convolving the observed source counts with an observed spectral index distribution at a low frequency and then making predictions for the high frequency without introducing any dependence of the properties of sources on luminosity or redshift. In this way the dependence of the fraction of flat-spectrum sources upon flux density can also be recovered and the high and low frequency counts can be shown to be consistent. A more satisfactory formulation was given by Fanaroff and Longair. By considering both an evolutionary luminosity function and spectral index function the above authors demonstrated that it was possible to account for the general features of the observations at both high and low frequencies. However, their model predicts much lower source counts at 5 GHz for the weak sources than has been observed, a discrepancy which reaches a factor of about 3 at $\sim$ 0.02 Jy. Moreover, at such low flux density levels the observed fraction of flat-spectrum sources is about 36 per cent, whereas the model predicts a value of only 18 per cent.

Fanaroff and Longair had made the following assumptions for the sake of simplicity: (a) the form of cosmological evolution is identical for sources with flat and steep spectra, (b) the spectral index function and the luminosity function are independent at a low frequency; any possible correlation between radio luminosity and spectral index is thus ignored.

However, recently from a study of luminosity-volume test for quasars and an analysis of radio source counts at low and high frequencies several investigators have suggested that the form of cosmological evolution is different for flat- and steep-spectrum radio sources. Also, a correlation between radio luminosity and spectral index has been reported by many authors in recent years.

It is clear that the above possibilities have to be taken into account in deriving the generalized luminosity

function for extragalactic radio sources. A generalized model, incorporating different forms of cosmological evolution for flat- and steep-spectrum sources and the correlation between radio luminosity and spectral index has been adopted for calculating the expected variations in spectral index distribution with flux density and frequency. It is shown that by an appropriate choice of the parameters of the model, the predictions can be made to have a good agreement with the observed source counts and spectral index distributions both at 408 MHz and 5000 MHz. The predictions are also found to be in reasonable agreement with the observations at 1400 MHz, 2380 MHz and 2700 MHz.

The generalized luminosity function is also used along with the radio size function in investigating the cosmological implications of the observed angular sizes of extragalactic radio sources. In these investigations an extension of the recent works of Swarup, Kapahi and Subrahmanya is attempted. The angular size counts of extragalactic sources are calculated by taking into account the spread in spectral indices and any possible luminosity-size correlation for extragalactic radio sources. A comparison of the predicted and observed counts indicates the presence of both density (or luminosity) and linear size evolution effects, in agreement with the conclusions reached by the above authors. The effects of the inclusion of spectral index distribution and power-size correlation are small.

To summarize, the improvement over earlier models is mainly due to the inclusion of different forms of cosmological evolution for flat- and steep-spectrum radio sources. The cosmological evolution is strong for the steep-spectrum sources but is confined only to the sources for which $P_{408} \gtrsim 10^{26}$ W Hz^{-1} ster^{-1}. For the flat-spectrum sources, the

cosmological evolution seems to take place for all sources with $P_{408} \gtrsim 10^{24}$ W Hz^{-1} $ster^{-1}$, but the evolution is not as strong as for the steep-spectrum sources. The effects of inclusion of the observed radio luminosity and spectral index correlation are comparatively small. The generalized luminosity function along with radio size function produces angular size counts that are in agreement with the observations. An important corollary of this result is that the spread in spectral indices does not significantly modify the results of earlier investigations of the cosmological implications of the observed angular size counts.

A knowledge of the generalized luminosity function along with radio size function is of considerable importance since it gives directly the relative populations of different types of sources with epoch and can possibly give information about the epoch of quasar and galaxy formation. More observations at low flux density levels, especially for flat-spectrum sources, are needed to determine the generalized luminosity function more accurately.

Statements required by the University

Statement No.(1) required under 0.770

I hereby declare that the work described in this thesis has not been submitted to this or any other university or body for a degree, diploma or any other academic award.

Statement No.(2) required under 0.771 stating 'Whether the work is based on the discovery of new facts by the candidate or of new relation of facts observed by others, and how the work tends to the general advancement of knowledge'.

In this thesis a Generalized Luminosity Function (GLF) is derived for extragalactic radio sources. The GLF is shown to predict source counts and spectral index distributions that are in agreement with observations both at low and high frequencies. It is also shown to produce angular size counts that are in agreement with the observations. A knowledge of GLF is of considerable importance since it gives directly the relative populations of different types of sources with epoch and can possibly give information about the epoch of quasar and galaxy formation.

Statement No.(3) required under 0.771 stating 'The sources from which his information has been derived and the extent to which he has based his work on the work of others, and shall indicate which portion or portions of his thesis he claims as original'.

Proper references have been made where the work of others are used or described in the thesis. The rest of the thesis can be claimed as original.

Statement No.(4) required under 0.771 stating 'Where a candidate presents a joint work, he shall clearly state the portion which is his own contribution as distinguished from the portion contributed by his collaborators'.

Only a small part of this thesis, study of redshifts of QSO's, has been in collaboration with Dr. A.K.Kembhavi. Proper references have been made when this joint work is described in the thesis.

"We wonder, Oh, we wonder,
what on earth the world
may be?"

W.S. Gilbert, The Mikado.

ACKNOWLEDGEMENTS

It is a pleasure to thank Professor Govind Swarup who initiated me to the ways and wonders of Radio Astronomy and continues to be a constant source of encouragement and advice for me. I am grateful to him for many valuable suggestions, comments and criticisms I received from him from time to time.

I would also like to express my gratefulness to Professor T.K. Menon for suggesting the problem and for many valuable discussions I had with him during different stages of this work. His encouragement and understanding nature made working with him a very pleasant experience for me.

It is a pleasure to thank my colleagues, Dr.M.N.Joshi, Dr. V.R.Venugopal, Dr. D.S.Bagri, Dr.T.Velusamy, Dr.V.K.Kapahi, Dr. C.R.Subrahmanya, Dr. A.P.Rao, Dr. S.Ananthakrishnan, Dr. Gopal-Krishna, V.Balasubramanian, S.Krishnamohan, D.K.Mohanty and D.J.Saikia for many fruitful discussions and constructive criticisms.

I would also like to thank Mathews for the fine job of typing the manuscript. Many thanks are due to Srinivasan, Premkumar and Siva for their help in tracing, Xeroxing and cyclostyling work. I gratefully acknowledge the willing help of Ashok Singal, Rajesh Kher, K.L.Venkatakrishna, B.K. Ravi, George Varkey, K.P.Dhaky and D.G.Banahatti in proof-reading.

I thank my friends, Dr.P.N.Bhat, Dr.N.Sundararajan, Dr.A.K.Kembhavi, A.D.Gangal, Miss Asha Padhye, Miss Suman Bhat and others for their interest and constant hospitality in Bombay and for making my stay in the institute a very pleasant experience.

Finally, I would like to express my gratitude to my parents for their constant encouragement and inspiration.

TABLE OF CONTENTS

		Page No.
Synopsis		i
Statements Required by the University		vi
Acknowledgements		vii
List of Figures		xi
List of Tables		xiii
1.	INTRODUCTION	1
1.1	Extragalactic Radio Sources	1
1.2	Radio Sources and Cosmology	4
1.2.1	Source Counts and Cosmology	4
1.2.2	Angular Sizes and Cosmology	6
1.2.3	Spectral Index Distributions and Cosmology	8
1.3	Present Work	11
2.	RADIO SOURCE COUNTS AT A SINGLE FREQUENCY, LOCAL LUMINOSITY FUNCTION AND EVOLUTION FUNCTION	15
2.1	Introduction	15
2.2	Number Counts at 408 MHz And Their Interpretation	17
2.2.1	Basic Ideas	17
2.2.2	Observations	18
2.2.3	Interpretation of Source Counts	20
2.3	Absolute Magnitudes and Hubble Plot for QSOs	26
2.3.1	Introduction	26
2.3.2	Analysis and Conclusions	29
2.4	The Determination of the Local Luminosity Function and Evolution Function	37
2.4.1	LLF and EF from Source Counts and Luminosity Distribution	37
2.4.2	LLF and EF from Luminosity-Volume Test	47
2.4.3	Derivation of LLF and EF from Angular Size Counts	56
2.5	Extended Free-Form Analysis of the Cosmological Evolution of Radio Sources	60

Page No.

3.	RADIO SOURCE COUNTS AND SPECTRAL INDEX DISTRIBUTIONS: Summary of Observations	69
3.1	Introduction	69
3.2	Source Counts at Different Frequencies	74
3.3	Spectral Index Distributions	79
3.3.1	The Spectral Index Distributions at 408 MHz	81
3.3.2	The Spectral Index Distribution at 1400 MHz	88
3.3.3	The Spectral Index Distribution at 2700 MHz	93
3.3.4	The Spectral Index Distribution at 5000 MHz	96
3.4	Summary	101
4.	RADIO SOURCE COUNTS AND SPECTRAL INDEX DISTRIBUTIONS: Models OR A GENERALIZED LUMINOSITY FUNCTION FOR EXTRAGALACTIC RADIO SOURCES	103
4.1.1	Introduction	103
4.1.2	Notation and Defenitions	104
4.2	Earlier Models	104
4.2.1	The Empirical Method	105
4.2.2	The Model of Fanaroff and Longair	112
4.3	The Present Model [illegible]	115
4.3.1	Cosmological Evolution of Flat- and Steep-Spectrum Sources	118
4.3.2	Radio Luminosity - Spectral Index Correlation	123
4.3.3	Form of the Generalized Luminosity Function	125
4.3.4	The Choice of World Model and Luminosity Function	128
4.3.5	The Calculations	129
4.3.6	The Models	131
4.4	The Results	134
4.4.1	The Source Counts and Spectral Index Distribution at 408 MHz	135
4.4.2	The Source Counts and Spectral Index Distribution at 5000 MHz	141

Page No.

4.4.3 The Source Counts and Spectral Index Distribution at 1400 MHz and 2700 MHz 151

4.4.4 Discussion 164

4.5 Summary 168

5. ANGULAR SIZE COUNTS AND COSMOLOGY 169

5.1 Introduction 169

5.2 Earlier Investigations 170

5.3 The Extended Luminosity Function and $N(>S,>\theta)$ Distributions 172

5.3.1 General Formalism for Calculating $N(>S,>\theta)$ Distributions 172

5.3.2 The Choice of World Model and GLF 174

5.3.3 The Size Functions $\varphi_a(\ell_a|P,z)$ 174

5.4 Model Calculations and Comparison with Observations 178

5.5 Discussion of Results 189

5.6 Summary 193

6. SUMMARY AND COMMENTS 194

6.1 Absolute Magnitudes and Hubble Diagram for QSOs.. 195

6.2 An Extended Free-Form Analysis Scheme for Investigating the Cosmological Evolution of Radio Sources 195

6.3 Generalized Luminosity Function, Source Counts, Spectral Index Distributions and Angular Size Counts 196

REFERENCES 201

LIST OF FIGURES

Figure		Page No.
2.1	The Observed Radio Source Counts at 408 MHz.....	19
2.2	The Observed Normalized Differential Source Counts at 408 MHz.....	19
2.3	Plot of Absolute Magnitude M_V Against Average Redshift $< z >$ for the Brightest and Faintest QSOs.....	33
2.4	Hubble Diagram for the Brightest QSOs.....	33
2.5a	Plot of the Absolute Magnitude M_V Against Average Redshift $< z >$	36
2.5b	Hubble Diagram for the Brightest QSOs Shown in Fig.2.5(a).....	36
2.6	Comparison of the Observed and Fitted Counts at 408 MHz.....	63
2.7	The Local Luminosity Function at 408 MHz.....	65
2.8	The Evolution Function E(z) as Determined from Free-Form Analysis.....	67
2.9	The Average of the Logarithm of Redshift as a Function of Flux Density.....	67
3.1	Frequency Dependence of Radio Source Counts.....	76
4.1	Plot of Average Spectral Index for Each Luminosity Bin Against Log of Luminosity.....	124
4.2a	Comparison of the Observed and the Predicted (Model A) Normalized Differential Source Counts at 408 MHz.....	138
4.2b	Comparison of the Observed and the Predicted (Model B) Normalized Differential Source Counts at 408 MHz.....	139
4.2c	Comparison of the Observed and the Predicted (Model C) Normalized Differential Source Counts at 408 MHz.....	140
4.3a	Comparison of the Observed and the Predicted (Model A) Normalized Differential Source Counts at 5000 MHz.....	146
4.3b	Comparison of the Observed and the Predicted (Model B) Normalized Differential Source Counts at 5000 MHz.....	147
4.3c	Comparison of the Observed and the Predicted (Model C) Normalized Differential Source Counts at 5000 MHz.....	148

Figure | Page No.

4.4 Comparison of the Observed and the Predicted (Model A) Normalized Differential Counts at 1400 MHz..... 156

4.5 Comparison of the Observed and the Predicted (Model A) Normalized Differential Counts at 2700 MHz..... 159

4.6 Comparison of the Observed and the Predicted (Model A) Normalized Differential Counts at 2380 MHz..... 161

4.7 Variation of the Effective Spectral Index $\alpha_{eff}(408,2380)$ with 2380 MHz Flux Density..... 161

5.1 Comparison of Predicted (Model X) and Observed Angular Size Distributions in Different Ranges of Flux Density S..... 184

5.2 Comparison of Predicted (Model Y) and Observed Angular Size Distributions in Different Ranges of Flux Density S..... 185

5.3 Comparison of Predicted (Model Z) and Observed Angular Size Distributions in Different Ranges of Flux Density S..... 186

LIST OF TABLES

Table		Page No.
2.1	Correlation of Log z and m_v for Various Samples of QSOs	31
3.1	The Parameters of Normalized Differential Source Counts at Different Frequencies	78
3.2	Features of the Spectral Index Distribution $f^{408}_{S(408)}[\alpha(408,5000)]$	80
3.3	Parameters of $f^{408}_{S(408)}[\alpha(178,1420)]$	82
3.4	The Spectral Index Distribution at 408 MHz	84
3.5	Dependence of Spectral Index Distribution $g^{408}_{S(408)}[\alpha(408,1415)]$ on S(408)	85
3.6	Flux Density Dependence of Effective Spectral Index	87
3.7	Parameters of Spectral Index Distribution $f^{1400}_{S(1400)}[\alpha(1400,\nu_2)]$	89
3.8a	Spectral Parameters of the Sources [S(1400) $\geq$ 0.5 Jy] in the GB2 Survey	91
3.8b	Spectral Parameters of the GB Sources	92
3.9	Dependence of $\alpha_{n\ med}(2700,\nu_2)$ on the 2700 MHz Flux Density	95
3.10	Spectral Index Distribution $f^{5000}_{S(5000)}[\alpha(5000,408)]$ as a Function of S(5000)	97
3.11	Spectral Index Distribution $f^{5000}_{S(5000)}[\alpha(5000,318)]$ as a Function of S(5000)	99
3.12	Spectral Index Distribution $f^{5000}_{S(5000)}[\alpha(5000,2695)]$ as a Function of S(5000)	100
4.1	Summary of $\langle V/V_m \rangle$ Results for Different Spectral Classes	120
4.2	Comparison of Predicted and Observed Spectral Index Distributions at 408 MHz	136
4.3a	Comparison of Predicted and Observed Values of Median Spectral Index α_{med} at 5000 MHz for All Sources	142
4.3b	Comparison of Predicted and Observed Values of $\alpha_{n\ med}$ at 5000 MHz for Sources with $\alpha \geq 0.5$	143
4.3c	Comparison of Predicted and Observed Values of the Fraction of Flat-Spectrum Sources at 5000 MHz	144

Table		Page No.
4.4	Comparison of Predicted and Observed Distributions $f^{5000}_{S(5000)}[\alpha(5000,2695)]$	150
4.5a	Comparison of Observed and Predicted Spectral Index Distributions $f^{1400}_{S(1400)}[\alpha(1400,\nu_2)]$	153
4.5b	Comparison of the Model Predictions with the Spectral Parameters of the Sources $[S(1400)\geq 0.5$ Jy] in the GB2 Survey	154
4.5c	Comparison of Model Predictions with the Spectral Parameters of the GB Sources	155
4.6	Comparison of Predicted and Observed Spectral Index Distributions at 2700 MHz	158
4.7	Variation (Predicted) of Effective Spectral Index $\alpha_e(2380,408)$ with S(2380)	162
4.8	Comparison of Predicted and Observed Values of $\alpha_e(408,1400)$	163
5.1	The Parameters of Model X	180
5.2	The Parameters of Model Y	182
5.3	The Parameters of Model Z	183
5.4	Chi-Square Values for the Three Models, X, Y and Z	190
5.5	χ^2 versus K, Q; K = no. of bins, Q = Significance Level	191

"From these our interviews, in which I

steal

From all I may be, or have been before,

To mingle with the Universe, and feel

What I can never express, yet cannot

all conceal."

George G. Byron.

CHAPTER 1

INTRODUCTION

1.1. Extragalactic Radio Sources

In the first thirty years of its existence, extragalactic radio astronomy has produced many startling discoveries and unexpected results. The first one was the identification by Baade and Minkowski (1954) of the strong radio source Cyg-A with a galaxy of redshift $z = 0.056$. This discovery led to a lot of excitement in the field because it implied that a majority of the radio sources have a high luminosity and can be observed at cosmological distances. The strong apparent luminosity of Cyg-A, in spite of its relatively large distance indicated by $z = 0.056$, suggested that the intrinsic luminosity of many of the radio galaxies must be very high. Observations made during the last two decades have shown that 'radio galaxies' i.e. radio sources identified with galaxies, have radio power outputs of about 10^{33} to 10^{37} Watt. These power outputs are thousands of times larger than those of our own galaxy or other normal galaxies. Also, it is now well established that the nonthermal radio emission is due to synchrotron process. Several models have been suggested to explain the observed features of extragalactic radio sources. However, the origin and evolution of radio sources are not yet well understood. The source of huge energies in radio sources still continues to be one of the most challenging problems in astrophysics.

In addition, the strong apparent intensity of Cyg-A meant that it should be possible to see sources similar to Cyg-A to much larger distances (redshifts). From this it follows that it should be possible to use radio sources as probes to investigate the large scale structure of the universe. A considerable amount of effort has, therefore, gone into improving receiving techniques and building of more and more powerful radio telescopes with the result that now radio sources millions of times fainter than Cyg-A can be easily detected. Several systematic surveys of the sky, going down to mJy (1mJy = 10^{-3} Jy) level in flux density have been carried out and over 30,000 sources have already been catalogued by radio astronomers.

The second startling discovery in the field of extragalactic astronomy was the identification of the radio source 3C 273 with a 13th magnitude stellar object by Hazard et al. (1963) and the measurement of its redshift ($z = 0.158$) by Schmidt (1963). This brought in a new class of radio sources with high redshifts. Many hundreds of such 'quasi stellar objects' or 'QSOs' as they are popularly known have now been identified and for about 700 of them redshifts have been measured.

The measured redshifts of QSOs are larger than those of galaxies and span a range of redshift $z = 0.04$ to 3.5. The origin and nature of QSO redshifts has been a matter of great controversy. The most widely believed view is that they are

cosmological in nature, although there is no direct confirmation of the corresponding very large distances. The radio properties of QSOs do not seem to be very different from those of powerful radio galaxies.

The third and most unexpected discovery in extragalactic radio astronomy was the detection, in 1965, of the universal microwave background radiation (3 K radiation), by Penzias and Wilson. This discovery provides the most convincing evidence against the Steady State model of the universe. In the Steady State model it is not possible to account for the presence of such a universal background radiation in any convincing manner. On the other hand in Big Bang cosmological models such radiation can be naturally interpreted as a leftover from the primordial fireball.

The observed distributions of different properties of radio sources depend both on the intrinsic properties of individual sources and the evolution in the gross properties of the radio source populations with cosmic epoch and it is necessary to separate these two effects before one can exploit the full potential of radio sources as probes for studying cosmology. It is the study of variation in statistical properties of radio source populations and the determination of distribution in space of radio sources with which the present thesis is mainly concerned. First, we present a review of several methods in which different parameters of radio sources are used to study cosmology. This is

followed by a brief introduction that gives an outline of the present investigations in which an attempt is made to explain the source counts and spectral index distributions in terms of evolutionary world models.

1.2. Radio Sources and Cosmology

If the radio sources are indeed at the cosmological distances, they are the most suitable objects for cosmological investigations and might provide important clues to us for understanding the large scale space-time structure of the universe. Radio observations provide information regarding several properties of radio sources such as flux density, angular size and spectral index. Optical observations can provide redshift information for the identified sources. The observed distributions of different properties of radio sources depend on the space density of radio sources and also on the geometry of the universe. This might lead one to think that the radio sources provide a simple and powerful tool for unfolding the nature of the universe. Unfortunately, it has turned out to be not so and the reasons for this unfortunate state of affairs are discussed below.

1.2.1. Source Counts and Cosmology

The very first method and perhaps the most popular (or easy ?) cosmological test employed by radio astronomers is the method of source counts i.e. study of the number of sources $N(>S)$ above a certain flux density S, as a function of

S (see reviews by Longair 1971; von Hoerner 1973; Jauncey 1975). Since S can be easily measured for a large number of sources, this was supposed to be a simple and a pure radio tool for determining the geometry of the universe. However, source counts have not revealed much about the geometry of the universe, because the observations show that the source counts cannot be explained without postulating a strong evolution of the source properties with cosmic epoch. The effects of this evolution dominate over the geometric differences between various world models. The most salient features of the evolutionary effects that have been inferred from the investigations of source counts from different surveys are:

(i) the evolution is confined to powerful sources $[P(408) > 10^{26}\ \mathrm{WHz^{-1}\ sr^{-1}}]$.

(ii) the evolution is quite strong; the comoving space density of sources at large redshifts ($z \sim 2$) is ~ 1000 times their density in the nearby space.

However, there is still much disagreement regarding the details of this evolution. This situation arises because the determination of evolution function (EF) from the observed source counts requires a knowledge of the local luminosity function (LLF) i.e. the local space density of sources with different luminosities. However, a determination of the LLF itself in turn requires the knowledge of EF, the geometry of the universe and involves assumptions regarding distances of

radio sources. The uncertainties of the LLF and the geometry of the universe permit a wide range of models. Hence we have to look for additional observational information such as that provided by $\langle z(S) \rangle$ versus S relation (radio 'Hubble relation') that places further constraints on the models (von Hoerner 1973). However, the z(S) relation for radio sources is blurred by too much of scatter in the data (Hoyle and Burbidge 1966). The observed scatter in the $\langle z(S) \rangle$ versus S plot is a direct consequence of a rather broad LLF. Moreover, the expected relation depends rather critically on the nature of the luminosity function employed. Several authors (von Hoerner 1973; Jauncey 1975) have, therefore, emphasized the need for including other distance dependent features like angular sizes and Spectral Index Distributions (SID) in addition to just fluxes and numbers.

1.2.2. Angular Sizes and Cosmology

The angular structure of a radio source is another important parameter that can be used to study cosmology. Observations over the last two decades have shown a remarkably high percentage of sources to have double structure(Fomalont 1969; Mackay 1971). The separation of components or the angular size (θ) of a radio source provides 'metric' diameters in contrast to 'isophotal' diameters measured in the case of optical galaxies. Since the θ-z relation for extragalactic objects depends on the cosmological model, observations of angular sizes can be used , in principle, to determine the

geometry of the universe. However, in the practical application of this test a complication arises because of the wide dispersion in the linear sizes of radio sources.

Several authors have investigated the angular size versus redshift (θ-z) plot for quasars and concluded that the data provide evidence for the evolution of linear sizes (Legg 1970; Miley 1971; Wardle and Miley 1974). This seems to be the most widely accepted interpretation although many investigators have questioned it and have attempted to explain the observed θ-z plot without invoking the evolution of linear sizes (Reinhardt 1972; Jackson 1973; Richter 1973).

As discussed above the θ-z test encounters some interpretational problems. In addition, it suffers from the following drawbacks. The first one is that it requires a knowledge of redshifts of radio sources. Secondly, it cannot be of much use in studying the evolutionary properties of radio galaxies because most of the redshifts measured for galaxies are small ($z < 0.3$) and at such small redshifts the effects of evolution are small.

A related test is the angular size vs flux density or θ-S test. The θ-S test is a pure radio test because it does not require the redshift information. Since the variation of θ and S with redshift depends on the specific cosmological model chosen, θ-S relation can be used to study cosmology. Early attempts (Longair and Pooley 1969; Fanaroff and Longair 1972) to use this test were not very fruitful mainly because of the small samples of sources involved.

A detailed analysis of the observed θ-S relation was first presented by Swarup (1975). From an analysis of the angular size data for sources from the Ooty occultation surveys, 3CR and the All-Sky catalogue (Robertson 1973), Swarup showed that the median value of angular sizes (θ_{med}) is correlated with flux density. Kapahi (1975a, 1975b) used the θ_{med} vs. S relation derived by Swarup and the angular size counts $N(> \theta)$ for the 3CR sources to obtain several important results in cosmology. He showed that the angular size data provide an independent means of deriving the local luminosity function without explicit use of redshifts. He further showed that the observed data imply the presence of density (and/or luminosity) and linear size evolution effects among radio sources. It was inferred that the overall linear sizes of radio sources vary as $(1+z)^{-n}$ where n lies in the range 1 to 1.5.

1.2.3. Spectral Index Distributions and Cosmology

Apart from flux density, spectral index is the most readily measured parameter of a radio source. Observations made during the last two decades have shown that the nonthermal radio emission from extragalactic radio sources arises in synchrotron process and that the spectra of radio sources can be represented by a power law of the form $S(\nu) \propto \nu^{-\alpha}$. A majority of the sources found in low frequency ($\nu < 1000$ MHz) surveys have straight line spectra i.e. α is a constant. Although the dispersion in spectral indices is rather large with a range of -0.5 to 1.2, most of the sources found in a low frequency

survey have spectral indices in a narrow range around 0.8. At low frequencies the distribution of spectral indices can be represented approximately by a normal distribution function. The non-zero width of SID influences the nature of observed source counts and SIDs at low and high frequencies. The steep-spectrum sources are preferentially observed in the low frequency surveys. On the other hand at high frequencies, flat-spectrum sources are more favourably observed.

The observed SIDs can be used in an indirect manner to gain information about certain features of the space distribution of radio sources. The redshift z upto which a source of luminosity $P(\nu)$ can be observed at a limiting flux density $S(\nu)$ depends on the spectral index and the specific cosmological model used. This spectral dependence of the effect of redshift on flux density is analogous to K-correction for the measurement of optical magnitudes. In a given cosmological model for a fixed luminosity P and flux density limit S $z(\alpha_1, P, S) > z(\alpha_2, P, S)$ if $\alpha_1 < \alpha_2$. In other words, sources with steep-spectra become fainter with increasing redshift more rapidly than sources with flat-spectra. This means that if there is a flux density-distance relation, then we expect a correlation between flux density and spectral index. The expected correlation is such that it causes an increase in the fraction of flat-spectrum sources for the weaker sources.

In uniform cosmological models in which comoving space density of radio sources remains constant the expected correlation between SID and flux density is blurred by the

wide dispersion in the intrinsic luminosities of radio sources. As a consequence of this no significant variations in SIDs with flux density are expected. On the other hand in evolving world models a strong dependence of SID on flux density is expected. In these models the comoving space density of radio sources increases rapidly with redshift upto $z \sim 3$. This has the effect of increasing the fraction of sources with large redshifts in a given flux density range. This increase is over and above the increase that is caused by the geometric effects alone. Since the overall effects of evolution are much larger compared to the geometric effects, in evolving world models significant variations in SIDs with flux density are expected. This means that by making use of source counts and SIDs for sources selected at low and high frequencies it should be possible to derive a Generalized Luminosity Function (GLF) that describes the space density of extragalactic sources as a function of luminosity (P), redshift z and spectral index α.

The interpretation of the observed source counts and SIDs in terms of evolutionary models and the derivation of the GLF has been discussed by Fanaroff and Longair (1973). They proposed a model to explain the source counts and SIDs for sources selected at 178 MHz and 5000 MHz. They assumed that the GLF $\psi(P,z,\alpha)$ can be factorized into spectral index function $\eta(\alpha)$ and luminosity function $\rho(P,z)$ i.e. the spectral index function is independent of luminosity at a low frequency. In addition, they assumed an identical form of cosmological

evolution for flat- and steep-spectrum sources. The model was then used to calculate the expected SIDs and source counts. The results showed that even in simplest types of evolutionary world models large variations in SIDs with flux density are expected for sources selected at high frequencies. The model was shown to account for the general features of the observations at both low and high frequencies. However, the model seems to run into difficulties in predicting source counts and SIDs in the low flux density region (~ 0.1 Jy) at 5000 MHz.

Moreover, recent investigations (e.g. Schmidt 1977; Masson and Wall 1977) show that the cosmological evolution is likely to be spectral index dependent. A correlation between radio luminosity and spectral index has also been reported by many authors in recent years (e.g. Veron, Veron and Witzel 1972).

It is clear that the observational features discussed in the preceding paragraph should be taken into account in deriving a GLF for extragalactic radio sources. It is the derivation of such a GLF with which the present thesis is mainly concerned.

1.3 The Present Work

In this thesis we discuss many topics that are related to the use of different properties of radio sources to study cosmology. Our main aim is to derive the space distribution of radio sources as a function of radio luminosity, spectral

index, redshift and linear size, by making use of observational data available at low and high frequencies. This involves determination of the LLF, EF, spectral index function and linear size function.

In Chapter 2, we review briefly the observations and interpretation of source counts at a single frequency (408 MHz). In this connection, we present a discussion of the observed absolute magnitude vs. redshift diagram and Hubble plot for a sample containing ~ 570 QSOs. This is followed by a critical review of different methods for determination of the LLF and the EF. After discussing the Free-Form Analysis Scheme (Robertson 1978) of solving for the EF, the scheme is extended to start from the observed luminosity distribution rather than the derived LLF. The LLF and the EF thus derived are shown to be in general agreement with the results obtained from conventional analysis of source counts (e.g. Wall et al. 1977).

The current observational situation of source counts and SIDs is reviewed in Chapter 3. The general features of the source counts at different frequencies are pointed out. The dependence of the SIDs on flux density and frequency are discussed. The observational data available at present show that the SIDs of sources from a high frequency survey show significant variations with flux density. On the other hand very small, if any, variations are observed in the SIDs of sources selected at a low frequency.

A discussion of the interpretation of the source counts and SIDs is given in Chapter 4. First a brief review of the earlier models is given (e.g. Kellermann, Pauliny-Toth and Davis 1968; van der Laan 1969; Fanaroff and Longair 1973; Petrosian and Dickey 1973; Schmidt 1972c). This is followed by a discussion of some of the drawbacks of these models. After pointing out some of the difficulties that these models encounter in the light of the recent data a new model is proposed. The new model includes (i) the observed correlation between radio luminosity and spectral index and (ii) spectral index dependent evolution function for extragalactic radio sources.

A GLF is derived by following a model fitting procedure. First a form for the GLF is assumed. The free parameters of the GLF are then estimated by comparing the model predictions with the observational data at 408 MHz. The model is then shown to predict source counts and SIDs that are in good agreement with the observations at 5000 MHz. The predictions are also found to be in reasonable agreement with observed source counts and spectral index distributions for sources selected from surveys at 1400, 2380 and 2700 MHz. In this way a GLF which gives source counts and SIDs that are consistent with observational data both at low and high frequencies is derived. The improvement over earlier models is mainly due to the inclusion of the spectral index dependence of the cosmological evolution. The effects of inclusion of radio luminosity-spectral index correlation are comparatively small.

Some of the limitations of the present model are pointed out and possible further refinements of the model are indicated.

In Chapter 5, the GLF derived in Chapter 4 is used along with the radio size function in investigating the cosmological implications of the observed angular sizes of extragalactic radio sources. These investigations form an extension of the recent works (Swarup 1975; Kapahi 1975a, 1975b; Subrahmanya 1977). The angular size counts are calculated by taking into account the dispersion in spectral indices and possible correlation between radio luminosity and linear size. From a comparison of the predicted and observed angular size counts the presence of density (and/or luminosity) and linear size evolution effects in radio source populations is inferred. The results obtained are found to be in agreement with those reported by the above authors and show that the dispersion in spectral indices does not significantly modify the results of earlier investigations of the cosmological implications of the observed angular size counts.

The GLF in conjunction with the radio size function gives us the Extended Luminosity Function (ELF). The ELF gives the number of sources per unit comoving volume as a function of luminosity, redshift, spectral index and linear size. The ELF derived here is found to be consistent with the source counts and SIDs both at low and high frequencies and also with the angular size counts of extragalactic radio sources.

The principal results of the present investigations are summarized in Chapter 6.

"Only that God who sees in highest heaven:
He only knows whence comes this universe,
and whether it was, made or uncreated.
He only knows, or perhaps he knows not."

Rig Veda X, 129.

CHAPTER 2

RADIO SOURCE COUNTS AT A SINGLE FREQUENCY, LOCAL LUMINOSITY FUNCTION AND EVOLUTION FUNCTION

2.1 Introduction

The most widely used method of using radio surveys for observational cosmology has been to count the number of radio sources, N(>S), above successively decreasing flux densities, S. The log N(>S)-log S relation has been extensively studied using radio surveys made with different telescopes at different observing frequencies now going upto 8000 MHz. In Chapter 4 we derive a Generalized Luminosity Function for explaining the observed counts at different frequencies. In this chapter a detailed review of interpretation of observed source counts at a single frequency is presented. Also, presented is a detailed discussion of the apparent magnitude-redshift relation for the QSOs. We have also proposed an extension of the Free Form Analysis Scheme of Robertson(1978).

For illustrative purposes, the source counts at 408 MHz are considered, because most extensive work on this subject has been carried out at this frequency from source surveys going down to flux levels of 0.01 Jy (1 Jy = 10^{-26} $Wm^{-2}Hz^{-1}$). The general features of the observed counts and different interpretations are summarized in Section 2.2. The most popular interpretation of radio source counts has

been in terms of evolving model cosmologies. However, this is not a straightforward procedure because the evaluation of source counts requires the knowledge of: (i) the Local Luminosity Function (LLF); (ii) the geometrical properties of the world model; and (iii) the evolution of the radio source properties with cosmic epoch. The determination of the LLF involves the distances of radio sources. However, it is not possible to determine the distances of these sources by radio observations alone. For this we need to use redshifts estimated by optical methods. Hence it is necessary to assume all radio sources including quasars lie at cosmological distances as given by their redshifts. In Section 2.3 we have made an analysis of the observed magnitude-redshift relation for the brightest quasars and have shown that the results are consistent with the cosmological hypothesis. In Section 2.4, the complications showing up in the determination of the LLF and the Evolution Function (EF) are pointed out and different methods of deriving these functions are reviewed. The Free-Form Analysis Method (FFAM), recently proposed by Robertson (1978), for investigating the cosmological evolution of radio sources, is discussed in some detail. An extension of FFAM, that starts from observed Luminosity Distributions (LD) rather than the derived LLF is proposed in Section 2.5.

2.2 Number Counts at 408 MHz and Their Interpretation

2.2.1. Basic Ideas

In a universe assumed to be Euclidean, static and uniformly filled with radio sources of luminosity P (measured in W Hz^{-1} sr^{-1}), the following relations hold

$$S \propto \frac{P}{r^2} \ , \ N(<r) \propto r^3 \qquad (2.1)$$

where S is the observed flux density and N(<r) the number of sources per steradian, in a sphere of radius, r . This is the same as the number of sources, N(>S), with flux density greater than S . Hence N(>S) is given by

$$N(>S) \propto S^{-3/2} \text{ or } \log N(>S) = -1.5 \log S + \text{const.} \qquad (2.2)$$

This is the famous log N-log S relation in the integral form. Since the relation is true for any luminosity, it will be true for any combination of the luminosities. As a consequence of this the form of source counts is independent of the LLF in a static-Euclidean world.

Sometimes the counts are presented in differential form, so that the numbers of sources n(s) counted in each flux density range Δs are statistically independent. For comparing the observations with the predictions of uniform cosmological models, it is convenient to show the counts in the normalized differential form - i.e. in the form

$n(S)/n_o(S)$ where $n_o(S)$ is the number of sources per unit flux density range expected in a uniform, static Euclidean universe. In an Euclidean universe in which sources are distributed uniformly, $n(S)/n_o(S)$ would be a constant for all flux densities. In real world models, however, the differential counts of sources depart significantly from the constant value, even at relatively small redshifts. Before considering the predictions of these world models, let us outline the general picture that emerges from observations.

2.2.2. Observations

For many years the experimental value of the radio source counts was a subject of great controversy because the experimental errors due to confusion, noise and incompleteness were underestimated. Today, as a result of the vastly increased sensitivity and resolution of modern telescopes, the experimental situation is much clearer and there is a good general agreement among radio source surveys (Longair 1971; Longair 1974; Scheuer 1975; Jauncey 1975).

The most extensive counts are those at 408 MHz spanning a range of about 5000:1 in flux density. They are presented in the normalized differential form in Fig.2.1 (Pearson and Kus 1978). Some 90 % of the sources found at this frequency are of the extended steep-spectrum type, so that as a first approximation one can ignore the dispersion in spectral indices and assume that spectral index $\alpha = 0.75$ ($S \propto \nu^{-\alpha}$) for all sources. Moreover, recent identifications

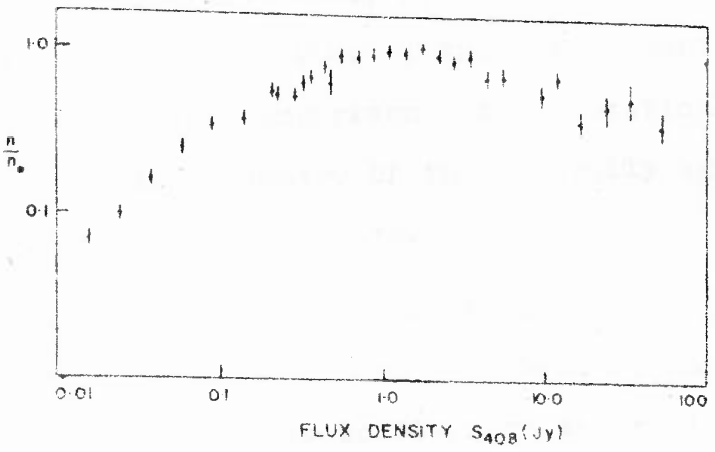

FIG 2·1 THE OBSERVED RADIO SOURCE COUNTS AT 408 MHz. IN NORMALIZED DIFFERENTIAL FORM. THE COUNTS ARE TAKEN FROM ROBERTSON (1973), COLLA et al (1973), AND THE CAMBRIDGE 5C SURVEYS (PEARSON & KUS 1978).

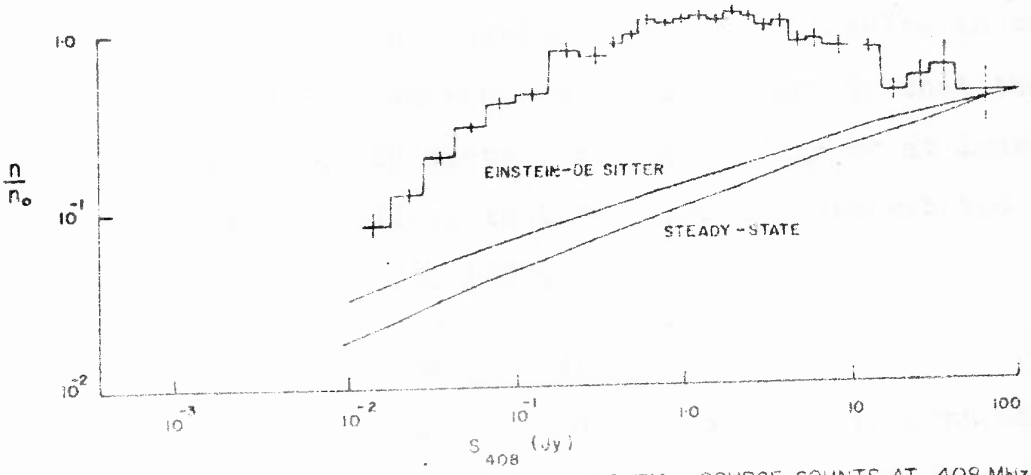

FIG 2·2 THE OBSERVED NORMALIZED DIFFERENTIAL SOURCE COUNTS AT 408 MHz THE LOWER CURVES REPRESENT AN EINSTEIN-DE SITTER MODEL WITH A UNIFORM DENSITY OF SOURCES, AND THE STEADY-STATE MODEL.

and redshift determinations, yield a well-defined Luminosity Distribution (LD). In view of this, the counts at 408 MHz are well suited for comparison with theoretical predictions. The following is a summary of the generally agreed features of the observed source counts.

a) The normalized differential counts $n_n(S)$ show a drop at the bright end, by a factor of about 2, implying a deficit of sources. The drop is confined to the region between 5 and 15 sources sr^{-1}.

b) There is a maximum or somewhat flat top at intermediate flux densities covering the region between 15 and 10^3 sources sr^{-1}.

c) Finally, there is the region of convergence at low flux densities where source density is greater than $\sim 10^3$ sources sr^{-1}.

d) The absence of any convincing positive results in the clustering or anisotropy searches naturally suggests that the radio sources are randomly distributed on the sky or at least there is no reason to believe that they are not distributed randomly(e.g. Webster 1976, 1977; Wall 1977).

2.2.3. Interpretation of Source Counts

Let us now turn our attention to the predictions of uniform cosmological models and their comparison with observations. The essential features of source counts expected in different models are outlined below.

i) Steady State Model: $n(S)/n_o(S)$ decreases as S decreases, provided only that spectral index $\alpha > -2.5$.

ii) Relativistic models: $n(S)/n_o(S)$ decreases as S decreases in all open models if $\alpha > -1$ and in all closed models with the cosmological constant $\Lambda = 0$ if $\alpha > 0$ (Longair 1971; Scheuer 1975).

Since the mean spectral index $< \alpha >$ of radio sources has a value of about 0.8, it follows that for a very wide range of cosmological models, in which it is assumed that there is a fixed number of sources per unit comoving volume, the source count $n(S)/n_o(S)$ is expected to decrease monotonically with decreasing flux density in contradiction with the observations. Thus the geometrical properties of the Robertson-Walker metric (i.e. use of different world models) cannot be of much help in accounting for the rise in $n(S)/n_o(S)$ with decreasing S; in fact they merely aggravate the problem. The observed source counts must therefore imply some inhomogeneity or evolution of the source population. This inference is quite independent of any knowledge of distances and in particular of the cosmological hypothesis for the redshifts of QSOs. However, it is not possible to distinguish between inhomogeneity and evolution, without some additional information on the nature of the sources involved. Attempts have been made to reconcile the theoretical predictions with observations either by postulating inhomogeneity or evolution and main results of these attempts are described below.

a) The evolution of radio source population: As pointed out above one of the possible implications of the discrepancy

between the observed and the predicted source counts is that the mean properties of radio sources have changed over cosmological time scales. Most authors who have compared source counts with models agree that such an evolution is needed. But there is much disagreement about all possible details regarding type of evolution and the class of sources involved in the evolution. This is because the evolution of the radio source population cannot be derived uniquely from the source counts without additional information regarding the distances of radio sources. In the most general form the unknowns involved in the derivation of evolutionary world models are: (i) the LLF $\rho(P\ z = o)$; (ii) the geometrical properties of the cosmological model and (iii) the EF describing the change in the mean properties of radio sources with epoch. In a satisfactory world model these three unknowns must be derived in such a way that the following observational data are accounted for: (i) the radio source counts; (ii) the luminosity distributions (LD) and (iii) the integrated emission from extragalactic radio sources. However, many complications show up immediately.

First, the determination of the LLF requires a knowledge of the distances of radio sources, including quasars. There is no way of estimating the distance of a radio source from radio observations alone; it must be obtained by identifying the source with an optical object and measuring its redshift. Hence it becomes necessary to assume that quasars

are at cosmological distances implied by their redshifts. This is discussed further in Section 2.3.

Secondly, the decrease in the percentage of identification with decreasing flux density and the dependence of LLF on EF and the geometrical properties of the world model, introduce further uncertainty in our knowledge of the LLF. A discussion of these points and a summary of the different methods employed in the derivation of LLF and EF is given in Section 2.4.

Because of the above-mentioned complications and lack of sufficient information, it is possible to work out a variety of evolutionary schemes within the uncertainties of the world model and the LLF, to fit the observed counts satisfactorily (Longair 1971; Scheuer 1975; von Hoerner 1973). The principal conclusions which emerge from all such analyses can be summarized as follows:

i) The evolution must be strong: the comoving space density of powerful radio sources ($P_{408} \gtrsim 10^{26}$ W $Hz^{-1}sr^{-1}$) must be about 1000-10000 times greater at earlier epochs (corresponding to redshifts of about 2-4) than it is at the present epoch.

ii) Strong evolution is indicated only up to redshifts of about 3. For larger redshifts, the comoving source density should decrease or rise much less rapidly with z in order to reproduce the rapid convergence observed at very low flux densities and to conform to the constraints imposed by the background radio emission measurements.

iii) The strong evolution is mostly confined to powerful radio sources. If low luminosity sources evolved as rapidly as strong sources, it would not be possible to reproduce the observed convergence of source counts at low flux densities. Moreover, since the total extragalactic background with a spectral index $\alpha = 0.75$ is about $3^{\circ}K$ at 408 MHz (Bridle 1967) and the sources with $S_{408} \geq 0.01$ Jy account for $1.4^{\circ}K$ (Pooley and Ryle 1968), it follows that a strong evolution of sources of all luminosity classes would result in a background radio radiation many times greater than the observed value.

It might be pointed out here that the presence of strong evolutionary effects among the powerful extragalactic radio sources has also been inferred from an application of the Luminosity-Volume test to QSOs and radio galaxies (Schmidt 1968; Rowan-Robinson 1971).

iv) Type of evolution: As pointed out earlier it is not possible to determine the EF uniquely. For example, the source counts can be explained by supposing an increase with z, in either the comoving space density of radio sources or in the mean luminosities of radio sources. There has been much discussion in the literature on whether 'density evolution' or 'luminosity evolution' or a combination of both gives a better fit to the observed source counts. However, it seems that it is not possible to distinguish among various viable forms of evolution, unless we find some source properties that can be used as labels to select the object of the same

intrinsic type at different epochs.

How important is the choice of world models in all these analyses of source counts ? It turns out that the above conclusions are not very sensitive to the choice of the world model. In Fig.2.2, the observed normalised differential counts at 408 MHz (Pearson and Kus 1978) are compared with the predicted counts in the Einstein-de Sitter model with a uniform density of sources, and in the Steady State model. It is clear from Fig.2.2 that the geometric differences between world models are small compared with the aggregate effects of evolution. In the flux density interval 1-4 Jy where $n(S)/n_o(S)$ is maximum, the effects of evolution are about 7 times greater than the differences between the predictions of the two cosmological models considered. A consideration of the mean square deviations (i) between observations and predictions of Steady State model and (ii) between predictions of Einstein-de Sitter model and Steady State model, also shows that the differences introduced by evolution exceed the geometric differences by a factor of ~ 6. The Steady State model is ruled out not because of this discrepancy alone, but because it does not allow evolution.

b) The above interpretation of source counts has often been questioned (e.g. Hoyle 1968; Brecher et al. 1971). It is sometimes argued that rise of $n(S)/n_o(S)$ with decreasing flux density observed at high flux densities can equally well be interpreted as a deficiency of nearby sources rather than as

an excess of distant sources. However, such models seem to have difficulty in accounting for the isotropy of source counts and for the fact that the sources detected in the surveys contribute at least ~ 1/3 of the total extragalactic radio background. A lively discussion of arguments for and against this 'local hole' model can be found in the review articles by Kellermann (1972) and Longair and Rees (1972), respectively. A detailed analysis by von Hoerner (1973) also argues against the local hole hypothesis.

To summarize, the observed counts cannot be convincingly explained in the Steady State theory or in the Friedmann cosmologies without recourse to evolutionary effects. In the rest of the thesis, we will accept this conventional interpretation of source counts and estimate counts and other relevant observables in the framework of an evolutionary world model only.

2.3. Absolute Magnitudes and Hubble Plot for QSOs

2.3.1. Introduction

Ever since the discovery of quasars there has been much lively discussion in the literature on the nature of their redshifts (e.g. Field et al. 1973; Burbidge 1973). It is not our intention to enter the controversy as to whether the quasar redshifts are cosmological or not. However, we would like to present our analysis of the observed apparent magnitude versus redshift relation for quasars and show that the

results are consistent with cosmological hypothesis of redshift of QSOs (Kembhavi and Kulkarni 1977).

The redshift-magnitude test has been one of the important tools in the study of cosmology. In the case of radio-galaxies, the dispersion in absolute magnitude is small and the redshift-magnitude diagram reflects a well-defined Hubble law. However, in most cases, the observed redshifts are smaller than about 0.4 and at such small redshifts the differences between world models are small. Hence the Hubble diagram for radio galaxies cannot be of much help in distinguishing among different world models.

On the other hand, quasar-redshifts are sufficiently large for cosmological effects to be important. However, investigations of the apparent magnitude vs. redshift relation for all quasars in various samples by Sandage (1965), Hoyle and Burbidge (1966), Longair and Scheuer (1967) and Schmidt (1968) showed the absence of any obvious redshift-magnitude correlation in QSOs. McCrea (1972) reasoned that this lack of correlation might be due to the large dispersion in luminosities and suggested that the brightest QSO at each redshift might have a well-defined Hubble relation. Following this suggesion , Bahcall and Hills (1973) grouped QSOs according to their redshifts, z and picked the intrinsically brightest member of each group as a standard candle. They made an estimate of observational selection effects by following a procedure that involves some assumptions about quasar

luminosity function and a series of computer experiments. Bahcall and Hills then constructed the apparent magnitude-redshift diagram for the brightest QSOs and obtained results consistent with the hypothesis of a cosmological origin for the redshifts. On the other hand Burbidge and O'Dell (1973), using the same data but a slightly different analysis to avoid the effects of selection concluded that the data do not provide strong evidence that the redshifts of QSOs are of cosmological origin.

Recently, Burbidge, Crowne and Smith (1977) have published a catalogue that contains the optical properties of 570* QSOs. Bahcall and Hills (1973) and Burbidge and O'Dell used a subset of this sample in their analysis. The new sample covers a larger redshift range and thus spans a larger volume of space. Moreover, because of its large size, it is better suited for statistical analysis. It is therefore worthwhile to investigate the absolute magnitude-redshift relation and the Hubble relation for this sample and see what trends are indicated by the data. However, some complications arise immediately because the sample is not complete to any optical or radio flux density and unknown selection effects may be present. In the second half of our analysis we have tried to eliminate the selection effect pointed out by Burbidge and O'Dell (1973).

---

* The analysis was done on the basis of a preprint available to us. The published catalogue contains a list of 633 QSOs.

2.3.2. Analysis and Conclusions

Though the catalogue contains 570 QSOs, all the relevant data is available for only 563 of them. We have used this sample of 563 QSOs in our study of the magnitude-redshift relation. However, it is necessary to apply the following corrections to apparent visual magnitude.

The first is the correction due to galactic absorption. Following Sandage (1968) and Schmidt (1968) we have applied the correction

$$\Delta m_v = -0.18(\mathrm{cosec}\,|b| - 1) \quad \text{for } |b| > 10^\circ$$

and

$$\Delta m_v = -0.9 \quad \text{for } |b| \leq 10^\circ$$

where b is the galactic latitude.

The second correction arises due to the general expansion of the universe. This expansion causes a shift in the QSO spectra toward red under a fixed observing bandpass $\Delta\nu$. Another effect of this expansion is to compress a bandwidth $\Delta\nu_o$ at emission over a bandwidth $\Delta\nu = \Delta\nu_o(1+z)^{-1}$ at reception. The correction applied to compensate for these two effects is usually referred to as the K-correction. We have assumed that in the case of QSOs the spectral flux density in the optical region varies as $\nu^{-1.0}$, ν being the proper frequency (Schmidt 1975). The K-correction then reduces to zero. Even if the optical spectral flux density is taken to be proportional to $\nu^{-0.7}$ as some authors do, no significant change will be

produced in the result as the maximum correction would be only ~ 0.2 mag.

We have done our calculations within the framework of the closed Friedmann universe ($k = 1$) with the deccleration parameter $q_o = 1$. If the QSO redshifts are true distance indicators, then the plot of log z versus the corrected apparent magnitude should produce a straight line with slope 0.2. The Hubble plot for the 563 QSOs shows a lot of scatter. The linear correlation coefficient (r) between log z and corrected apparent magnitude is 0.38. The slope of the least squares fit line $\log z = a+bm_v$, differs from the theoretical value of 0.2 by 4.76σ (See Table 2.1). However, if the redshifts are cosmological, this large scatter can be attributed to a broad luminosity function. As discussed earlier, if this is true, then the Hubble plot for the brightest QSOs at every redshift should show much less scatter and give a large value for the linear correlation coefficient r .

We have ordered the QSOs in the sample according to z and grouped them into 36 redshift bins, each bin (except the last) containing 16 QSOs, so that the first bin contained the QSOs having the 16 smallest redshifts and so on. For each QSO we calculate the absolute visual magnitude M_v using

$$M_v = m_v - 5\log z - 43.88 \text{ for } H_o = 50 \text{ km/(s Mpc) and } q_o = 1 \qquad (2.3)$$

We also find, for each bin, the value of the average redshift $\langle z \rangle$ and the absolute magnitude of the brightest QSO assuming

TABLE 2.1 : Correlation of log z and m_v for various samples of QSOs

Sample	Number of QSOs	Slope b	Uncertainty σ_b	Correlation coefficient r	Probability of exceeding r for uncorrelated parent population	$t = (b-0.2)\sigma_b^{-1}$	Probability of exceeding t if the slope is 0.2	Significance level 0.05	Significance level 0.01
All QSOs	565	0.134	0.014	0.379	$< 10^{-4}$	-4.762	$< 10^{-4}$	Yes	Yes
Brightest QSOs	36	0.312	0.045	0.765	$< 10^{-4}$	2.484	~ 0.018	Yes	No
Brightest QSOs with selection effect removed	11	0.209	0.052	0.799	$\sim 4 \times 10^{-3}$	0.164	~ 0.89	No	No

its redshift to be <z> . The plot of the absolute visual magnitude M_v of the brightest QSO in each bin against the average redshift <z> for that bin is shown in Fig.2.3. It is seen that the absolute magnitude of the brightest QSO increases with redshift up to z = 1, after which it remains nearly constant, with a mean value of M_v = -29.4 mag (corresponding to a luminosity of 2×10^{32} ergs/(s Hz) at λ = 5517 A^o) and a standard deviation of 0.5 mag. Based on his investigations of H_β or L_α fluxes for 57 Seyfert galaxies and QSOs, Weedman (1976) has reported similar results.

The constancy of M_v for z > 1 suggests, that the maximum luminosity that QSOs can reach is independent of epoch. The initial rise in M_v seen for redshifts z < 1 can be simply explained with a luminosity function that makes the more luminous QSOs sufficiently rare, so that they cannot be found until a large volume of the universe is surveyed i.e. until a high enough redshift is reached. We also plot in Fig.2.3, the absolute magnitude of the faintest QSOs in each bin. The absolute magnitudes of all 563 QSOs lie between the upper and lower envelopes. It might be pointed out that the lower envelope is determined by the prevailing observational cut-off magnitude. In the same figure, we show the absolute luminosity versus redshift plot for all the QSOs with z>2.75. It is seen that at the high-redshift end, all the observed QSOs come from the brighter side of the luminosity function. This is expected because at high redshifts the low luminosity QSOs would be below the detection limit.

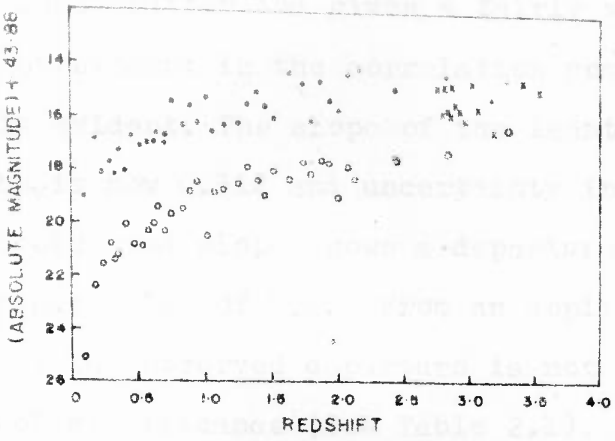

FIG.2·3 PLOT OF ABSOLUTE MAGNITUDE M_V AGAINST AVERAGE REDSHIFT $\langle z \rangle$ FOR THE BRIGHTEST (CLOSED CIRCLES) AND FAINTEST (OPEN CIRCLES) QSOs IN EACH OF 36 REDSHIFT BINS. CROSSES INDICATE ALL QSOs WITH $z > 2{\cdot}75$

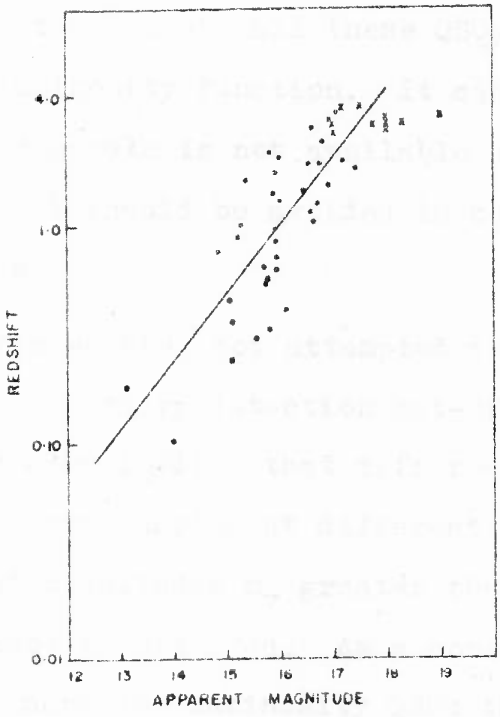

FIG. 2·4 HUBBLE DIAGRAM FOR THE BRIGHTEST QSOs (CLOSED CIRCLES) SHOWN IN FIG. 2·3. CROSSES INDICATE ALL QSOs WITH $z > 2{\cdot}75$

The Hubble plot for the brightest QSOs (Fig.2.4) shows much less scatter and gives a fairly well-defined Hubble line. The improvement in the correlation coefficient, which is now, 0.76 is evident. The slope of the least squares line $\log z = a+bm_v$ is now 0.312 and uncertainty in the slope is 0.045. The observed slope shows a departure of 2.484σ from the theoretical value of 0.2. From an application of t test we infer that the observed departure is not significant at 0.01 level of significance (See Table 2.1).

The consistency of Fig.2.3 and 2.4 is obvious. The presence of many points (at low redshifts) to the right of the Hubble line in Fig.2.4 can be attributed to a decrease (at low redshift end) in the luminosity of the brightest QSOs seen in Fig.2.3. All the QSOs with $z > 2.75$ are also plotted in Fig.2.4. These QSOs show a small spread about the Hubble line. This is expected because all these QSOs come from the brighter end of the luminosity function. It can be concluded that a good standard candle is not available at low redshifts and QSOs with $z < 1$ should be avoided in constructing a Hubble plot for QSOs.

So far we have not attempted to compensate for biased bin widths and a sharp detection cut-off. The broad luminosity function for QSOs implies that different parts of the luminosity function are sampled at different redshift, because QSOs with apparent magnitudes m_v greater than some cut-off magnitude m_v^* cannot be detected. As a consequence of this a given bin contains more low luminosity QSOs than the next bin with

higher redshifts. This preferential selection of intrinsically faint QSOs at low redshifts manifests as an increase in the slope. We have followed the procedure suggested by Burbidge and O'Dell (1973), to eliminate this selection effect. The 563 QSOs are divided into two groups by the line

$$\log z = -3.35+0.2\ m_v \qquad (2.4)$$

For $z = 3.53$ (largest in the sample), the above equation gives a value of 19.5 for the apparent magnitude. It follows that if we assume a detection cut-off of 19.5 mag. then every QSO to the left of the line would be visible at all redshifts upto 3.53. We use only these QSOs in choosing redshifts ranges. This ensures that every redshift range contains samples from the same part of the luminosity function. We ordered all the QSOs to the left of the line according to z and grouped them into 11 redshifts bins, each bin (except the last) containing 15 QSOs. A plot of the absolute magnitude of the most luminous QSO in each bin vs average redshift $< z >$ is shown in Fig.2.5(a). The initial rise in M_v with redshift seen in Fig.2.3, is no longer present. The plot also shows that the absolute magnitudes of the brightest QSOs remain nearly constant.

The log z-apparent magnitude plot for these brightest QSOs (Fig.2.5b) shows a correlation coefficient of 0.80. A least squares estimate of the slope is 0.209 ± 0.052 and is in close agreement with the theoretical value of 0.2.

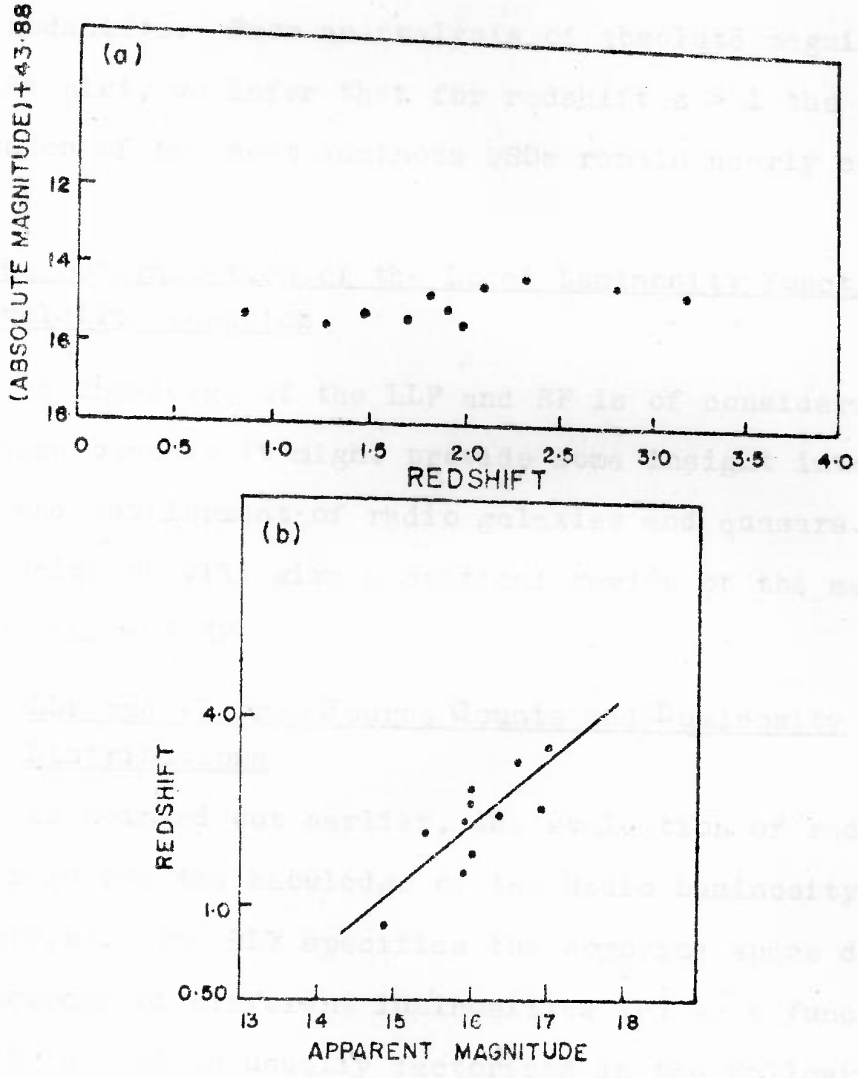

FIG. 2·5(a) PLOT OF THE ABSOLUTE MAGNITUDE M_v AGAINST AVERAGE REDSHIFT $<z>$

(b) HUBBLE DIAGRAM FOR THE BRIGHTEST QSOs SHOWN IN (a)

To summarize, our findings are consistent with the hypothesis that QSOs are at cosmological distances implied by their redshifts. From an analysis of absolute magnitude vs redshift plot, we infer that for redshift $z > 1$ the absolute magnitudes of the most luminous QSOs remain nearly constant.

2.4 The Determination of the Local Luminosity Function and Evolution Function

A knowledge of the LLF and EF is of considerable importance because it might provide some insight into the origin and development of radio galaxies and quasars. In this section we will give a critical review of the methods of deriving LLF and EF.

2.4.1. LLF and EF from Source Counts and Luminosity Distributions

As pointed out earlier, the evaluation of radio source counts requires the knowledge of the Radio Luminosity Function (RLF) $\rho(P,z)$. The RLF specifies the comoving space density of radio sources of different luminosities (P) as a function of redshift z and is usually factorized in the following manner,

$$\rho(P,z) = \rho(P,z=0)F(P,z) \qquad (2.5)$$

where $\rho(P,z=0) = \rho_0(P)$ is the LLF and $F(P,z)$ is the evolution function (EF). The EF describes the dependence of the mean properties of the radio source population on cosmic epoch. Another closely related concept is that of Luminosity

Distribution (LD). The LD denoted by $n(P,S_o)$ gives the number of radio sources of different luminosities P in a radio source survey that contains all radio sources which have flux densities (S) greater than some limiting value (S_o). It is important to distinguish between the LLF and the LD. In any given cosmological model these quantities and the differential source counts $n(S)$ are related in the following manner

$$n(P,S_o) = \int_o^{z^*} \rho(P,z=o)F(P,z)dV(z) \qquad (2.6)$$

and

$$n(S) = \int_o^{\infty} \rho(P=SD^2(1+z)^{\alpha-1},z=o)F(P=SD^2(1+z)^{\alpha-1},z)$$

$$D^2(z)(1+z)^{\alpha-1}dV(z) \qquad (2.7)$$

where

$D(z)$ = luminosity distance
α = spectral index
$dV(z)$ = volume element at z

The luminosity distance $D(z)$ and the volume element $dV(z)$ depend on the choice of the world model. The upper limit of integration z^* in eqn.(2.6) corresponds to the distance up to which a radio source of luminosity P can be placed and still be included in the sample and is given by

$$P = S_o D^2(z^*)(1+z^*)^{\alpha-1} \qquad (2.8)$$

From eqn.(2.6) we can write

$$\rho_o(P) = \rho(P,z=o)=n(P,S_o)/\int_o^{z^*} F(P,z)dV(z) \qquad (2.9)$$

It is clear from eq.(2.9) that if a complete luminosity distribution $n(P,S_o)$ for $S > S_o$ is available, the LLF can be derived provided we have knowledge of the world model and the EF. Let us now consider methods of circumventing the above problems and determining the LLF.

The first method is rather simple. From a well-defined luminosity distribution we choose only those objects with redshifts $z \lesssim 0.1$ and derive a modified LD $n'(P)$. At such small redshifts, the evolutionary effects and the difference between world models can be ignored. Therefore, we can make the following approximations:

$$F(P,z) \simeq 1$$

$$P = S_o z^2 (c/H_o)^2$$

c = velocity of light

H_o = Hubble constant

and $$dV(z) = (c/H_o)^3 z^2 dz$$

Eq(2.9) then reduces to

$$\rho(P,z=o) \propto n'(P) / \int_o^{z^*} z^2 dz \qquad (2.10)$$

giving a simple expression for the LLF. Once the LLF is known in any world model, the EF can be determined in the following manner. A plausible form of EF with some free parameters is assumed and the optimum values of these parameters are obtained by requiring a close agreement between the predicted and observed number counts. However, this method introduces

considerable uncertainty in our knowledge of the LLF at the high luminosity end. The reason for this uncertainty becomes clear from the following argument. In order to reduce the uncertainty we need many more intrinsically luminous sources in the sample. However, intrinsically luminous sources are rare and therefore they would not be detected until a large enough volume is sampled, i.e. until high enough redshifts are reached. Thus the local volume density of the intrinsically powerful sources cannot be determined without the knowledge of the world model and without correcting for evolutionary effects which one is trying to determine !

Recently, Wall, Pearson and Longair (1977) have proposed a scheme for determining both LLF and EF in a self-consistent manner. We give below, a summary of this scheme. Consider the equations,

$$\rho(P,z=o)=n(P,S_o)/\int_o^{z^*} F(P,z)dV(z) \qquad (2.11)$$

and

$$n(S)=\int_o^{\infty} \rho(P=SD^2(1+z)^{\alpha-1},z=o)F(P=SD^2(1+z)^{\alpha-1}D^2(z)(1+z)^{\alpha-1}$$

$$dV(z) \qquad (2.12)$$

In these equations $n(P,S_o)$ and $n(S)$ are known from observations. Assume (a) a world model and (b) an EF with some free parameters and follow the steps described below:

i) Use eq.(2.11) and estimate $\rho(P,z=o)$

ii) Use this estimated $\rho(P,z=o)$ in eq.(2.12) and predict source counts

iii) Compare the observed and predicted counts using χ^2-test and vary free parameters of EF, so as to minimize the value of χ^2.

iv) Repeat the steps (i)-(iii) until a close agreement is obtained between the observational data and model predictions. Since this scheme does not require the $n(P,S_o)$ distribution to contain local sources (z small) only, the problem of inadequate sample size and the resultant uncertainty in LLF (especially at the bright end) encountered in the first method can be avoided. Wall et al. (1977) have used this scheme to derive a variety of evolutionary world models to explain the source counts at 408 MHz.

In both the methods described above, either an exponential form or a power law form is used to represent the EF. However, there is no clear astrophysical reason why the evolution should be of this particular form (see. e.g. Rees 1972). Thus the choice of any particular form to represent EF, seems to be governed by considerations of mathematical simplicity and computational convenience. In these parametric evolution schemes, as they are popularly known, the results obtained depend to some extent on the assumed functional form. For example, a cut-off redshift is clearly required when the EF has the form $(1+z)^{\beta}$ while it is not compulsory if EF has an exponential form. Moreover, with the availability of increasingly accurate source counts over a wide range of flux density (0.01 Jy-100 Jy), the number of free parameters

required to represent EF will increase. As a consequence of this, the derivation of a suitable EF will become more difficult, because it is necessary to follow a nonlinear minimization procedure to estimate the optimum values of the free parameters.

It is thus clear that it is desirable to devise a scheme in which it is possible to solve for the EF without making any prior assumptions about its functional form. In fact such a scheme was given by Ringenberg and McVittie(1970). These authors showed that after imposing some restrictions concerning which classes of radio sources should evolve, it is possible to solve for the comoving space density of sources at different epochs, by transforming the integral equation for EF (eq.2.12) to an equation similar to a Fredholm equation of the second kind. However, because of its complex nature, their scheme does not seem to have attracted much attention in the literature. Recently, Robertson (1978) has proposed a simple iterative scheme for finding EF. In the following pages we give a summary of this 'Free-form Analysis Method' (FFAM) for investigating radio source counts.

Consider the following eq. for source counts,

$$n(S)=\int_0^{\infty} \rho(P=SD^2(1+z)^{\alpha-1}, z=o)F(P=SD^2(1+z)^{\alpha-1}, z)$$

$$D^2(z)(1+z)^{\alpha-1} dV(z) \qquad (2.13)$$

It is very difficult to solve for $F(P,z)$ in this general case. Therefore we make the following simplifying assumptions:

a) The local luminosity function is known

b) The cosmological evolution is confined only to those sources which have luminosities greater than a critical luminosity P_c, i.e.

$$F(P,z) = 1 \qquad P < P_c$$
$$= E(z) \quad P \geq P_c$$

In this way the problem of solving for an unknown function of two variables (P and z) is reduced to that of finding an unknown function $E(z)$ of one variable and one parameter P_c.

Since the geometrical differences between world models are small compared to gross effects of evolution, the choice of world model is not important. For the sake of definiteness the Einstein-de Sitter model is employed.

With the above assumptions, the eq. for source counts reduces to

$$n(S)=\int_0^\infty \rho_o(P)E(z)dV(z)D^2(z)(1+z)^{\alpha-1} \qquad (2.14)$$

where $P = S(1+z)^{\alpha-1}D^2(z)$

and $\rho_o(P) = \rho(P,z=o)$

In evaluating these counts, it is convenient to use logarithmic integration and specify $E(z)$ at $N(\sim 100)$ equally spaced

points on the log z axis. The ith element of the array is represented by $E(z_i)$. With $Z=\log z$ and the $dV(z)D^2(z)(1+z)^{\alpha-1} = H(z)dz$ the above equation reduces

$$n(S) \propto \int_{-\infty}^{\infty} \rho_o(P)E(z)z\, dZ\, H(Z) \qquad (2.15)$$

or

$$n(S) \propto \int_{-\infty}^{\infty} I(z,S)dZ$$

where $I(z,S) = \rho(P,z=o)E(z)H(z)z$

The above equation can be written in the following form

$$n(S_j) = \sum_{i=1}^{N} I(z_i, S_j)\Delta Z_i \qquad (2.16)$$

where S_j's are the values of the flux density at which counts have to be evaluated. In his analysis Robertson considered the Molongolo source counts. The counts were plotted in normalized differential form. A smooth curve was then drawn through these observed points and from this curve the values $n'_n(S_j)$ were read at flux densities S_j's(j=1....M), covering the range between 0.020 Jy to 50 Jy. The iterative scheme for deriving E(z) proceeds as follows.

STEPS

i) $E(z)=E_1(z)$ where initial guess $E_1(z)$ is given by

$$E_1(z_i) = 10i \ , \ i = 1, 2....N$$

2) Calculate $n(S_j)$ for $j = 1, 2 \ldots M$

3) Calculate $R_j = \frac{n'_n(S_j)}{kn(S_j)S_j^{2.5}}$ where k is a normalizing constant. It is clear that if instead of $E(z_i)=E_1(z_i)$ we use $E_1(z_i)R_j$ in eq.(2.16) an exact agreement between observed and predicted counts will be obtained at S_j. However, the scale factor R_j will be different in general at different S_j. The problem is how to obtain next approximation $E_{r+1}(z_i)$ from $E_r(z_i)$ by using these scale factors R_j at different S_j. It is clear that some average or effective scaling factor has to be used in deriving $E_{r+1}(z_i)$ from $E_r(z_i)$. Now $I(z_i,S_j)$ has in general a peak at some redshift z_p and the location of this peak changes with flux density (S_j) i.e. there is some correlation between average redshift $\langle z \rangle$ and flux density. Consider sources with flux density S_j. Most of them have redshifts $\sim z_i$. Hence in calculating the average (or effective) scaling factor for $E_r(z_i)$, scaling factors R_js at and around S_j have to be given more weightage. This is accomplished by choosing the weights as given by the following equation.

$$W_{ij} = \left[\frac{I(z_i,S_j)}{n(S_j)}\right]^2 \qquad (2.17)$$

The next approximation to $E(z_i)$ is given by

$$E_{r+1}(z_i) = E_r(z_i)\frac{\sum_j R_j W_{ij}}{\sum_j W_{ij}} \qquad (2.18)$$

We have assumed that only sources with $P > P_c$ take part in evolution. This constraint is implemented by putting $E(z)=1$ in eq.(2.15) and by setting $W_{ij}=0$ for (z_i, S_j) pairs corresponding to $P \leq P_c$. The scheme for finding $E(z)$, thus reduces to one of iterative application of eq.(2.18). Robertson (1978) used a value of 4.5×10^{26} W $Hz^{-1} sr^{-1}$ for P_c. With an initial guess $E_1(z_i)=10i$, $i=1,2,...N$, convergence was obtained in about 15 iterations. He derived EF and redshift distributions for three types of LLFs which he refers to as (a) Standard LLF (b) Steep LLF and (c) Flat LLF. The important conclusions from Robertson's analysis can be summarized as follows:

1) The resulting EF is basically similar to the results of previous studies but, being a free-form function, it is able to take a more complex shape. It leads to a good fit to the observed counts. The evolution function is not very sensitive to moderate changes in LLF.

2) The predicted redshift distributions agree with the observational data available at high flux densities from identifications of 3CR sources. Considerably higher redshifts are predicted at low flux densities (0.1 to 10 Jy). The redshift distributions are sensitive to changes in LLF and only the redshift distributions derived with the standard LLF are in reasonable agreement with the observations.

The free-form analysis method (FFAM) is a simple and iterative method of solving for the EF. However, in this scheme, the LLF is assumed to be known. This seems to be one

of the drawbacks of the method. We have extended this scheme so that free-form evolution function can be derived starting from the observed luminosity distribution rather than the derived LLF. A discussion of this extension of the scheme and the results obtained is postponed to Section 2.5. In the next two sections we continue the discussion of different methods of deriving LLF and EF.

2.4.2. LLF and EF from Luminosity-Volume Test

The luminosity-volume test or V/V_m test is a method (Schmidt 1968; Rowan-Robinson 1968a) of testing whether the objects, such as QSOs or radio galaxies in certain kinds of samples have been drawn from a population with a uniform distribution in space. In our discussion of the test, we follow the procedure described by Schmidt. Suppose the sample of objects is complete i.e. all objects having flux densities greater than some limiting value S_m (at a particular wavelength) have been detected and the redshifts of all these objects are measured. We can calculate for each object in the sample the maximum redshift z_{max} at which the object would still belong to the sample (i.e. $S=S_{lim}$). If $V(z)$ is the volume of space within redshift z and $V(z_{max})=V_m$, then V/V_m is a measure of the position of the object within the volume V_m that is available to it within the sample limit. We have

$$\frac{V}{V_m} = \int_0^z dV(z) / \int_0^{z_{max}} dV(z) = \int_0^z H(z)dz / \int_0^{z_{max}} H(z)dz \qquad (2.19)$$

where the comoving volume element $dV(z)$ is written as $dV(z)=H(z)dz$. For a uniform distribution of sources, the mean value of V/V_m for all sources of a single luminosity class P , in the complete sample is given by

$$\left\langle \frac{V}{V_m} \right\rangle = \frac{\int_0^{z_{max}} (V/V_m)H(z)dz}{\int_0^{z_{max}} H(z)dz} = \frac{\int_0^{z_{max}} \left(\int_0^{z} H(z)dz\right)H(z)dz}{\left(\int_0^{z_{max}} H(z)dz\right)^2}$$

$$= \frac{\int_0^{z_{max}} \left[\left(\int_0^{z} H(z)dz\right)\frac{d}{dz}\left(\int_0^{z} H(z)dz\right)\right]dz}{\left(\int_0^{z_{max}} H(z)dz\right)^2}$$

$$= \frac{\frac{1}{2}\left(\int_0^{z_{max}} H(z)dz\right)^2}{\left(\int_0^{z_{max}} H(z)dz\right)^2} = \frac{1}{2}$$

The standard deviation is given by

$$\sigma^2(V/V_m) = \langle (V/V_m - \langle V/V_m \rangle)^2 \rangle$$

$$= \langle (V/V_m)^2 \rangle - \langle V/V_m \rangle^2$$

$$= \frac{\int_0^{z_{max}} (V/V_m)^2 H(z)dz}{\int_0^{z_{max}} H(z)dz} - 0.5^2$$

$$= \frac{\int_0^{z_{max}} [(\int_0^z H(z)dz)^2] H(z)dz}{(\int_0^{z_{max}} H(z)dz)^3} - 0.25$$

$$= \frac{\int_0^{z_{max}} [(\int_0^z H(z)dz)^2 \frac{d}{dz}(\int_0^z H(z)dz)]dz}{(\int_0^{z_{max}} H(z)dz)^3} - 0.25$$

This reduces to

$$\sigma^2(V/V_m) = \frac{\frac{1}{3}(\int_0^z H(z)dz)^3 \Big|_0^{z_{max}}}{(\int_0^{z_{max}} H(z)dz)^3} - 0.25 = \frac{1}{12}$$

Thus if the objects are drawn from a uniformly distributed population, then V/V_m should have a uniform distribution between 0 and 1 with mean 0.5 and standard deviation $\frac{1}{\sqrt{12}} \simeq 0.28$. For sufficiently large sample size, we can apply the central limit theorem and show that the probability distribution of

mean value of V/V_m for the sample can be approximated by a normal distribution with standard derivation $\sigma_m = \frac{\sigma}{\sqrt{N}}$ where N is the number of objects in the sample. Note that the method is independent of any luminosity variations among objects: V and V_m depend on luminosity but V/V_m does not.

An attractive feature of the V/V_m test is that it can be applied even if the objects in a sample are limited in two or more observables. For example, the complete sample of 3CR QSOs is defined by two limits. First, there is the radio flux density limit i.e. S_{178}=9 Jy. Secondly, there is an optical limit. This is because redshift determination is possible only at optical wavelengths and complete searches for QSOs have not been carried out to apparent magnitude $m_v \gtrsim 19$. The optical selection effects unavoidably play a role and as a result in some cases V_m is determined by the radio limit (S_{lim}) and in some others by the optical limit(m_{lim}). The mean value of V/V_m is still expected to be 0.5 for a uniform distribution of sources provided $V_m = \min[V_{m\ rad}, V_{m\ opt}]$ for each source and this makes the test applicable even when the sample is limited in more than one observables.

Many authors have used the V/V_m test in investigating the space distribution of QSOs (e.g. Schmidt 1968; Rowan-Robinson 1968a). Schmidt (1968) showed that for a complete sample of 33 3CR QSOs $< V/V_m >$ is 0.69. The results are not sensitive to the kind of the cosmological model adopted; for $q_o = 0.0$, $< V/V_m > = 0.75$ (in Steady State model V and V_m

refer to proper volumes). All these (for a summary see Schmidt 1977; Wills and Lynds 1978) values of $< V/V_m >$ are significantly above 0.5 implying a nonuniform space distribution of QSOs i.e. the results are incompatible with a Steady State model and with non-evolving luminosity function in the Friedmann models. Rowan-Robinson(1968b) and Petrosian (1969) showed that in certain Lemaitre world models the mean value of V/V_m is close to 0.5, consistent with a uniform space distribution of sources. However, it can be shown that the distribution is not uniform even in these models, if attention is restricted to the region of the model in which the flux density S decreases monotonically with redshift (Longair and Scheuer 1970).

A question that naturally arises is: in what way are the source counts and the V/V_m test related ? Longair and Scheuer (1970) investigated the relation between the two tests and showed that in the case of Static Euclidean Universe (i.e. $N(>S) \propto S^{-\beta}$) and only one flux-density limit, the mean value of V/V_m and the slope β are related in the following manner:

$$< V/V_m > = \frac{\beta}{\beta+1.5} \qquad (2.20)$$

In a Friedmann model the situation becomes more complicated and the exact equivalence breaks down. On the basis of explicit calculations for the Einstein-de Sitter model and some numerical experiments Longair and Scheuer (1970) showed that

the expected value of $< V/V_m >$ depends to some extent on the range of redshifts in which sources lie and on the cosmological model but not upon the detailed distribution of redshifts among the QSOs. This led them to conclude that, as compared with the counts of QSOs, the V/V_m test

i) adds an estimate $< z >$ of the sources in the sample

ii) allows incorporation of cosmological model so that the effects of high redshifts of QSOs are properly taken into account (for a further discussion of these and other related points see Carswell and Weymann 1971; Rees and Schmidt 1971; Lynds and Petrosian 1972).

The V/V_m test can also be used to determine the LLF and the EF, by following the procedure outlined below. Suppose that the space distribution of QSOs is found to be non-uniform; we can derive the EF, $E(z)$, by requiring that $\frac{V'}{V_m}$, where $V' = \int E(z)dV(z)$, has a uniform distribution between 0 and 1. Note, however, that the EF $E(z)$ cannot be determined uniquely. For example Schmidt (1970, 1972a) found that $E(z) \propto (1+z)^6$ and $E(z) \propto 10^{5\tau}$, where τ is the light-travel or look-back time expressed in terms of the age of the universe, give good fit to the 3CR data. Lynden-Bell (1971) has suggested a method of determining $E(z)$ from the V/V_m values. The method makes optimum use of redshift data available for radio and optically limited samples of QSOs. The derivation of LLF is also quite straight forward. Once we know $E(z)$, we can determine LLF just by summing $(V'_{max})^{-1}$ over all objects in the complete sample.

Schmidt (1970) has shown that it is possible to extend the above formalism to derive a Generalized Luminosity Function $\Phi(P_{rad}, P_{opt}, z, \alpha)$ where

P_{rad} = radio luminosity at 500 MHz in the source's frame of reference in WHz^{-1}.

P_{opt} = optical luminosity at 2500 Å in the source's frame of reference in WHz^{-1}

α = radio spectral index defined by $S(\nu) \propto \nu^{-\alpha}$

There is some evidence to believe that the z-dependent part of GLF i.e. $E(z)$, might depend on spectral index α . A detailed discussion of this point is given later. In this general case we can write

$$\Phi(P_{rad}, P_{opt}, z, \alpha) = E(z,\alpha)\rho(P_{opt}, P_{rad}, \alpha) \qquad (2.21)$$

To make further progress in the determination of the Multi-variate Luminosity Function (MLF), $\rho(P_{opt}, P_{rad}, \alpha)$, it is necessary to make some simplifying assumptions. For example, if spectral index α and P_{opt} and P_{rad} are independent, we can write

$$\rho(P_{opt}, P_{rad}, \alpha) = \rho_b(P_{opt}, P_{rad})\eta(\alpha) \qquad (2.22)$$

where $\eta(\alpha)$ = Spectral Index Function (SIF) and $\rho_b(P_{opt}, P_{rad})$ is the Bi-variate Luminosity Function (BLF). Schmidt (1970) noted that the observed redshift distributions of radio quasars and optically selected quasars at optical magnitude 18

appear identical and that it would be difficult to understand this result if the radio and optical power are treated as independent variables. To explain the result Schmidt proposed that P_{rad} appears in the luminosity function only through its ratio to P_{opt}, i.e.

$$\rho_b(P_{opt},P_{rad}) = \varphi(P_{opt})\,\Psi(R) \qquad (2.23)$$

where $R = P_{rad}/P_{opt}$

The function $\Psi(R)$ has been studied by many authors (e.g. Fanti and Perola 1977; Wills and Lynds 1978). On the basis of the above form for BLF, it is also possible to account for the peak in the optical magnitude distribution of 3CR quasars at 18.5 magnitude (Schmidt 1977). However, recently, the validity of the above factorization, in the region of low radio power has been questioned. From a study of optical identifications of background source survey, extending down to ~ 10 mJy, de Ruiter(1978) has inferred that:

a) the number of quasars decreases beyond m (blue magnitude) = 19 and possibly falls to zero at m ~ 22 or 23.

b) the quasar count log n(S,m<21.5) is remarkably flat between S_{1400} ~ 10 mJy and 100 mJy. He suggested that these observed features can be accounted for by factorizing the BLF in the following manner

$$\rho_b(P_{opt},P_{rad}) = \varphi(P_{opt})\varepsilon(P_{opt},P_{rad}) \qquad (2.24)$$

where $\int_0^\infty \varepsilon(P_{opt},P_{rad})dP_{rad}=1$ and $\varepsilon(P_{opt},P_{rad}) \longrightarrow \psi(R)$ at large P_{rad}. Further, de Ruiter, claims that the above modification of BLF is also able to explain the apparent discrepancy, noted by Fanti et al. (1973) and Fanti et al. (1977), between $\psi(R)$ as determined from radio selected and as determined from optically selected quasars. More optical observations of quasars with the radio flux density in the range 10 mJy-100mJy are clearly needed to throw further light on the nature of $\varepsilon(P_{opt},P_{rad})$ at low radio power. In Lynden-Bell's method (mentioned earlier) of determining EF using V/V_m test, the validity of eq.(2.23) is assumed. In view of the above discussion it is clear that it might be necessary to modify Lynden-Bell's method.

Several authors (e.g. Rowan-Robinson 1971; Schmidt 1972b) have investigated the luminosity function of radio galaxies using the V/V_m test. However, because of the small redshifts involved, the picture regarding the evolution of the LF is not very clear. There is some evidence to believe that V/V_m for radio galaxies depends on radio power i.e. $< V/V_m >$ increases with radio power and for $P_{178} \gtrsim 10^{25}$ WHz^{-1}, $<V/V_m>$ is significantly higher than 0.5 which is the value expected in a static Euclidean universe with uniform distribution of objects in space. The results indicate a strong evolution for the more powerful radio galaxies (de Ruiter 1978). This view is supported be Grueff and Vigotti's (1977) analysis of identified B2 radio sources. They noted a sharp

increase in the percentage of identification with galaxies just beyond the plate limit of the red Palomar Sky Survey. They pointed out that this increase is larger than expected on the basis of Schmidt's (1972b) model and proposed an evolution model for radio sources in which quasars and radio galaxies are linked in a single evolutionary sequence. The most interesting features of this model are its simplicity, the small number of independent parameters involved and a unification of luminosity functions for quasars and for radio galaxies. This is in contrast to the models proposed earlier, where two luminosity functions, one for quasars and the other for radiogalaxies, are employed. The model is shown to produce excellent agreement with the available observational data. Further investigations along these lines might prove to be very fruitful.

2.4.3 Derivation of LLF and EF from Angular Size Counts

From investigations of the cosmological implications of the observed angular sizes of radio sources, Kapahi (1975a, 1975b) derived several important results regarding Local Luminosity Function (LLF) and evolutionary effects in radio source populations. A summary of these investigations is given below.

The angular size counts or the log N-log θ relation (where N is the number of sources with an angular size greater than a value θ in a radio survey complete to a certain flux density) depends on the world model, the radio

luminosity function (RLF) and the distribution of physical sizes of radio sources (radio size function RSF). The log N-log θ relation is constructed for 3CR complete sample. A subsample within $\theta > 125''$ arc consists of essentially of radio galaxies of small redshifts with luminosities in the range of about $10^{23} \lesssim P_{178} \lesssim 10^{26}$ W $Hz^{-1}sr^{-1}$ and because of the small values of z , the slope of the log N-log θ relation for this subsample depends mainly on the radio luminosity function and is practically independent of the cosmological model and the radio size function. Any evolutionary effects in the comoving space density or overall sizes of radio sources with cosmological epoch should also be relatively unimportant, because of small z. Kapahi made use of this fact and showed that LLF of radiogalaxies in the range of about $10^{23} \leq P_{178} \leq 10^{26}$ W $Hz^{-1}sr^{-1}$ is given by

$$\rho(P,z=0) \propto P^{-2.1\pm0.15} \qquad (2.25)$$

This is in good agreement with the conventional determinations of the luminosity function from measured redshifts and optical magnitudes of identified radio galaxies. An attractive feature of this method is that it provides an independent determination of the LLF without the explicit use of redshift data. This is so because in the log N-log θ relation the redshift information for radio sources has been used only to derive the radio size function which, in any case, is not very important in determining the slope of the log N-log θ relation at large θ. The knowledge of the range of redshifts involved, however, is

important in order to determine the range of luminosities to which the LLF refers. A drawback that this method shares with other methods of determining LLF is that it cannot be used to derive the LLF for the more luminous sources without the knowledge of the cosmological model and the evolutionary properties of the radio source population.

Kapahi (1975a; 1975b) also calculated the expected θ_{med} vs. flux density relation for a uniform distribution of sources in space and compared it with the observed θ_{med} vs. S relation (Swarup 1975) derived from the 3CR, the All-Sky and the Ooty occultation surveys. Some of the important conclusions that emerged from Kapahi's investigations are as follows:

1) The observed θ_{med} vs. S relation over a flux density range of $\sim$ 300:1 does not agree with the predictions of reasonable world models for any LLF and provides strong evidence for evolutionary effects in source properties. The data also suggest that evolutionary effects are more important than the geometric differences between various world models. The angular-size data cannot be explained in the Steady State model and this conclusion holds true even if the QSOs are excluded from the analysis. Furthermore, the angular-size data and the prediction of Steady State theory remain incompatible even if a local deficiency of strong sources is postulated.

2) It is not possible to explain the angular size data without recourse to evolution both in the space density (and/or luminosity) and in the overall physical sizes of radio sources.

The main features of the evolutionary scheme which fits the data in the Einstein-de Sitter world model are:

a) For luminosities $P_{178} \gtrsim 10^{26}$ W $Hz^{-1}sr^{-1}$, the LLF steepens considerably and the comoving space density rises with increasing redshift as $\sim (1+z)^{5.5}$. The form of LLF is similar to that inferred from the log N-log S data(e.g.Longair 1971). The evolution function derived from angular-size data is also in general agreement with the EF estimated from log N-log S data (Longair 1966; Doroshkevich, Longair and Zeldovich 1970) or from the V/V_m test for quasars (Schmidt 1968).

b) The overall physical sizes of radio sources change with redshift roughly as $(1+z)^{-1}$. This is similar to the type of evolution required to explain the observed θ-z relation for QSOs (e.g. Wardle and Miley 1974).

Recently, Narlikar and Chitre (1977) claimed that with the presently available angular size data it is not possible to distinguish between evolutionary and non-evolutionary models. They claimed further that a non-evolutionary model, in which there is a correlation between radio luminosity and linear size is not inconsistent with the data. However, on the basis of a more detailed consideration of the available data on the source counts and angular size counts, Subrahmanya (1977) concluded that (a) the Steady State model cannot be reconciled with the observations and (b) the angular size counts provide an independent evidence for the evolution of radio sources with cosmic epoch, thus supporting Kapahi's (1975a, 1975b) conclusions.

2.5 Extended Free-Form Analysis of the Cosmological Evolution of Radio Sources

In the Free-Form Analysis scheme outlined in Section 2.4.1, a Local Luminosity Function was assumed together with a turn-on luminosity P_c above which the source density evolves and the EF was then derived without imposing any restrictions on its form. However, as emphasized earlier, the determination of LLF requires the knowledge of EF i.e. the derivations of LLF and EF are coupled and one cannot be determined without the knowledge of the other one. A better approach, therefore, would be to use the observed luminosity distribution along with source counts n(S) and determine both LLF and EF in a self-consistent manner. Such an approach is described below.

Consider the following expressions for LLF and source counts

$$\rho(P,z=o) = n(P)/\int_o^{z^*} F(P,z)dz \qquad (2.26)$$

and

$$n(S) \propto \int_o^{\infty} \rho(P=S\ D^2(1+z)^{\alpha-1},z=o)F(P=S\ D^2(1+z)^{\alpha-1})$$
$$D^2(1+z)^{\alpha-1}dV(z) \qquad (2.27)$$

where $z^*=z(P,S_o)$. Assume, as before, $F(P,z)=E(z)$ for $P\geq P_c$ and $F(P,z)=1$ for $P < P_c$. With the substitutions $dV(z)=f(z)dz$ and $\zeta = \log z$, the above equations reduce to

$$\rho(P,z=o)=n(P)/\int_{o}^{Z^{*}} E(z)zf(z)dZ \qquad (2.28)$$

and

$$n(S) \propto \int_{-\infty}^{\infty} \rho(P=SD^{2}(1+z)^{\alpha-1},z=o)E(z)f(z)D^{2}(1+z)^{\alpha-1}z\ dZ$$

$$\propto \int_{-\infty}^{\infty} \rho(P=SD^{2}(1+z)^{\alpha-1},z=o)E(z)zH(z)dZ \qquad (2.29)$$

where $H(z)=f(z)D^{2}(1+z)^{\alpha-1}$. For the purpose of integration we divide the redshift range into (N-1) equal logarithmic intervals. The source counts are specified at S_j's, j=1,2,...M. The above equations can be written in the following discretized form;

$$\rho(P,z=o) = \frac{n(P)}{\sum_{i=1}^{N'} E(z_i)z_i f(z_i)\Delta Z_i} \qquad (2.30)$$

and

$$n(S_j) = \sum_{i=1}^{N} \rho(P,z=o)E(z_i)z_i H(z_i)\Delta Z_i \qquad (2.31)$$

where N' is chosen in the following manner:

We find j such that $Z_j<Z^{*}<Z_{j+1}$ and then set N'=j+1 and replace Z_{j+1} by Z^{*}. Note that in eq.(2.30) the value of $E(Z^{*})$ is required. This value is obtained using quadratic interpolation. The determination of LLF and EF proceeds along the following lines:

STEPS:

1) The choice of the observed n(P) distribution: we have considered the 408 MHz Luminosity distribution. This is

well-defined for $S_{408} > 10$ Jy. The sample contains 87 radio sources. About 90 % are steep-spectrum sources (Wall, Pearson and Longair 1977).

2) Specification of source counts at different S_j's, $j=1,2,...M$: For this purpose we considered the source counts at 408 MHz given by Pearson and Kus (1978). From the log $n'_n(S)$ value log S (i.e. source counts in normalized differential form), plot we specified the values of the normalized differential counts $n'_n(S_j)$, at S_j's where $j=1,2,3,...M$.

3) Initial guess for E(z): Our choice of $E_1(z_i) = \exp[8(1-(1+z_i)^{-1.5}]$ as initial guess was guided by the fact that in general the exponential evolution function is known to give a good fit to the data. However, the method is not very sensitive to the choice of the initial guess provided that the initial guess is roughly similar to a sufficiently fast rising (with redshift) function.

4) The choice of the world model: the geometric differences between world models are small compared to the gross effects of evolution. Hence the choice of the world model is not crucial. We have done our analysis within the frame work of the Einstein-de Sitter model.

5) With the initial guess for E(z) given in (3), we determined the first approximation to LLF, using eq.(2.30). The ith approximation to LLF is denoted by $\rho_i(P,z=o)$. Thus $\rho_1(P,z=o)$ is the first approximation to LLF.

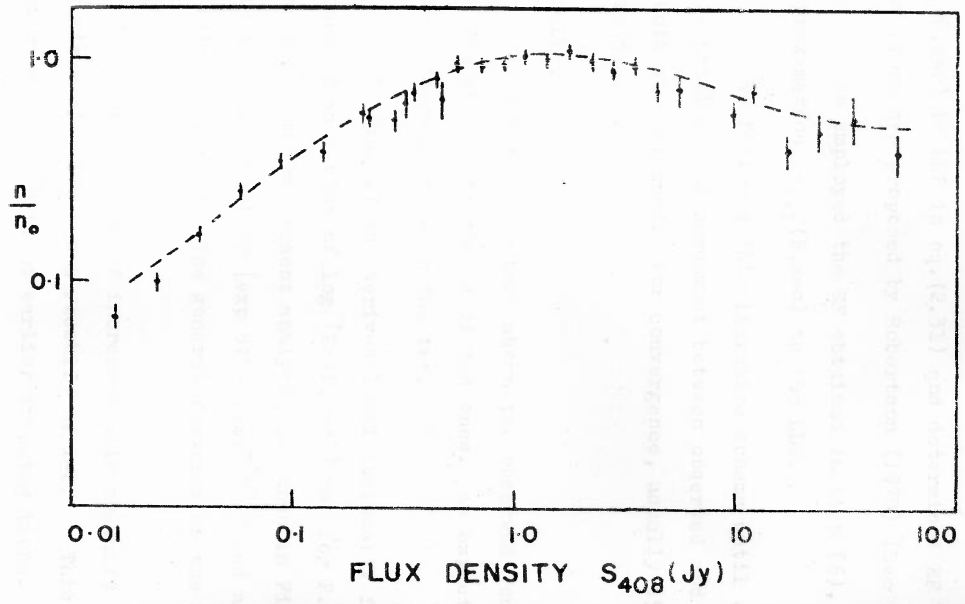

FIG. 2·6 COMPARISON OF THE OBSERVED (PEARSON & KUS 1978 AND REFERENCES THEREIN) AND FITTED COUNTS AT 408 MHz. THE DASHED CURVE REPRESENTS COUNTS DERIVED FROM FREE-FORM ANALYSIS.

6) We used this ith (in the beginning i = 1) approximation $\rho_i(P,z=o)$ to LLF in eq.(2.31) and determined EF by following the procedure proposed by Robertson (1978) (See Section 2.4.1).

7) We employed the EF obtained in Step (6), to derive next approximation $\rho_{i+1}(P,z=o)$ to the LLF.

8) We followed this iterative scheme until convergence - i.e. until a good agreement between observed and predicted counts was obtained. For convergence, usually 15-20 iterations were needed.

RESULTS:

In Fig.2.6 we have shown the observed source counts at 408 MHz along with the predicted ones. As expected, there is a close agreement between the two.

In Fig.2.7 the derived local luminosity function is presented as a plot of log $[P\rho(P,z=o)]$ vs. log P. The EF obtained from the present analysis is shown in Fig.2.8 along with an exponential EF $[\exp 8\{1-(1+z)^{-1.5}\}]$ and a power law EF $[(1+z)^{\beta}, \beta \sim 6]$. The general features of the free-form EF are:

i) Initially the EF increases with redshift z and reaches a maximum of $\sim$ 1000 at a redshift of 1-2. This is in agreement with the results of earlier investigations.

ii) The EF saturates or becomes flat after $z \sim 3.5$. However, it is not clear whether a cut-off really is needed or not.

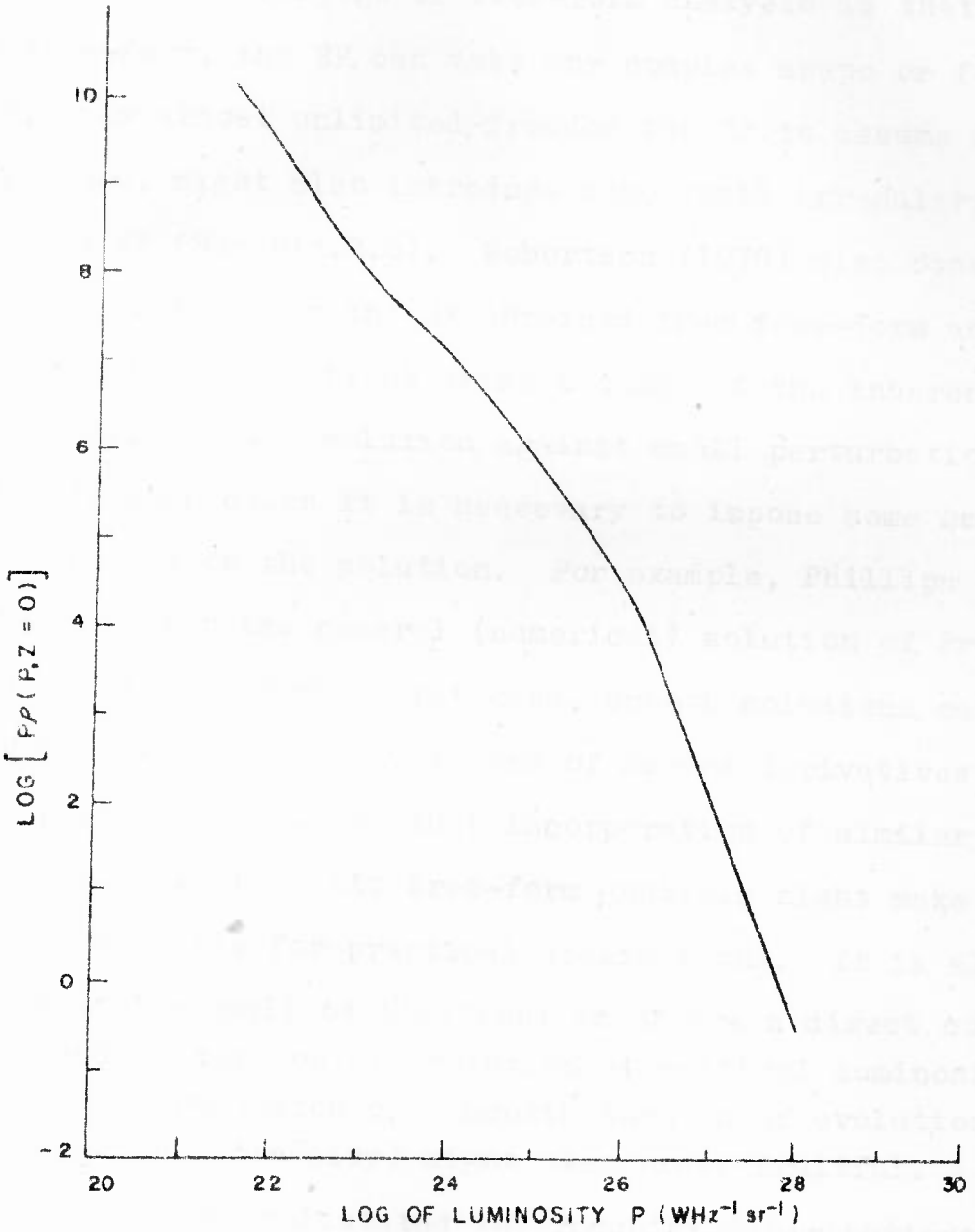

FIG. 2·7 THE LOCAL LUMINOSITY FUNCTION AT 408 MHz. (DETERMINED FROM FREE-FORM ANALYSIS). THE LOGARITHM OF $P\rho$ (P, Z = 0) IS PLOTTED AGAINST LOG P_{408}.

iii) The main advantage of free-form analysis is that because of its free-form, the EF can take any complex shape or form. However, this almost unlimited freedom for EF to assume any complex shape, might also introduce some small irregularities in the derived EF (See Fig.2.8). Robertson (1978) also observed similar oscillations in the EF obtained from free-form analysis. Such unphysical oscillations arise because of the inherent unstable nature of the solution against small perturbations in the data. In such cases it is necessary to impose some smoothness constraints on the solution. For example, Phillips (1962) suggested that for the general (numerical) solution of Fredholm integral equations of the First kind, smooth solutions can be obtained by minimising the variance of second derivatives of the solution vector. We believe that incorporation of similar smoothness constraints into free-form analysis might make the method more suitable for practical applications. It is also possible that the small oscillations in EF are a direct consequence of sudden turn on of evolution at critical luminosity P_c. In that case introduction of a smooth turn on of evolution (over a range in luminosity) might also prove fruitful.

We have also calculated the redshift distributions using the derived LLF and EF. In Fig.2.9, we have plotted $\langle \log z(S) \rangle$ versus $\log S_{408}$. The distribution is similar to the one given by Robertson (1978). We have not attempted any comparison with the observed redshift distributions, because our main aim was to see whether one can extend the free-form analysis scheme, rather than derive a model to account for the observations in detail.

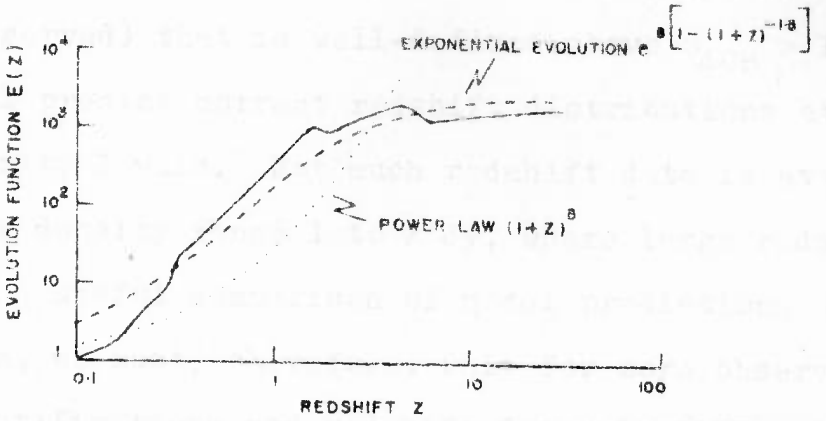

FIG. 2·8 THE EVOLUTION FUNCTION E (Z), AS DETERMINED FROM FREE-FORM ANALYSIS SCHEME IS PLOTTED AGAINST REDSHIFT. FOR COMPARISON POWER LAW (DOTTED CURVE) AND EXPONENTIAL LAW (DASHED CURVE) OF EVOLUTION ARE ALSO SHOWN.

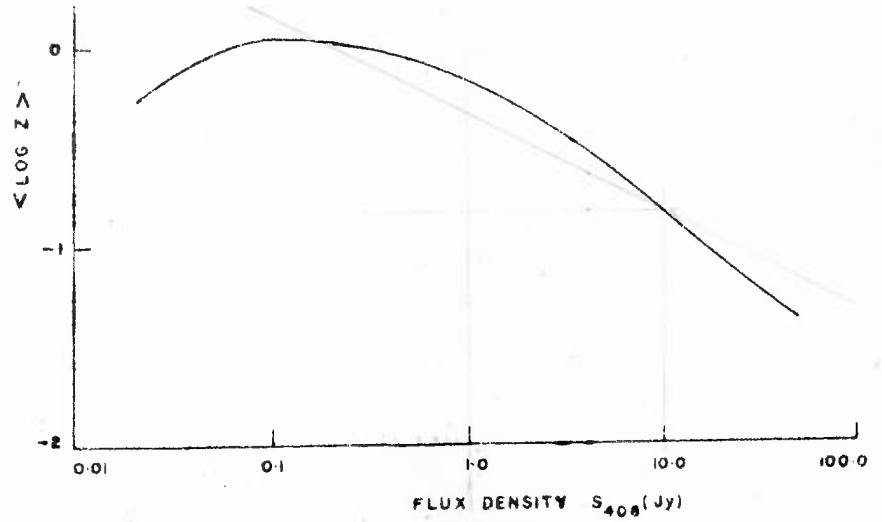

FIG. 2·9 THE AVERAGE OF THE LOGARITHM OF REDSHIFT, AS A FUNCTION OF FLUX DENSITY, FOR THE LOCAL LUMINOSITY FUNCTION AND THE EVOLUTION FUNCTION SHOWN IN FIGURES 2·7 & 2·8 RESPECTIVELY.

Moreover, since we started with a luminosity distribution (observed) that is well-defined above $S_{408} > 10$ Jy, the model will predict correct redshift distributions at such high flux density levels. Not much redshift data is available in the flux density range 1 to 2 Jy, where large redshift are predicted. For a useful comparison of model predictions and observational data, we must, therefore, wait for more observations regarding identifications and redshift determinations at low flux densities.

"It is a capital mistake to theorize before one has data"

Sir Arthur Conan Doyle

'A Scandal in Bohemia' from

The Adventures of Sherlock Holmes.

CHAPTER 3

RADIO SOURCE COUNTS AND SPECTRAL INDEX DISTRIBUTIONS: Summary of Observations

3.1 Introduction

So far in our discussion we have assumed that all the radio sources have the same spectral index ~ 0.75 i.e. the spectral index distribution is characterized by a delta function $\delta(\alpha-\alpha_o)$ where $\alpha_o = 0.75$. However, observations of radio sources made at several frequencies show a finite spread in the spectral index distribution. The spectral indices of radio sources vary over a range ~ -1.5 to 1.5. Moreover, if the spectral index distribution was a delta function, then the source counts at different frequencies would have been the same except for a scale factor. But the observed source counts at different frequencies exhibit quite different features. This is expected, because, as a result of the finite width of spectral index distribution, the surveys at low and high frequencies select sources belonging to different spectral classes. Observations also indicate that spectral index is related to other properties of a source such as luminosity and angular size (e.g. Kellermann, Pauliny-Toth and Williams 1969; Fanaroff and Longair 1972). Most of the compact radio sources which are believed to be in early stages of evolution have flat spectra whereas the extended sources that are presumably in later stages of evolution have mostly steep spectra. In

view of these properties, the spectral indices are likely to provide information regarding origin, evolution and age of radio sources. Moreover, for a given luminosity and in a flux density limited sample, sources with flat-spectra are seen to larger redshifts than the steep-spectrum sources. This property can be made use of in gaining information about the space distribution of radio sources. Also, the spectral indices can be measured for a large number of sources without much difficulty, making them suitable for use in any statistical studies of radio source properties.

It is thus clear that we must make use of information regarding spectral indices of radio sources either in studying the physical evolution of radio sources or in investigating the cosmological evolution of radio sources. In this chapter, we give a summary of the results that emerge from analysis of source counts and spectral index distributions. The interpretation of these observational results and their implications are discussed in the next chapter.

Before discussing observations, we will give a summary of definitions and notations used in our discussion. Our definitions and notations are similar to those of van der Laan (1969). The flux density at frequency ν is denoted by $S(\nu)$. The spectral index α is defined by the relation $S(\nu) \propto \nu^{-\alpha}$. The radio sources with $\alpha \leq 0.5$ are called the flat-spectrum sources and those with $\alpha > 0.5$ are called the steep-spectrum sources. Note that in general α may be a function of frequency

and for this reason it is possible to define different types of spectral indices. For example the two-point spectral index $\alpha(\nu_1, \nu_2)$ is determined by the following relation,

$$\alpha(\nu_1, \nu_2) = -\log [S(\nu_2)/S(\nu_1)]/\log(\nu_2/\nu_1) \qquad (3.1)$$

On the other hand, the spectral index $\alpha(\nu)$ at a frequency ν is defined by

$$\alpha(\nu) = -d \log S(\nu)/d \log \nu \qquad (3.2)$$

For a source with a straight spectrum $\alpha(\nu_1, \nu_2) = \alpha(\nu)$.

Consider a complete survey $CS(\nu_i, S_{lim})$ in which all the sources above a limiting flux density S_{lim} at frequency ν_i are detected. Suppose that the two-point spectral indices for all the sources in the survey have been determined by observing the sources at frequencies ν_j and ν_m. The spectral index distribution in integral form is the distribution $g^{\nu_i}_{S_{lim}}[\alpha(\nu_m, \nu_j)]$ of the spectral index $\alpha(\nu_m, \nu_j)$ among the sources of a complete sample $CS(\nu_i, S_{lim})$. The spectral index distribution $f^{\nu_i}_{S(\nu_i)}[\alpha(\nu_m, \nu_j)]$ in differential form is defined by

$$g^{\nu_i}_{S_{lim}}[\alpha(\nu_m, \nu_j)] = \int_{S_{lim}}^{\infty} f^{\nu_i}_{S(\nu_i)}[\alpha(\nu_m, \nu_j)]\, dS(\nu_i) \qquad (3.3)$$

Also note that the integral source counts at frequency ν_i are given by

$$N(>S, \nu_i) = \int_{-\infty}^{\infty} g^{\nu_i}_{S_{lim}}[\alpha(\nu_m, \nu_j)]\, d\alpha(\nu_m, \nu_j) \qquad (3.4)$$

and the differential counts by,

$$n(S,\nu_i) = \int_{-\infty}^{\infty} \int_{S(\nu_i)}^{\nu_i} [\alpha(\nu_m,\nu_j)]\, d\alpha(\nu_m,\nu_j) \qquad (3.5)$$

Sometimes it is convenient to introduce the concept of the 'effective spectral index'. The 'effective spectral index' is defined in the following manner.

Let $n_1(S_1,\nu_1) \int_{S_1(\nu_1)}^{\nu_1} [\alpha(\nu_1,\nu_2)]\, dS_1\, d\alpha(\nu_1,\nu_2)$ be the number of sources, at frequency ν_1, with their flux densities in the range $S_1(\nu_1)$ to $S_1(\nu_1)+dS_1(\nu_1)$ and with spectral indices in the range $\alpha(\nu_1,\nu_2)$ to $\alpha(\nu_1,\nu_2)+d\alpha(\nu_1,\nu_2)$. Let $S_2(\nu_2)$ to $S_2(\nu_2)+dS_2(\nu_2)$ be the corresponding flux density range, at frequency ν_2, in which these sources will be observed. From this it follows that,

$$n_1(S_1,\nu_1) \int_{S_1(\nu_1)}^{\nu_1} [\alpha(\nu_1,\nu_2)]\, dS_1(\nu_1)\, d\alpha(\nu_1,\nu_2)$$

$$= n_2(S_2,\nu_2) \int_{S_2(\nu_2)}^{\nu_2} [\alpha(\nu_1,\nu_2)]\, dS_2(\nu_2)\, d\alpha(\nu_1,\nu_2) \qquad (3.6)$$

Since $S_2(\nu_2) = S_1(\nu_1)(\nu_1/\nu_2)^{\alpha(\nu_1,\nu_2)}$, we can write

$$dS_2(\nu_2) = dS_1(\nu_1)(\nu_1/\nu_2)^{\alpha(\nu_1,\nu_2)} \qquad (3.7)$$

Let us now assume that all these sources have the same spectral index α_{eff}. This is equivalent to writing,

$$f^{\nu_1}_{S_1(\nu_1)}[\alpha(\nu_1,\nu_2)] = \delta[\alpha(\nu_1,\nu_2)-\alpha_{eff}]$$

$$= f^{\nu_2}_{S_2(\nu_2)}[\alpha(\nu_1,\nu_2)] \qquad (3.8)$$

Making use of eqs. (3.7) and (3.8) in eq.(3.6) and integrating we can easily show that

$$n_1(S_1,\nu_1) = n_2[S_1(\nu_1/\nu_2)^{\alpha_{eff}},\nu_2]\,(\nu_1/\nu_2)^{\alpha_{eff}} \qquad (3.9)$$

The fraction of flat-spectrum sources $F(\nu_m,\nu_j,S_1(\nu_i), S_2(\nu_i)]$ for the sources with flux densities in the range $S_1(\nu_i)$ to $S_2(\nu_i)$ is given by,

$$F[\nu_m,\nu_j,S_1(\nu_i),S_2(\nu_i)] = \frac{\int_{S_1}^{S_2} dS(\nu_i)\int_{-\infty}^{0.5} f^{\nu_i}_{S(\nu_i)}[\alpha(\nu_m,\nu_j)]d\alpha(\nu_m,\nu_j)}{\int_{S_1}^{S_2} dS(\nu_i)\int_{-\infty}^{\infty} f^{\nu_i}_{S(\nu_i)}[\alpha(\nu_m,\nu_j)]d\alpha(\nu_m,\nu_j)} \qquad (3.10)$$

Two more parameters that are useful in studying the spectral index distributions are (i) the median spectral index (MSI) $\alpha_{med}[\nu_m,\nu_j]$ and (ii) the median spectral index $\alpha_{n\ med}[\nu_m,\nu_j]$

for the normal component of the spectral index distribution i.e. sources for which $\alpha(\nu_m, \nu_j) > 0.5$ and are defined so that

$$\int_{-\infty}^{\alpha_{med}(\nu_m,\nu_j)} d\alpha(\nu_m,\nu_j) \int_{S_1(\nu_i)}^{S_2(\nu_i)} f_{S(\nu_i)}^{\nu_i} [\alpha(\nu_m,\nu_j)]dS(\nu_i)$$

$$= \int_{\alpha_{med}(\nu_m,\nu_j)}^{\infty} d\alpha(\nu_m,\nu_j) \int_{S_1(\nu_i)}^{S_2(\nu_i)} f_{S(\nu_i)}^{\nu_i} [\alpha(\nu_m,\nu_j)]dS(\nu_i) \quad (3.11)$$

and

$$\int_{\alpha(\nu_m,\nu_j)>0.5}^{\alpha_{n\ med}(\nu_m,\nu_j)} d\alpha(\nu_m,\nu_j) \int_{S_1(\nu_i)}^{S_2(\nu_i)} f_{S(\nu_i)}^{\nu_i} [\alpha(\nu_m,\nu_j)]dS(\nu_i)$$

$$= \int_{\alpha_{n\ med}(\nu_m,\nu_j)}^{\infty} d\alpha(\nu_m,\nu_j) \int_{S_1(\nu_i)}^{S_2(\nu_i)} f_{S(\nu_i)}^{\nu_i} [\alpha(\nu_m,\nu_j)]dS(\nu_i) \quad (3.12)$$

3.2 Source Counts at Different Frequencies

In the last few years, there has been considerable progress in the observational aspects of radio source counts. The synthesis arrays at Westerbork and Cambridge are mapping more and more area of the sky to mJy (1 mJy = 10^{-3} Jy) flux densities at frequencies of 408, 610, 1400 and 5000 MHz(e.g. Katgert 1975; Pearson and Kus 1978). The Molonglo (e.g. Davies, Little and Mills 1973; Sutton et al. 1974;

Robertson 1977a, 1977b) and Bologna (Colla et al. 1970, 1972, 1973) surveys now give fairly well-defined counts at 408 MHz, while the Greenbank (e.g. Maslowski 1972; Machalski 1978a), the Cambridge 5C (Pearson and Kus 1978) and Westerbork (Katgert 1977; Willis et al. 1976, 1977) surveys provide data for number counts at 1400 MHz. The source counts at 2700 MHz are derived from the Parkes 2.7 GHz survey (covers an area of 7.36 sr and contains ~ 7500 sources) and from the background deflection analysis i.e. P(D) analysis of the Parkes data (Wall and Cooke 1975). At 5000 MHz the NRAO surveys (Kellermann, Pauliny-Toth and Davis 1968; Davis 1971; Pauliny-Toth et al. 1972; Pauliny-Toth et al. 1978a) are now supplemented by deep 4.85 GHz survey at Bonn (Pauliny-Toth et al. 1978b). These surveys have strengthened the observational basis for source counts and have provided fairly well-defined log n - log S relations at frequencies of 408, 1400, 2700 and 5000 MHz, covering a wide range (10^{-2} Jy to 10^{2} Jy) in flux density. These counts are great improvement over previous ones. This availability of well-defined source counts at many different frequencies has led to a general agreement regarding the observational features (e.g. Longair 1974; Jauncey 1975). Here we give a summary of the principal features of the n(S) relations that emerge from an analysis of these observations.

i) There is a deficit of sources at high flux densities. This is inferred from the observed steep slope (>2.5) of the log n-log S relation in the high flux density region. However,

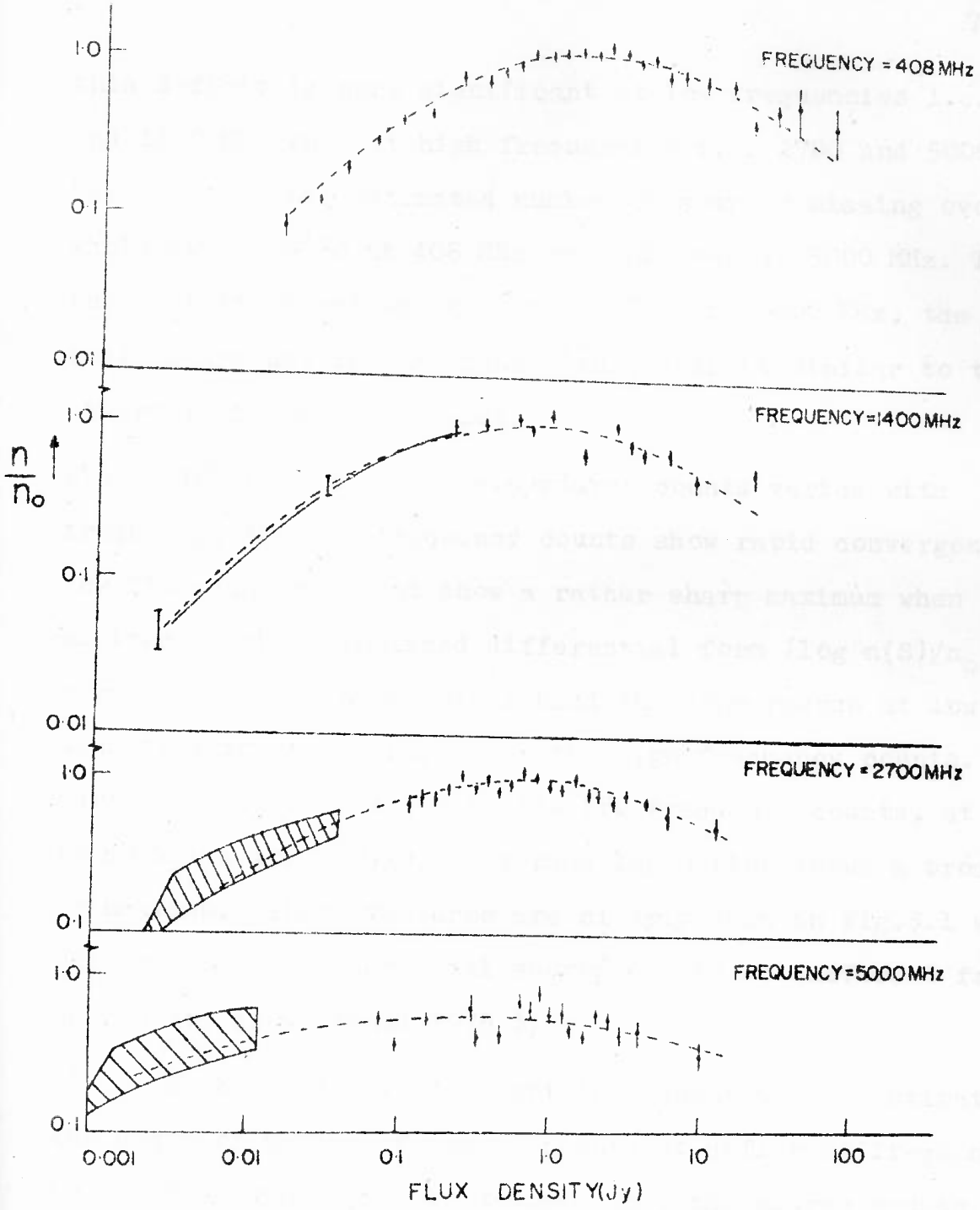

FIG 3·1 FREQUENCY DEPENDENCE OF RADIO SOURCE COUNTS. THE OBSERVED COUNTS AT DIFFERENT FREQUENCIES ARE PLOTTED IN RELATIVE DIFFERENTIAL FORM (SEE WALL 1978 AND REFERENCES THEREIN). THE VERTICAL NORMALIZATION IS ARBITRARY. THE DASHED LINES REPRESENT THE ADOPTED FITS (SEE TEXT)

this deficit is more significant at low frequencies i.e. 408 and 1400 MHz than at high frequencies i.e. 2700 and 5000 MHz. For example, the estimated number of sources missing over the whole sky is ~250 at 408 MHz and only ~50 at 5000 MHz. Though the deficit is not so evident at 2700 and 5000 MHz, the observations are not inconsistent with a deficit similar to that observed at low frequencies.

ii) The form of the radio source counts varies with frequency; the low frequency counts show rapid convergence at low flux densities and show a rather sharp maximum when plotted in the normalized differential form (log $n(S)/n_o(S)$ versus log S). On the other hand the convergence at low flux densities is not so rapid for the high frequency counts. Furthermore, in contrast to the low frequency counts, at high frequencies log $n(S)/n_o(S)$ versus log S plot shows a broad top or maximum. These features are clearly seen in Fig.3.1 where the normalized differential source counts at different frequencies are shown (Wall 1978).

We have attempted to obtain a quantitative estimate of the width of maxima of source counts at different frequencies, in the following way. We assumed that the source counts at each frequency can be represented adequately by an equation of the form $n(S)/n_o(S) \propto S^{-x-y\ln S}$ (Willis et al. 1977). The values of the parameters x and y as estimated by a least-squares analysis are given in Table 3.1. It can be shown that '1/e width' for log $n(S)/n_o(S)$ versus log S curve is given by

TABLE 3.1 : The Parameters of Normalized Differential Counts at Different Frequencies

Frequency (in MHz)	x	y	The ratio $\frac{SR}{SL}=e^{2/\sqrt{y}}$
408	-0.119	0.116	350
1400	0.08	0.105	480
2700	0.098	0.086	900
5000	0.075	0.033	60,000

$$\ln W = \ln S_R - \ln S_L = 2/\sqrt{y} \qquad (3.13)$$

where S_L and S_R are flux densities at which $n(S)/n_o(S)$ has dropped by a factor 'e' from the peak value. From eq.(3.13) we get $W = S_R/S_L = e^{2/\sqrt{y}}$. The values of W for the source counts at different frequencies are also given in Table 3.1. It is seen that the width W increases fairly rapidly with increasing frequency (see also, Fomalont, Bridle and Davis 1974; Wall 1978).

iii) At high frequencies, the flat-spectrum sources contribute significantly to the source counts; at low frequencies the contribution of flat-spectrum sources to the source counts is small. In addition at high frequencies pronounced variations are observed in the spectral index distribution with flux density: for example, at the highest flux density levels the fraction of flat-spectrum sources increases with decreasing flux density but for low flux densities there is a decrease in this fraction. At low frequencies such variations are much smaller. These points are discussed in detail in the next section.

3.3 Spectral Index Distributions

There are two important features to be looked for in the spectral index distributions of radio sources. First is the difference in spectral index distributions for samples complete at the same frequency but to different depths i.e. we can study the variation

TABLE 3.2 : Features of the Spectral Index Distribution $\frac{408}{S(408)} f [\alpha(408,5000)]$

(Pauliny-Toth and Kellermann,1972a)

Flux density S at 408 MHz (Jy)	Median spectral index $\alpha_{med}(408,5000)$	Fraction of flat spectrum sources F(408,5000)
S > 11.8	0.75±0.02	0.10
11.8 > S > 8.7	0.80±0.03	0.06
8.7 > S > 6.9	0.83±0.03	0.10
6.8 > S > 4.1	0.83±0.03	0.06
4.0 > S > 2.21	0.82±0.03	0.15
2.19> S > 0.89	0.83±0.02	0.10
0.86> S > 0.48	0.78±0.03	0.13

of $f^{\nu_i}_{S(\nu_i)}[\alpha(\nu_m,\nu_j)]$ with $S(\nu_i)$. When the sample size is small it might be more meaningful, from the statistical point of view, to study the dependence of $g^{\nu_i}_{S_{lim}}[\alpha(\nu_m,\nu_j)]$ on S_{lim}.

The second feature of the spectral index distribution that we can study is the difference in distributions for samples complete at different frequencies but at comparable depths i.e. we can look for the dependence of $f^{\nu_i}_{S(\nu_i)}[\alpha(\nu_m,\nu_j)]$ or $g^{\nu_i}_{S_{lim}}[\alpha(\nu_m,\nu_j)]$ on frequency ν_i. The main results that follow from investigations of samples selected at different frequencies are discussed below.

3.3.1 The Spectral Index Distribution at 408 MHz

Several authors have studied the spectral index distribution for sources selected at 408 MHz. Pauliny-Toth and Kellermann (1972a) considered the distribution of spectral index $\alpha(408,5000)$ for a sample containing ~ 400 sources selected at 408 MHz and determined the values of median spectral index $\alpha_{med}[408,5000]$ for different flux density ranges. They discussed also the variation in the fraction of flat-spectrum sources $F[408,5000]$ with $S(408)$. From the results (summarized in Table 3.2) of these investigations, Pauliny-Toth and Kellermann concluded that there is no significant change in $f^{408}_{S(408)}[\alpha(408,5000)]$ with $S(408)$. Using distribution of spectral index $\alpha(178,1420)$ for sources selected at 408 MHz, Willson (1972b) estimated the values of mean spectral

TABLE 3.3 : Parameters of $f_{S(408)}^{408}$ [$\alpha(178,1420)$]

(Wilson 1972b)

Flux density at 408 MHz (Jy)	Mean spectral index $\bar{\alpha}(178,1420)$
$S \geq 3.0$	0.65 ± 0.04
$3.0 > S \geq 1.75$	0.60 ± 0.03
$1.75 > S \geq 1.25$	0.70 ± 0.04
$1.25 > S \geq 1.0$	0.68 ± 0.04
$S \geq 1.0$	0.656 ± 0.019

index $\bar{\alpha}(178,1420)$ in different flux density intervals (see Table 3.3) and reached similar conclusions.

However, the investigations of Murdoch (1976) have given somewhat different results. In his investigations Murdoch considered a 'weak source sample' and a 'strong source sample' both selected at 408 MHz. The weak source sample contains sources from the Molonglo MC2 and MC3 surveys (Sutton et al. 1974). The 'strong source sample' consists of all the sources from an all-sky catalogue of strong sources (Robertson 1973). A comparison of $\bar{\alpha}(408,2695)$ for these samples (see Table 3.4) led Murdoch to suggest that the mean spectral index increases with decreasing flux density.

The nature of spectral index distribution in the flux density range S(408)=0.1Jy to 0.03 Jy has been investigated by Katgert(1976, 1977). Katgert derived the distribution of spectral index $\alpha(408, 1415)$, for a source sample selected at 408 MHz by making use of the data from the third 1415 MHz Westerbork survey and 5C2 survey at 408 MHz. He used the spectral index distribution thus derived along with the spectral index distribution derived from a sample complete down to 5.5 Jy taken from the Bologna 408 MHz survey, to study possible dependence of spectral index distribution on flux density. The essential features of these distributions are given in Table 3.5. On the basis of these studies Katgert suggested that:

i) There appears to be an increase in the average spectral index $\bar{\alpha}(408,1415)$ of 0.09 ± 0.07 on lowering the completeness

TABLE 3.4 : The Spectral Index Distribution at 408 MHz

(Murdoch 1976)

Flux density S at 408 MHz (Jy)	Mean Spectral Index	
	$\bar{\alpha}(408,1400)$	$\bar{\alpha}(408,2695)$
$S \geq 1$	0.934 ± 0.017	0.957 ± 0.018
$S \geq 10$	0.863 ± 0.015	0.856 ± 0.014

TABLE 3.5 : Dependence of Spectral Index Distribution $g_{S(408)}^{408}[\alpha(408,1415)]$ on S(408)

(Katgert 1977)

Flux density S at 408 MHz (Jy)	Mean spectral index $\bar{\alpha}(408,1415)$	α_o	Fraction of sources with $\alpha \leq \alpha_o$
S > 5.5	0.74	0.55	0.12 ± 0.04
S > 0.06 (extended sources)	0.83	0.50	0.07 ± 0.05
S > 0.06 (non-ext)	0.91	0.58	0.06 ± 0.04
0.06 > S > 0.03	0.81	0.58	0.18 ± 0.04

limit from 5.5 to 0.06 Jy. However, this apparent steepening is not significant as it represents only 1.3σ result.

ii) Below 0.06 Jy, $\bar{\alpha}$(408,1415) decreases by 0.10$\pm$0.06. In addition there is an increase in the fraction of flat-spectrum sources below $\sim$ 0.06 Jy. Again these results are only marginally significant.

The flattening of spectrum (decrease in α) at lower flux density levels has also been inferred from a comparison of source counts at 408 MHz and 1415 MHz (Katgert 1976, 1977; Oosterbaan 1978). Katgert determined the values of the 'effective spectral index' (van der Laan 1969) in different 408 MHz flux density ranges by demanding consistency between 408 MHz and 1415 MHz source counts and studied the change in α_{eff} with 408 MHz flux density. The results summarized in Table 3.6, seem to imply a flattening of the spectrum towards lower flux densities. Also, note that flattening in this case is much more pronounced than that inferred from the analysis of spectral index distributions discussed earlier. Similar conclusions have been reached by Oosterbaan (1978). From a comparison of source counts at 408 MHz and 1415 MHz, Oosterbaan suggested that the effective spectral index α_{eff}(610, 1415) changes from 0.89 at S(610)=3.0 Jy to 0.55 at S(610)=0.01 Jy, in agreement with Katgert's results. More observations especially for the faint sources are clearly needed to confirm or disprove the trends indicated by the observations available at present.

TABLE 3.6 : Flux Density Dependence of Effective Spectral Index (Katgert 1977)

Flux Density S at 408 MHz (Jy)	Effective Spectral Index $\alpha_{eff}(408,1415)$
2.8	0.8
1.1	0.8
0.39	0.7
0.12	0.5
0.032	0.2

3.3.2 The Spectral Index Distribution at 1400 MHz

Many authors have investigated α-S dependence for sources selected at 1400 MHz (Willson 1972a; Maslowski 1977; Katgert et al. 1977; Pearson and Kus 1978). From a study of spectral index $\alpha(1407, 408)$ for the sources from the Cambridge 5C2, 5C3 and 5C4 surveys, Willson (1972a) suggested that the spectral index distribution $g^{1407}_{S(1407)}[\alpha(1407,408)]$ is practically independent of flux density down to S(1407)=0.2 Jy, but changes significantly at lower flux densities.

However, on the basis of similar investigations for the sources from the 5C5, 5C6 and 5C7 surveys and using accurately determined spectral indices, Pearson and Kus (1978) concluded that there is no variation of the distribution $g^{1407}_{S(1407)}[\alpha(1407, 408)]$ with flux density (see Table 3.7).

Investigations similar to those referred above have been carried out by Maslowski (1977). In his analysis Maslowski used spectral indices for the sources in GB (Maslowski 1972) and GB2 (Machalski 1978a) surveys. For all the GB2 sources with S(1400) > 0.5 Jy, the two-point spectral indices $\alpha(1400,5000)$ were derived by observing them at 5000 MHz with the NRAO 300-ft telescope.

In addition, the two-point spectral indices $\alpha(1400,408)$ were also determined for the sources in GB2 survey; for this the Bologna 408 MHz flux densities from the B2 survey were used. The complete sample of GB2 sources with $0.5 < S(1400) < 2.0$ Jy was then split into two subsamples in two flux density

TABLE 3.7 : Parameters of Spectral Index Distribution $\int_{S(1400)}^{1400} f\,[\alpha(1400,\nu_2)]$

(Pearson and Kus 1978)

Sample	ν_2 (MHz)	No. of sources	Mean Spectral index $\bar{\alpha}(1400,\nu_2)$	Median Spectral Index $\alpha_{med}(1400,\nu_2)$	Fraction of Flat Spectrum sources $F(1400,\nu_2)$	Mean Spectral index for sources with $\alpha \geq 0.3$ $\bar{\alpha}_h(1400,\nu_2)$
5C5: all sources detected at 1407 MHz S(1400)>1.8 mJy	408	47	0.67±0.07	0.79	0.21±0.06	0.85±0.03
5C6: all sources detected at 1407 MHz S(1407)>1.5 mJy	408	48	0.69±0.04	0.74	0 25±0.06	0.76±0.03
5C7: all sources selected at 1407 MHz S(1407)>1.5 mJy	408	44	0.75±0.05	0.80	0.18±0.06	0.83±0.04
Samples with 10<S(1400)<200 mJy						
5C2,3 and 4 (Willson 1972a)	408	38	0.72±0.06	0.77	0.26±0.07	0.83±0.04
5C5,6 and 7	408	60	0.66±0.06	0.77	0.23±0.05	0.84±0.03
5C2-7	408	98	0.67±0.04	0.77	0.24±0.04	0.84±0.03
Comparison samples:						
Westerbork S(1400)>20 mJy (Katgert et al. 1977)	610	174*	0.64±0.03		0.25±0.04	
Half-mile S(1400)>10 mJy (Gillespie 1975)	408	140	0.71±0.03	0.80	0.21±0.04	0.81±0.03
BDFL/B2(2Jy) (Katgert et al. 1977)	408	50	0.61±0.05		0.25±0.07	

* Notes The Westerbork sample contains a further 9 sources for which S(610) is not available.

The statistics have been calculated by including both upper limits and the estimates with equal weight (For details see Pearson and Kus 1978).

intervals. For each flux density interval, the median spectral index α_{med}, the median spectral index for the normal component $\alpha_{n\ med}$ and the fraction of flat-spectrum sources F were calculated. The results are given in Table 3.8(a). Some of the important features that are apparent from Table 3.8(a) are:

i) For sources with S(1400)>0.7 Jy, $\alpha_{n\ med}(1400,408)$ and $\alpha_{n\ med}(1400,5000)$ differ by an amount of $\sim 0.14\pm0.03$ implying a strong mean spectral curvature for the sources in the normal component. Such a difference is not observed for sources with S(1400)<0.7 Jy. This means that sources with S(1400)<0.7 Jy have straight spectra over the range of 408-1400-5000 MHz.

ii) The median spectral index for the normal component $\alpha_{n\ med}(1400,408)$ increases from 0.75 for the strong source subsample [S(1400)>0.7] to 0.85 for the weak source sample [S(1400)< 0.7 Jy]. The result seems to be significant. On the other hand, $\alpha_{n\ med}(1400,5000)$ changes from 0.89 for the strong source sample to 0.86 for the weak source sample. However, not much significance can be attached to this change.

Maslowski (1977) has investigated the α-S dependence for the GB sources also. The two-point spectral indices α(1400,2695) were determined for all the sources (in the GB survey) with S(1400)>0.2 Jy, by observing them at 2695 MHz using the NRAO 300-foot telescope. Maslowski then determined the spectral index distribution for the GB sources and made an analysis of α-S dependence. The results (see Table 3.8(b))

TABLE 3.8(a) : Spectral Parameters of the Sources [S(1400)≥0.5 Jy] in the GB2 Survey (Maslowski 1977)

Flux Density at 1400 MHz (Jy)	Median spectral index		Median spectral index for the normal component sources		Fraction of flat-spectrum sources	
	$\alpha_{med}(1400,408)$	$\alpha_{med}(1400,5000)$	$\alpha_{n\ med}(1400,408)$	$\alpha_{n\ med}(1400,5000)$	F(1400,408)	F(1400,5000)
0.70-2.0	0.74 ± 0.028	0.82 ± 0.031	0.75 ± 0.017	0.89 ± 0.019	0.20 ± 0.044	0.17 ± 0.042
0.50-0.69	0.80 ± 0.028	0.84 ± 0.025	0.85 ± 0.014	0.86 ± 0.019	0.21 ± 0.045	0.12 ± 0.035

TABLE 3.8(b) : Spectral Parameters of the GB Sources
(Maslowski 1977)

Flux density at 1400 MHz (Jy)	Median spectral index $\alpha_{med}(1400,2695)$	Median spectral index for the normal component sources $\alpha_{n\ med}(1400,2695)$	Fraction of flat-spectrum sources F(1400,2695)
0.50-∞	0.89±0.036	0.92±0.022	0.21±0.039
0.33-0.49	0.79±0.035	0.81±0.017	0.20±0.039
0.24-0.32	0.89±0.025	0.94±0.016	0.11±0.030
0.20-0.23	0.85±0.036	0.92±0.020	0.20±0.038

showed that there is a rapid change in $\alpha_{n\ med}(1400,2695)$ in the narrow flux density range 0.33 Jy to 0.5 Jy. For the sources stronger than 0.49 Jy and weaker than 0.33 Jy, $\alpha_{n\ med}$ is considerably larger. However, an application of the chi-square test shows that the differences between the subsamples are not significant.

The apparent independence of average spectral index $\bar{\alpha}(1400,408)$ and 1400 MHz flux density has also been inferred from a detailed and careful analysis of the spectral index distributions for (a) a strong source sample with S(1400)>2 Jy and (b) a weak source sample with S>0.02 Jy (see Katgert et al. 1977 for details).

3.3.3 The Spectral Index Distribution at 2700 MHz

The flux density dependence of the spectral index distribution of sources found in 2700 MHz surveys has been investigated by many authors (Wall 1972; Condon and Jauncey 1974a; Balonek et al. 1975). We give a discussion of these investigations.

From a study of the spectral index distribution for the sources from the Parkes 2700 MHz survey, Wall (1972) suggested that (a) the median spectral index $\alpha_{med}(2700,178)$ changes from 0.57 for a sample of 80 sources with S(2700)>1.01 Jy to 0.64 for 68 sources with 1.01>S(2700)>0.64 Jy and (b) the fraction of flat-spectrum sources changes from 0.38 to 0.28. It might be pointed out that neither (a) nor (b) is by itself significant

even at the 2σ level, although they are supported by the difference between low- and high-frequency source counts (Shimmins, Bolton and Wall 1968).

Conclusions similar to those of Wall (1972) have been reported recently by Condon and Jauncey (1974a) and Balonek et al. (1975). Condon and Jauncey made an analysis of the distribution of $\alpha(2700,318)$ for sources selected from the Parkes 2700 MHz survey and found both the steep- and flat-spectrum portions of the spectral index distribution of 258 sources (forming a sample statistically complete down to 0.35 Jy at 2700 MHz) to be flux density dependent. Balonek et al. extended the above analysis down to 0.1 Jy at 2700 MHz by considering the distribution of $\alpha(2700,430)$. Condon and Jauncey and Balonek et al. have estimated the values of $\alpha_{n\ med}$ and F in different flux density intervals. These values are shown in Table 3.9. The median ($\alpha_{n\ med}$) of the nearly Gaussian 'normal' spectrum component was estimated by passing a mathematical window of width 0.6 in α over each spectral index distribution (for details see Condon and Jauncy 1974a). The principal results from these investigations may be summed up by saying that there is a change in both $\alpha_{n\ med}$ and F in the range of $0.5 < S(2700) < 0.8$ Jy but there is no evidence of further change down to 0.1 Jy. More investigations with much larger sample sizes are clearly required to detect any changes that might be present.

TABLE 3.9 : Dependence of $\alpha_{n\ med}(2700, \nu_2)$ on the 2700 MHz Flux Density
(Condon and Jauncey 1974a; Balonek et al.1975)

Flux density at 2700 MHz (Jy)	ν_2 (MHz)	Median spectral index for the normal component sources $\alpha_{n\ med}(2700, \nu_2)$	Fraction of flat-spectrum sources $F(2700, \nu_2)$
$S \geq 0.80$	318	0.698 ± 0.017	0.38 ± 0.05
$0.80 > S \geq 0.51$	318	0.813 ± 0.016	0.35 ± 0.05
$0.51 > S \geq 0.35$	318	0.802 ± 0.016	0.26 ± 0.05
$0.35 > S \geq 0.10$	430	0.76 ± 0.02	0.27 ± 0.05

3.3.4 The Spectral Index Distribution at 5000 MHz

Perhaps the most convincing evidence regarding the dependence of spectral index distribution on flux density comes from the surveys conducted at 5000 MHz. In what follows we give a summary of the investigations carried out using surveys at 5000 MHz and highlight the essential features of the results that follow from these investigations.

1) The dependence of $f^{5000}_{S(5000)}[\alpha(5000,408)]$ on S(5000): The dependence of $\alpha_{med}(5000,408)$ on flux density and the variation in the fraction of flat-spectrum sources F with sample depth were derived by Pauliny-Toth and Kellermann (1972b, 1974). The spectral index distributions were derived for the S1, S2, S3 and D surveys (see Pauliny-Toth and Kellermann 1974 and references therein) using data at 408 MHz and 5000 MHz. Using these distributions, the values of $\alpha_{med}(5000,408)$ and F(5000, 408) were calculated for different flux density ranges (see Table 3.10). On the basis of these investigations Pauliny-Toth and Kellermann showed that (i) the median spectral index $\alpha_{med}(5000,408)$ increases with decreasing S(5000) and (ii) the fraction of flat-spectrum sources F(5000,408) decreases as S(5000) decreases.

2) The dependence of $f^{5000}_{S(5000)}[\alpha(5000,318)]$ on S(5000): Condon and Jauncey (1974b) have investigated the spectral index distributions for a sample of 278 sources from the NRAO 5000 MHz S-survey. The spectral indices of these 278 sources

TABLE 3.10 : Spectral Index Distribution $\int_{S(5000)}^{5000} f\,[\alpha(5000,408)]$ as a Function of S(5000)

(Pauliny-Toth and Kellermann 1972b,1974)

Flux density S at 5000 MHz	Median Spectral index $\alpha_{med}(5000, 408)$	Fraction of flat-spectrum sources F(5000,408)
$S \geq 1.5$	0.30 ± 0.06	0.57 ± 0.10
$1.5 > S \geq 1.0$	0.35 ± 0.05	0.60 ± 0.09
$1.0 > S \geq 0.8$	0.54 ± 0.06	0.47 ± 0.09
$0.8 > S \geq 0.6$	0.55 ± 0.05	0.45 ± 0.07
$0.6 > S \geq 0.1$	0.60 ± 0.07	0.43 ± 0.10
$0.1 > S \geq 0.067$	0.63 ± 0.04	0.40 ± 0.09

were determined from 318 MHz flux densities measured at Arecibo. For different flux density ranges, the median spectral index $\alpha_{med}(5000,318)$, the median spectral index for the normal component sources $\alpha_{n\ med}(5000,318)$ and the fraction of flat-spectrum sources F(5000,318) were calculated. The results show (Table 3.11) that (a) $\alpha_{n\ med}(5000,318)$ increases with decreasing flux density S(5000) and (b) the fraction of flat-spectrum sources F(5000,318) decreases with decreasing S(5000).

3) The dependence of $f_{S(5000)}^{5000}[\alpha(5000,1400)]$ on S(5000): From a study of spectral index distribution $f_{S(5000)}^{5000}[\alpha(5000,1400)]$ for 61 sources from the Bonn 5000 MHz (4850 MHz to be precise but we ignore the small difference) deep survey Davis (1977) showed that:

i) For 61 sources with S(5000)>9 mJy, $\alpha_{med}(5000,1400)=0.60$ and $F(5000,1400)=0.34$.

ii) For sources with S(5000)>20 mJy, F(5000,1400)=0.36

This means that, at these very low flux densities, the fraction of flat-spectrum sources does not continue to decrease with decreasing flux density. The median value of spectral index $\alpha_{med}(5000,1400)$ also does not vary with S(5000) at very low flux densities. These conclusions are supported by the investigations of Willis and Miley (1979). Willis and Miley derived the spectral index distribution for a sample containing

TABLE 3.11 : Spectral Index Distribution $f_{S(5000)}^{5000}$ [$\alpha(5000,318)$] as a Function of S(5000)

(Condon and Jauncey 1974b)

Flux density range (Jy)	Median Spectral index $\alpha_{med}(5000,318)$	Median spectral index for the normal component sources $\alpha_{n\ med}(5000,318)$	Fraction of flat-spectrum sources F(5000,318)
$S \geq 1.15$	0.34 ± 0.15	0.66 ± 0.027	0.56 ± 0.05
$1.15 > S \geq 0.8$	0.43 ± 0.07	0.73 ± 0.030	0.57 ± 0.05
$0.8 > S \geq 0.6$	$0.55^{+0.04}_{-0.11}$	0.70 ± 0.024	0.48 ± 0.05
$0.6 > S \geq 0.25$	$0.49^{+0.10}_{-0.15}$	0.79 ± 0.05	0.52 ± 0.08
$0.25 > S \geq 0.067$	$0.57^{+0.02}_{-0.03}$	0.76 ± 0.021	0.43 ± 0.04

TABLE 3.12 : Spectral Index Distributions $f_{S(5000)}^{5000}[\alpha(5000,2695)]$ as a Function of S(5000)

(Pauliny-Toth et al. 1978a)

Flux density range (Jy)	Median spectral index $\alpha_{med}(5000,2695)$	Fraction of flat-spectrum sources F(5000,2695)
$S \geq 2.1$	0.43 ± 0.09	0.54 ± 0.07
$2.1 > S \geq 1.3$	0.30 ± 0.11	0.58 ± 0.06
$1.3 > S \geq 0.96$	0.36 ± 0.10	0.56 ± 0.05
$0.96 > S \geq 0.8$	0.54 ± 0.08	0.48 ± 0.06
$0.8 > S \geq 0.6$	0.47 ± 0.05	0.50 ± 0.04
$0.6 > S \geq 0.5$	0.52 ± 0.11	0.48 ± 0.09
$0.6 > S \geq 0.067$	0.45 ± 0.04	0.49 ± 0.06

~ 20 sources from the Westerbork 6-cm survey. The results gave a value of 0.35 ± 0.13 for F(5000,1400). This value is in excellent agreement with the results of Davis (1977) discussed above.

4) The dependence of $f^{5000}_{S(5000)}$ [5000,2700)] on S(5000):

Pauliny-Toth and Kellermann (1974) and Pauliny-Toth et al. (1978a) studied the variations in spectral index distributions with flux density. They used the flux density measurements at 2700 MHz and 5000 MHz to estimate $f^{5000}_{S(5000)}$ [α(5000,2700)] for the sources in the S1, S2, S3 and D surveys and calculated α_{med}(5000,2700) and F(5000,2700) for different flux density intervals. The results, summarized in Table 3.12 show that α_{med}(5000,2700) and F(5000,2700) do not vary with 5000 MHz flux density in any significant manner.

3.4 Summary

The observations indicate that the counts of radio sources at different frequencies are similar in form, but not identical. When expressed in the form log $n(S)/n_o(S)$ vs. log S, the high frequency counts show a broader top than the low frequency counts, i.e. the high frequency source counts differ from those derived at low frequencies in that there is less evidence for either a steepening of the counts at high densities or for their convergence at low flux densities.

The spectral index distributions depend on frequency. The spectral index distribution is seen to depend on flux density when sources are from a high (ν >2000 MHz) frequency

survey and the spectral indices are determined from the flux density measurements at the survey frequency and some low frequency ($\nu < 2000$ MHz). The spectral index distribution does not depend on flux density when the spectral indices are derived from data at the survey frequency ($\nu > 2000$ MHz) and some high frequency. On the other hand, for sources selected at low frequencies, there does not seem to be any really convincing evidence to believe that spectral index distribution depends on flux density. Further observations are clearly needed to throw more light on the nature of spectral index distribution at low frequencies. In the mean time the theoretical models of spectral index distribution can be tested using data from the high frequency surveys.

"Now entertain conjecture
of a time, when creeping
murmur and the poring
dark fills the wide vessel of
the universe"

: William Shakespeare

KING HENRY V

"If we indulge in fanciful imagination and build worlds of our own, we must not wonder at our going wide from the path of truth and nature ... On the other hand, if we add observation to observation, without attempting to draw not only certain conclusions, but also conjectural views from them, we offend against the very end for which only observations ought to be made"

: William Herschel.

CHAPTER 4

RADIO SOURCE COUNTS AND SPECTRAL INDEX DESTRIBUTIONS : Models

OR

A GENERALIZED LUMINOSITY FUNCTION FOR EXTRAGALACTIC RADIO SOURCES

4.1.1. Introduction

In Chapter 3 we discussed the current observational status of radio source counts and spectral index distributions, the essential features of which, both at low and high frequencies, were highlighted. In this chapter, we will consider the interpretation of these observed features in terms of models. In Section 4.2, we give a brief review of earlier models put forward by various workers to explain the observational data. Some of the important assumptions made in these models and the difficulties encountered in view of the recent data on source counts and spectral index distributions are pointed out. In Section 4.3 a new model is proposed and the expected source counts and spectral index distributions are calculated. The possibility of a spectral index dependent cosmological evolution function has been considered, together with the known correlation between radio luminosity and spectral index. By comparing the predicted source counts and spectral index distributions with those observed both at low and high frequencies, a Generalized Luminosity Function is derived. The GLF describes

the comoving space density of extragalactic radio sources as a function of radio luminosity P (measured in W Hz^{-1} sr^{-1}), redshift z and spectral index α. The chapter concludes with a summary of conclusions and the effects of the assumptions made in the present model. Possible lines of investigations for improving the model are also indicated.

4.1.2. Notation and Definitions

We use the same notation that was introduced in Chapter 3. In addition, we will define the following entities.

The Generalized Luminosity Function (GLF) denoted by $\psi(P,z,\alpha)$ describes the comoving space density of radio sources as a function of radio luminosity, redshift and spectral index. The comoving space density of radio sources with spectral index between α and $\alpha+d\alpha$ is denoted by $\eta(\alpha)$ and is referred to as 'Spectral Index Function' (SIF). Note that SIF is associated with a unit volume of space and is not directly derivable from observations unlike the Spectral Index Distribution (SID) $f^{\nu}_{S(\nu)}(\alpha)$. Entities with subscripts f and s refer to flat and steep-spectrum sources respectively. For instance the cosmological Evolution Function (EF) for flat-spectrum sources is represented by $F_f(P,z)$.

4.2 Earlier Models

The problem of predicting radio-source counts at different frequencies and the related problem of calculating the expected variations in spectral index distributions with

flux density has been discussed by many authors (Kellermann, Pauliny-Toth and Davis 1968; van der Laan 1969; Fanaroff and Longair 1973; Petrosian and Dickey 1973). In these investigations essentially two approaches have been taken. In the first, described by Kellermann, Pauliny-Toth and Davis (1968) and van der Laan (1969), the spectral index distributions and source counts at one frequency are used to calculate the spectral index distributions and source counts at another frequency. This is an empirical formalism. In the second approach (Fanaroff and Longair 1973; Petrosian and Dickey 1973; Schmidt 1972c) the spectral index distributions and source counts are estimated from the models of space distribution of radio sources i.e. from the GLF $\psi(P,z,\alpha)$. A short account of these approaches is given below.

4.2.1. The Empirical Method

Kellermann, Pauliny-Toth and Davis (1968; see also van der Laan 1969) employed the empirical method in investigating the dependence of radio source counts and spectral index distributions on frequency. The formalism is quite simple and straight forward. Let $g^{\nu_i}_{S(\nu_i)}[\alpha(\nu_i,\nu_j)]$ be the normalized distribution of the spectral index $\alpha(\nu_i,\nu_j)$ at frequency ν_i for all sources with a flux density $\geq S(\nu_i)$ and let $g^{\nu_j}_{S(\nu_j)}[\alpha(\nu_j,\nu_i)]$ be the corresponding quantity for ν_j. The integral counts at ν_i and ν_j are denoted by $N(>S(\nu_i),\nu_i]$ and $N'[>S(\nu_j),\nu_j]$ respectively. Let us assume that $g^{\nu_i}_{S(\nu_i)}[\alpha(\nu_i,\nu_j)]$ is independent of flux density $S(\nu_i)$. Suppose further that

$N[>S(\nu_i),\nu_i]$ and $g^{\nu_i}_{S(\nu_i)}[\alpha(\nu_i,\nu_j)]$ are known from observations. The aim is to derive $N'[>S(\nu_j),\nu_j]$ and $g^{\nu_i}_{S(\nu_j)}[\alpha(\nu_j,\nu_i)]$ from the observations at ν_i. Now consider a source with flux density $> S(\nu_j)$ at ν_j and spectral index $\alpha(\nu_j,\nu_i)$. This source will have a flux density $> S(\nu_j)(\frac{\nu_i}{\nu_j})^{-\alpha}$ at frequency ν_i. Note that for convenience we have set $\alpha(\nu_i,\nu_j) = \alpha$. It follows that

$$g^{\nu_j}_{S(\nu_j)}[\alpha]N'[>S(\nu_j),\nu_j] = g^{\nu_i}_{S(\nu_i)}[\alpha]N[>S(\nu_j)(\frac{\nu_i}{\nu_j})^{-\alpha},\nu_i] \quad (4.1)$$

Note that $g^{\nu_j}_{S(\nu_j)}[\alpha]$ will be independent of $S(\nu_j)$ only if the source counts can be expressed in the form $N(>S(\nu),\nu]=k\ S(\nu)^{-x}$ where k and x are constants. In this case, eq.(4.1) reduces to

$$g^{\nu_j}_{S(\nu_j)}[\alpha] = \frac{N[>S(\nu_j),\nu_i]}{N'[>S(\nu_j),\nu_j]}\ (\frac{\nu_i}{\nu_j})^{\alpha x}\ g^{\nu_i}_{S(\nu_i)}[\alpha] \quad (4.2)$$

In general, the slope x is not constant but depends on flux density. For example, x takes smaller values at low flux densities i.e. the number-flux density curve becomes flatter at low flux densities. As a consequence of this $g^{\nu_j}_{S(\nu_j)}[\alpha]$ will in general depend on $S(\nu_j)$ even if $g^{\nu_i}_{S(\nu_i)}[\alpha]$ is assumed to be independent of $S(\nu_i)$.

The source counts at frequency ν_j are given by

$$N'[>S(\nu_j),\nu_j] = \int_{-\infty}^{\infty} N[>S(\nu_j)(\frac{\nu_i}{\nu_j})^{-\alpha},\nu_i]\; g^{\nu_i}_{S(\nu_i)}[\alpha]d\alpha \qquad (4.3)$$

With the form $N[>S(\nu),\nu] = k\, S(\nu)^{-x}$ for the source counts, eq.(4.3) reduces to

$$N'[>S(\nu_j),\nu_j] = N[>S(\nu_j),\nu_i] \int_{-\infty}^{\infty} (\frac{\nu_i}{\nu_j})^{\alpha x}\; g^{\nu_i}_{S(\nu_i)}[\alpha]d\alpha \qquad (4.4)$$

Starting with the source counts and spectral index distributions at low frequency (ν_i=408 MHz or 178 MHz) and the assumed independence of $g^{\nu_i}_{S(\nu_i)}[\alpha]$ and $S(\nu_i)$, Kellermann, Pauliny-Toth and Davis computed the spectral index distribution $g^{\nu_j}_{S(\nu_j)}[\alpha]$ and number counts $N'[>S(\nu_j),\nu_j]$ at a high frequency (ν_j = 2700 or 5000 MHz). The computed values were compared with the observational data from 2700 MHz (Parkes) and 5000 MHz (NRAO) surveys. On the basis of this comparison, Kellermann, Pauliny-Toth and Davis concluded that there were no significant differences between the computed and observed source counts and spectral index distributions except at low flux levels at 5000 MHz, where there may be an excess of sources with flat spectra.

From similar investigations, Pauliny-Toth et al. (1978b) found the source counts from the Bonn 4.85 GHz deep survey were consistent with those derived from the 408 MHz counts and the spectral index distributions for the 408 MHz sources.

Although the above formalism has some disadvantages, as pointed out at the end of this subsection, it can be quite useful in bringing out the different features of source counts at different frequencies. We give below a modified formalism and use it to derive some general features of source counts at different frequencies.

Let $\Sigma(S,\nu,\alpha)$ be the Generalized Source Counts (GSC) at frequency, ν. The GSC gives the number of radio sources (selected at frequency ν) with flux densities and spectral indices in the ranges S to S+dS and α to $\alpha+d\alpha$. The differential counts $n[S(\nu),\nu]$ and the GSC are related by

$$n[S(\nu),\nu] = \int_{-\infty}^{\infty} \Sigma(S,\nu,\alpha)d\alpha \qquad (4.5)$$

Consider generalized source counts $\Sigma[S(\nu_i),\nu_i,\alpha]$ and $\Sigma'[S(\nu_j),\nu_j,\alpha]$ at frequencies ν_i and ν_j respectively (in our discussion ν_i=408 MHz, ν_j=5000 MHz). These are connected by

$$\Sigma'[S(\nu_j),\nu_j,\alpha] = \Sigma[S(\nu_i),\nu_i,\alpha]\,\frac{dS(\nu_i)}{dS(\nu_j)} \qquad (4.6)$$

The source counts at frequency ν_j are given by

$$n'[S(\nu_j),\nu_j] = \int_{-\infty}^{\infty} \Sigma[S(\nu_i),\nu_i,\alpha](\frac{\nu_j}{\nu_i})^{\alpha}\, d\alpha \qquad (4.7)$$

We can factorize the GSC at ν_i in the following manner

$$\Sigma[S(\nu_i),\nu_i,\alpha] = n[S(\nu_i),\nu_i]\, f^{\nu_i}_{S(\nu_i)}(\alpha) \qquad (4.8)$$

Note that in general $f^{\nu_i}_{S(\nu_i)}(\alpha)$ may be a function of flux density $S(\nu_i)$. At low frequencies $f^{\nu_i}_{S(\nu_i)}(\alpha)$ can be represented approximately by a normal distribution function - i.e. $\frac{1}{\sigma\sqrt{2\pi}} \exp[-\{\alpha-\alpha_o(S)\}^2/2\sigma^2]$. In general $\alpha_o(S)$ is a function of S. Also we will assume that the source counts can be represented by

$$n[S(\nu),\nu] = k\, S^{-x-y \ln S} \qquad (4.9)$$

where x and y are parameters and k is a constant of normalization. From eqs.(4.8) and (4.9) we get

$$n'[S(\nu_j),\nu_j] = \frac{1}{\sigma\sqrt{2\pi}} \int_{-\infty}^{\infty} kS^{-x-y \ln S}\, e^{\frac{-[\alpha-\alpha_o(S)]^2}{2\sigma^2}} \left(\frac{\nu_j}{\nu_i}\right)^{\alpha} d\alpha \qquad (4.10)$$

Note that we have set $S(\nu_i) = S$ for convenience of writing. Let us assume that the flux density dependence of $\alpha_o(S)$ can be represented by

$$\alpha_o = a_o + b_o \ln[S]$$

$$= a_o + b_o[\ln S(\nu_j) + \alpha_o z], \text{ where } z = \ln\frac{\nu_j}{\nu_i}$$

or

$$\alpha_o = \frac{a_o + b_o \ln S(\nu_j)}{1 - b_o z} = a_1 + b_1 \ln S(\nu_j) \qquad (4.11)$$

Using eq. (4.11) in eq. (4.10) and integrating, we can show that

$$n'[S(\nu_j), \nu_j] = \frac{k\, e^{c_o}\, S'^{-x'-y'\ln S'}}{\sigma\sqrt{2(yz^2+\varepsilon)}} \qquad (4.12)$$

where $\varepsilon = \frac{1}{2\sigma^2}$

$S' = S(\nu_j)$

$$c_o = \frac{(xz - z - 2a_1\varepsilon)^2 - 4a_1^2\varepsilon(yz^2+\varepsilon)}{4(yz^2+\varepsilon)} \qquad (4.13)$$

$$x' = x + \frac{2a_1\varepsilon\, yz(1+b_1 z) + z(1-x)(yz - b_1\varepsilon)}{yz^2+\varepsilon} \qquad (4.14)$$

and

$$y' = \frac{y(1+b_1 z)^2}{\frac{yz^2}{\varepsilon} + 1} \qquad (4.15)$$

Thus the source counts at frequency ν_j (in our case ν_j = 5000 MHz) are characterized by the parameters x' and y'. It is clear from eq. (4.12) that the form of source counts at ν_j is similar to that at ν_i. Let us now consider some special cases.

a) Suppose the Universe is static and Euclidean i.e. y=0 and at a low frequency (ν_i=408 MHz) the spectral index distribution is independent of flux density i.e. b_1=0. In this case,

from eq.(4.14) we get

$$x' = x + (x-1)b_1 z = x$$

Thus the slope x remains the same.

b) Consider the case x=2.5, y=0 but $b_1 < 0$ i.e. mean spectral index $\alpha_o(S)$ increases (steepens) with decreasing flux density at ν_i . Then the expression for x' reduces to

$$x' = x + xb_1 z - b_1 z$$

$$= x + (x-1)b_1 z$$

Since $z = \ln \frac{\nu_j}{\nu_i} = \ln 5000/408 > 0$ and $b_1 < 0$, it follows that $(x-1)b_1 z < 0$. Hence $x' < x$ i.e. at high frequencies the slope of log n(S)-log S curve becomes less steep.

c) Assume that (i) x=2.5, $y \neq 0$ and (ii) $b_1 = 0$. An examination of the observational data at low frequencies indicates that these assumptions are quite realistic. In this case expression for y' reduces to

$$y' = \frac{y}{\frac{yz^2}{\varepsilon} + 1}$$

Since $\frac{yz^2}{\varepsilon} > 0$, we have $y' < y$. As pointed out in Chapter 2, the width of source counts $n(S)/n_o(S) \propto \frac{1}{\sqrt{y}}$. Therefore it follows that the high frequency source counts, expressed as $n(S)/n_o(S)$ should have a broader maximum than those at low frequencies. This view is supported by the observational data from low and high frequency surveys.

It is clear from the above discussion that it is possible to reconcile the observed counts and spectral index distributions at different frequencies, within the framework of the empirical formalism. However, this formalism is unsatisfactory for two reasons. The first is the assumption that spectral index distribution is independent of flux density at some frequency. The second and the more important one is the neglect of the detailed information present in the source counts regarding differential cosmological evolution of radio sources in widely different luminosity ranges.

Fanaroff and Longair (1973) (see also Petrosian and Dickey 1973; Schmidt 1972c) have given a more general and satisfactory formalism. They estimated the spectral index distributions and source counts from models of space distributions of radio sources i.e. from the GLF $\psi(P,z,\alpha)$. The essential features of this model and the conclusions that follow are summarized in the next subsection.

4.2.2. The Model of Fanaroff and Longair

Fanaroff and Longair (1973) have discussed the problem of predicting radio-source counts at different frequencies and the related problem of calculating the expected variations in spectral index distributions with flux density. The calculations were performed in terms of evolutionary world models which incorporate strong evolution of the radio source population. The following assumptions were made for the sake of simplicity:

1) At low frequencies, the spectra for most of the radio sources can be represented by power-law spectra $S(\nu) \propto \nu^{-\alpha}$ where α, the spectral index is a constant.

2) There is, if any, only a weak correlation between radio luminosity and spectral index for sources selected at 178 MHz (in general any low frequency). With this assumption the spectral index function $\eta(\alpha)$ can be treated to be independent of radio luminosity. Further if $\eta(\alpha)$ is assumed to be independent of z also, the GLF can be factorized (at a low frequency) in the following manner

$$\Psi(P,z,\alpha) = \eta(\alpha)\rho(P,z) \qquad (4.16)$$

3) The form of cosmological evolution is same for sources with flat and steep spectra -i.e. the evolution function $F(P,z)$ is independent of spectral index α.

In their calculations, Fanaroff and Longair (1973) considered only Einstein-de Sitter model (i.e. $q_o = 0.5$). This is not crucial because the geometric differences between world models are small in comparison with the gross effects of evolution. The evolutionary world models selected were similar to those employed by Doroshkevich, Longair and Zeldovich(1970) to explain the counts of radio sources. The evolution was described by 'density' evolution. The essential features of these models are:

i) the comoving space density of sources increases rapidly with redshift z

ii) There is a cut-off redshift z_c i.e. for $z > z_c$ the density of sources decreases or remains constant.

iii) Evolution is confined to powerful sources only.

The spectral index function $\eta(\alpha)$ was derived by following a model-fitting procedure. For this purpose the spectral index distributions observed at 178 MHz and 5000 MHz in the high flux density range, were used. The spectral index distributions at 178 MHz and 5000 MHz and in the low flux density region were then estimated using the spectral index function $\eta(\alpha)$. These calculations showed that

i) At 178 MHz (in general any low frequency), there are no significant variations in spectral index distribution with flux density.

ii) At 5000 MHz (in general any high frequency), significant variations in spectral index distributions with flux density are expected. At the highest flux densities $S(5000) \gtrsim 6$ Jy, the fraction of flat-spectrum sources increases with decreasing flux density but for lower flux densities, there is a very marked decrease in this fraction. These changes can be easily understood as follows. At 178 MHz the spectral index function $\eta(\alpha)$ and $\rho(P,z)$ are assumed to be independent of each other; but at 5000 MHz a strong correlation is induced between small α and high radio power. As a consequence, for a given luminosity P at 178 MHz, sources with flat spectra can be observed to much larger redshifts in the high frequency surveys (at a given flux density) than those

with steep-spectra. In evolutionary world models the comoving space density of radio sources increases with redshift. This rapid increase in $\rho(P,z)$ leads to an enhancement in the fraction of flat-spectrum sources in the high frequency sample. However, since even at $S(5000) \simeq 6$ Jy powerful sources with $\alpha < 0.5$ are observed at $z \sim 3$ and since $\rho(P,z)$ remains constant or decreases for $z > 3$, at low flux densities at 5000 MHz, the fraction of flat-spectrum sources starts decreasing rapidly.

iii) The spectral index α and radio luminosity P are assumed to be independent at a low frequency. This means that the spread in the luminosity of the evolving component of the radio sources is smallest at a low frequency. As a consequence, counts of radio sources should exhibit sharpest features at low frequencies.

Fanaroff and Longair showed that the above results are in general agreement with the observational data available. They noted that (a) only a small error is made in assuming that most of the sources have straight-line spectra over a wide range in frequency (b) the α-P correlation is unlikely to influence the results in any significant manner.

4.3 The Present Model

In this section some of the assumptions made in the model of Fanaroff and Longair are examined and the difficulties that this model encounters in the light of the recent

observational data are pointed out. A new model is proposed to incorporate some observational features that have been reported recently. The details of the model are also discussed. The predictions of the new model are then compared with the observational data.

From the discussion of previous section it is clear that the predictions of the model proposed by Fanaroff and Longair are in fairly good agreement with the observational data. However, Pauliny-Toth (1977) has pointed out that this model predicts consistently lower counts at 5000 MHz for the weak sources, a discrepancy which reaches a factor of 3 at 0.02 Jy, the limiting flux density of the deep surveys. This disagreement has also been noted by Davis and Tauber (1974) from the P(D) [background deflection] analysis of data from the NRAO 5 GHz deep survey (Davis 1971). A comparison of the model counts with the data from the Westerbork 6 cm survey (Willis and Miley 1979) and data from P(D) analysis (Wall 1978) leads to similar conclusions. It might be pointed out, however, that contrary to the nearly Euclidean nature or the nonconvergence of source counts (in the low flux density range) suggested by Wall, the Westerbork results indicate a convergence of source counts in the range from $\sim$ 100 mJy to 4 mJy (1 mJy = 10^{-3} Jy).

The model of Fanaroff and Longair seems to run into further difficulties in predicting spectral index distribution at very low flux densities. Davis (1977) has measured spectral

indices between 1.4 and 4.8 GHz for a sample of weak radio sources selected at 4.8 GHz. In a sample of 61 sources with flux densities > 0.009 Jy at 4.8 GHz, 34 per cent of the sources have flat spectra ($\alpha < 0.5$). The fraction of flat-spectrum sources is essentially unchanged (36 per cent) for sources with flux densities > 0.02 Jy. These results are supported by the investigations of Willis and Miley (1979). From a study of spectral index distribution for a sample containing ~ 20 sources from the Westerbork 6 cm survey, Willis and Miley derived a value of 35 ± 13 % for the fraction of flat-spectrum sources. This value is in excellent agreement with the results of Davis (1977) discussed above. The observations, thus indicate a value of ~ 35 per cent for the fraction of flat-spectrum sources. On the other hand, the model of Fanaroff and Longair predicts a value of ~ 18 per cent for the fraction of flat-spectrum sources at very small flux density levels. A comparison of the predicted and the observed values for the median spectral index also seems to imply a disagreement between the model predictions and observational data at very low flux densities.

In their model, Fanaroff and Longair made the following assumptions for the sake of simplicity:

a) The form of evolution is the same for sources with flat- and steep-spectra.

b) The spectral index function $\eta(\alpha)$ and the luminosity function $\rho(P,z)$ are independent at a low frequency.

These assumptions are examined below.

4.3.1. Cosmological Evolution of Flat- and Steep-spectrum Sources

The possibility that the cosmological evolution function for radio sources might depend on spectral index has been inferred from the V/V_m test for quasars and also from a comparison of source counts at low and high frequencies.

In Chapter 2, the V/V_m or the luminosity-volume test was described and it was shown that it can be used to determine the evolution function $E(z)$ and multivariate local luminosity function. We also mentioned some investigations in which the V/V_m test was used to infer the presence of strong evolutionary effects among quasars. In these investigations, identical evolution function was assumed for both flat- and steep-spectrum sources, i.e. any possible dependence of evolution function $E(z,\alpha)$ on α was ignored. However, in the last few years many authors have suggested that there might be differences in the evolution of flat- and steep-spectrum quasars (e.g. Rowan-Robinson 1972; 1976; Setti and Woltjer 1973; Fanti et al. 1975). In the case of steep-spectrum quasars, $< V/V_m >$ is significantly higher than 0.5 implying strong evolution of quasar populations with cosmic epoch. On the other hand $< V/V_m >$ for flat-spectrum quasars is not significantly different from 0.5, the value expected for a uniform distribution of these objects in space.

Schmidt (1976, 1977), for example, has analysed a sample of 51 quasars from the NRAO 5000 MHz survey, using the

V/V_m test. The three subsamples $\alpha > 0.45$, $0.45 > \alpha > 0.05$ and $\alpha < 0.05$, each of which contains 17 objects, yield values for $< V/V_m >$ of 0.71 ± 0.05, 0.60 ± 0.07 and 0.52 ± 0.06 respectively, indicating that there are indeed differences in the evolution of quasars present in different subsamples. From a study of a complete sample selected at 2700 MHz, Masson and Wall (1977) reached similar conclusions. They used spectral indices which are virtually identical to two-point 2700-5000 MHz spectral indices and found values $< V/V_m > = 0.52\pm0.05$ for a subsample of 42 flat-spectrum quasars with $\alpha < 0.5$ and 0.67 ± 0.05 for a subsample of 15 steep-spectrum quasars. From these results, along with the source counts and the relation between evolution and radio structure (Rowan-Robinson 1972), Masson and Wall suggested that the cosmological evolution of both quasars and galaxies is confined to the powerful sources with extended structure.

The dependence of V/V_m on radio spectral index is also indicated by the investigations of Wills and Lynds (1978). They combined new spectroscopic observations of nearly 100 QSOs with earlier data to compile observationally complete samples of QSOs selected from the 4C (178 MHz) and Parkes (2700 MHz) radio source surveys. The samples thus assembled were used to study, among other things, the possible differences between the cosmological evolution schemes for flat- and steep-spectrum quasars. The results summarized in Table 4.1 show that flat- and steep-spectrum sources have different values of $< V/V_m >$

TABLE 4.1 : Summary of $\langle V/V_m \rangle$ Results for Different Spectral Classes ($q_o = 1$)

(Wills and Lynds 1978)

Sample	Type of spectral index (α) used	$\langle V/V_m \rangle$ for sources with		No. of objects	
		Flat-Spectrum $\alpha \leq 0.5$	Steep-spectrum $\alpha > 0.5$	Flat-spectrum	Steep-spectrum
3CR *	α_{LF}	0.471 ± 0.105	0.751 ± 0.040	7	27
$S \geq 2$	α_{LF}	0.676 ± 0.083	0.690 ± 0.038	5	36
$S \geq 3$	α_{LF}	0.615 ± 0.060	0.720 ± 0.026	16	60
Combined 178 MHz	α_{LF}	0.590 ± 0.046	0.718 ± 0.019	28	123
$\pm 4^c$	α_{HF}	0.625 ± 0.057 for $\alpha \leq 0$	0.757 ± 0.052	18	15
		0.600 ± 0.048 for $0 < \alpha \leq 0.5$		27	
All samples	α_{LF}/α_{HF}	0.602 ± 0.028	0.722 ± 0.018	73	138

i.e. sources belonging to different spectral classes have different evolution functions.

However, from an application of V/V_m test to a complete sample of quasars selected at 1400 MHz, Blake (1978) has reached different conclusions. In his analysis Blake used a sample of 56 quasars from the BDFL (Bridle et al. 1972) catalogue. He used 1400-178 MHz spectral indices and calculated $< V/V_m >$ for the three subsamples with $\alpha < 0.0$, $0.0 < \alpha < 0.5$ and $\alpha > 0.5$. He carried out similar investigations using $\alpha(1400,2700)$. On the basis of these investigations, Blake concluded that powerful flat-spectrum quasars may take part in the cosmological evolution.

It is clear from the above discussion that although data at present do not allow us to draw any definite conclusions they indicate that the cosmological evolution for flat-spectrum quasars is not as strong as the evolution for steep-spectrum quasars. In our investigations, therefore, we use different evolution functions for flat- and steep-spectrum quasars. In addition, in accordance with the findings of Masson and Wall (1977), we will assume that the cosmological evolution of both quasars and galaxies is confined to the powerful sources with extended structure. Since a majority of the powerful extended sources have steep spectra, this implies that in general the evolution of sources with steep-spectra is stronger than that of flat-spectrum sources.

The fact that the flat- and steep-spectrum sources might differ in their evolutionary properties can also be inferred from a comparison of source counts at low and high frequencies. As discussed in Chapter 3, the source counts when expressed as $n(S)/n_o(S)$ show a broader maximum at high frequencies than at low frequencies. The range in flux density over which this maximum occurs corresponds to some luminosity range $\Delta P=P_2-P_1$ (Longair 1971). The cosmological evolution is confined to those sources which have their luminosity in the range P_1 to P_2. Thus the broader maximum of source counts at high frequencies implies that this range ΔP is larger. Also, at high frequencies the contribution to the source counts from flat-spectrum sources is comparatively large. Hence it is natural to assume that this range ΔP is larger for the flat-spectrum sources.

We have given above only the simplest explanation of the broader maximum in the high frequency counts. The truth is probably much more complex. For instance, ΔP may be epoch-dependent, and in different ways for flat- and steep-spectrum sources, or ΔP may be the same width but centered differently for flat- and steep-spectrum sources. Both these effects also give rise to a broader maximum at high frequencies. However, these factors are not included in our model because they would make it more complex, with added free parameters.

4.3.2. Radio Luminosity-spectral Index Correlation

Several authors have reported a correlation between radio luminosity P and spectral index α for sources selected at 178 MHz (Kellermann, Pauliny-Toth and Williams 1969; Bridle, Kesteven and Guindon 1972; Macleod and Doherty 1972; Véron, Véron and Witzel 1972). It appears that this correlation is statistically significant for a class of radio sources consisting mostly of radio galaxies with spectral index $\alpha > 0.5$.

We have also studied the radio luminosity-spectral index correlation. For this we considered a sample of 96 sources consisting of all the identified radio sources with S(408) > 10 Jy (Grueff and Vigotti 1977). For these sources, two-point spectral indices between 408 and 5000 MHz are available (see Grueff and Vigotti 1977). We divided the sources into 12 luminosity bins, each bin containing eight sources (Luminosities were calculated in an Einstein-de Sitter model for which $q_o = \frac{1}{2}$ and cosmological constant $\Lambda = 0$; a value of 50 km s^{-1} Mpc^{-1} was used for the Hubble constant H_o). From each bin, sources with $\alpha(408,5000) < 0.6$ were removed and averages $< \log P >$ and $< \alpha >$ were calculated. From a plot of $< \alpha >$ versus $< \log P >$ (Fig.4.1), it is seen that $< \log P >$ and $< \alpha >$ are correlated. The straight line obtained by least-squares analysis is given by

$$< \alpha > = -0.14+0.037 <\log P> \qquad (4.17)$$

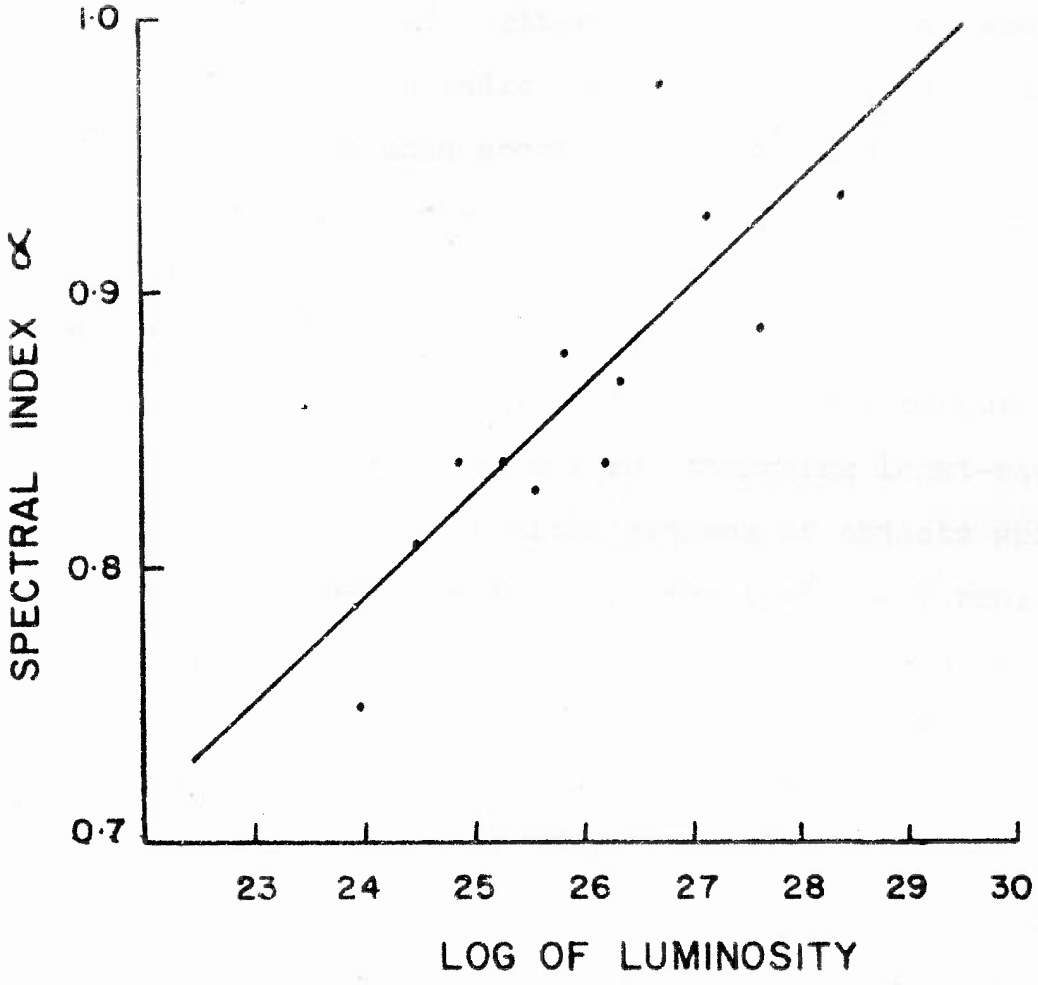

FIG. 4·1 PLOT OF AVERAGE SPECTRAL INDEX FOR EACH LUMINOSITY BIN AGAINST LOG OF LUMINOSITY (EXPRESSED IN $WHz^{-1}sr^{-1}$)

As mentioned earlier, many authors have noted a correlation between radio luminosity and spectral index. Most of these authors used spectral indices that were determined from measurements over a range of frequencies, whereas we have used two-point spectral indices $\alpha(408,5000)$. Also these investigators obtain lines fitted by least-squares without preaveraging the data, in contrast to our procedure in which we have preaveraged data before attempting least-squares analysis. Moreover, specific classes of objects were used in investigating α-P correlation. For instance Veron, Veron and Witzel (1972) used elliptical radio galaxies in their investigations. For these reasons the relation for $< \alpha >$ given above cannot be directly compared with those given by others. Moreover, our main aim was not a study of spectral index-radio luminosity correlation but derivation of an approximate relation between $\alpha(408,5000)$ and $P(408)$. This relation is used later in the derivation of GLF for extragalactic radio sources.

4.3.3. Form of the Generalized Luminosity Function

Let us assume that there are two classes of sources. Most of the steep-spectrum sources for which radio luminosity and spectral index are correlated form one class. The remaining ones, mostly the flat-spectrum sources for which radio luminosity and spectral index are not correlated, form another class. The GLF $\Psi(P,z,\alpha)$ can be written in the following form.

$$\Psi(P,z,\alpha) = \rho(P,z=0)[C_f F_f(P,z)\eta_f(\alpha) + C_s F_s(P,z)\eta_s(\alpha|P)\ ] \qquad (4.18)$$

where

$\rho(P,z=0)$ = local luminosity function

C_f = fraction of flat-spectrum sources

C_s = fraction of steep-spectrum sources

$F_f(P,z)$ = evolution function for flat-spectrum sources

$F_s(P,z)$ = evolution function for steep-spectrum sources

$\eta_f(\alpha)$ = normalized spectral index function for the flat-spectrum radio sources

$\eta_s(\alpha|P)$ = normalized spectral index function (i.e. the conditional probability function) for steep-spectrum sources for a given luminosity P.

A suitable form for $\eta_f(\alpha)$ and $\eta_s(\alpha|P)$ needs to be chosen. Petrosian and Dickey (1973) have shown that a bimodal spectral index function consisting of two Gaussians, one centred around $\alpha = 0.4$ and another around $\alpha = 0.8$, gives good agreement at 408 MHz. The 178 MHz spectral index function (Fanaroff and Longair 1973) also has a similar form. In view of this we have chosen the following forms:

$$\eta_f(\alpha) = \frac{1}{\sigma_f\sqrt{2\pi}} \exp[-(\alpha-\alpha_{of})^2/2\sigma_f^2] \qquad (4.19)$$

and

$$\eta_s(\alpha|P) = \frac{1}{\sigma_s\sqrt{2\pi}} \exp[-(\alpha-\alpha_{os})^2/2\sigma_s^2] \qquad (4.20)$$

where σ_f and σ_s and α_{of} are treated as free parameters. In general α_{os} is a function of radio luminosity. The correlation

between P and α is introduced into the formalism through α_{os}. A larger value of P would imply a larger value of α_{os} around which $\eta_s(\alpha|P)$ will be centred. If α_{os} is independent of luminosity P, then $\eta_s(\alpha|P) = \eta_s(\alpha)$ will be independent of luminosity P. However, in general both α_{os} and σ_s are functions of radio luminosity. With a view to keep the model as simple as possible but still including dependence of spectral index on luminosity, we have considered only luminosity dependence of α_{os}. In the absence of any observational evidence to believe in the contrary, it is quite reasonable to assume that σ_s is independent of P. In any case, as pointed out by Famaroff and Longair (1973) and Petrosian and Dickey (1973), these correlations are not likely to cause any appreciable changes in the results. A relation between α_{os} and P can be obtained by using the relation

$$< \alpha > = \int \alpha \eta_s(\alpha|P) d\alpha = \alpha_{os}(P) \qquad (4.21)$$

Using relation (4.17) between $< \alpha >$ and $<\log P>$ we can write

$$\alpha_{os}(P) = -0.14 + 0.037 <\log P> \qquad (4.22)$$

It is more convenient to write the above equation in the form

$$\alpha_{os}(P) = -0.14 + 0.037 <\log P> + a_o \qquad (4.23)$$

and treat a_o as an adjustable free parameter. Appropriate values of C_f and C_s can be estimated by considering the

observed spectral index distributions at low frequencies. Since ~ 5-10 per cent of sources in the low frequency surveys have flat-spectra, it is reasonable to assume $C_f \sim 0.05$. Since $C_f + C_s = 1$, it follows that $C_s \sim 0.95$.

4.3.4. The Choice of World Model and Luminosity Function

We have considered only the Einstein-de Sitter model in our calculations because the geometric differences between various world models are small in comparison with the overall effects of evolution. The local luminosity function was derived by following a procedure similar to that of Wall et al. (1977) and using the 408 MHz luminosity distribution (histogram) given by them. We employed the evolution function of model 4b of Wall et al. We used model 4b because Wall et al. seem to prefer it after comparing redshift distributions predicted by different models with the identifications of the 5C3 survey. Moreover, this (model 4b) is shown to produce angular size counts of extragalactic radio sources that are in agreement with the observational data (Subrahmanya 1977). We have assumed the same local luminosity function for flat- and steep-spectrum sources, because with the data available at present it is not possible to derive the local luminosity function for flat- and steep-spectrum sources separately.

The choice of evolution function for flat- and steep-spectrum sources presents another problem. The evolution function for the steep-spectrum sources was taken to be the

same as the one given by Wall et al. This assumption is a reasonable one because Wall et al. used the 408 MHz source counts in their investigations and ~ 90 per cent of the sources selected at 408 MHz have steep spectra. Since we do not know much about the evolution function for flat-spectrum sources, we represented it by some analytic form that contains some free parameters and estimated these free parameters. In the choice of a suitable form for $F_f(P,z)$ we were guided by the results of the V/V_m test for flat-spectrum quasars.

4.3.5. The Calculations

In the Einstein-de Sitter model the redshift $z(P,S,\alpha)$ upto which a radio source of spectral index α and luminosity $P(\nu)$ at the frequency of observation ν(νbeing 408 MHz in our case) can have a flux density greater than the limiting flux density $S(\nu)$, is the solution of

$$P(\nu) = \frac{4c^2}{H_o^2} S(\nu)\left[1-(1+z)^{-\frac{1}{2}}\right]^2 (1+z)^{\alpha+1} \qquad (4.24)$$

The number of sources with spectral index in the range α and $\alpha+d\alpha$, luminosities in the range P and P+dP and in the volume bounded by $z(P,S,\alpha)$ is

$$\int_o^{z^*} \psi(P,z,\alpha)\frac{dV(z)}{dz}\, dz\, d\alpha\, dP \qquad (4.25)$$

where dV is the comoving volume element and $z^*=z(P,S,\alpha)$.

The number of sources with flux density $\geq S(\nu)$ and spectral index in the range α and $\alpha+d\alpha$ is

$$N[>S(\nu),\nu,\alpha]\, d\alpha = \int_{P(\nu)} dP \int_{0}^{z^*} \Psi(P,z,\alpha)\frac{dV(z)}{dz}dz\, d\alpha \qquad (4.26)$$

The spectral index distribution at frequency ν is then given by

$$g^{\nu}_{S(\nu)}[\alpha] = \frac{N[>S(\nu),\nu,\alpha]}{\int_{\alpha} N[>S(\nu),\nu,\alpha]d\alpha} \qquad (4.27)$$

and the source counts (integral) at frequency ν by

$$N[>S(\nu),\nu] = \int_{\alpha} N[>S(\nu),\nu,\alpha]\, d\alpha \qquad (4.28)$$

The differential counts at frequency ν can be calculated using the relation

$$n[S(\nu),\nu] = \frac{N[>rS(\nu),\nu]-N[>\frac{S(\nu)}{r},\nu]}{[rS(\nu)-\frac{S(\nu)}{r}]} \qquad (4.29)$$

as $r \longrightarrow 1$.

The above formalism can be easily modified to calculate the source counts and spectral index distributions at some other frequency. Let $g^{\nu'}_{S(\nu')}[\alpha]$ be the spectral index

distribution of all the sources with flux density $\geq S'(\nu')$ at frequency ν' (=5000 MHz in the present case), and let $N'[>S'(\nu'),\nu']$ be the number of sources with flux density $\geq S'(\nu')$ at ν'. Now a source with luminosity P at frequency ν will have a luminosity P' at frequency ν', given by

$$P' = P(\nu/\nu')^{\alpha} \qquad (4.30)$$

Using this relation for P', equations similar to (4.27) and (4.28) can be obtained for $g^{\nu'}_{S'(\nu')}[\alpha]$ and $N'[>S'(\nu'),\nu']$.

4.3.6. The Models

We have considered three models A,B and C depending on whether radio luminosity P and spectral index α are correlated or not and on whether flat- and steep-spectrum sources differ in their density evolution. We have not followed any systematic optimizing procedure for deriving model parameters because we only wish to demonstrate that the incorporation of some observed effects into source-count models leads to consistency with observed source counts and spectral index distributions at 408 MHz and 5000 MHz.

1) Model A:

In this model P and α are correlated. The evolution of flat-spectrum sources is different from the evolution of steep-spectrum sources. We then assume that

$$\psi(P,z,\alpha) = \rho(P,z=0)[C_f F_f(P,z)\eta_f(\alpha)+C_s F_s(P,z)\eta_s(\alpha|P)] \qquad (4.31)$$

where

$$F_f(P,z) = \exp[M_f(P)(1-t/t_o)];\ \frac{t}{t_o} = (1+z)^{-1.5},$$

t_o = present-epoch

with

$$M_f(P) = 0 \text{ for } \log P \leq \log P_{f1} = 22.5$$

$$= M_{f\ max} = 8.0 \text{ for } \log P \geq \log P_{f2} = 28.0$$

$$= M_{f\ max} \frac{(\log P - \log P_{f1})}{(\log P_{f2} - \log P_{f1})} \text{ for } \log P_{f1} < \log P < \log P_{f2}$$

$$F_f(P,z) = 0 \text{ if } z > z_c = 3.5$$

and

$$F_s(P,z) = \exp[M_s(P)(1-t/t_o)],$$

with

$$M_s(P) = 0 \text{ for } \log P \leq \log P_{s1} = 25.0$$

$$= M_{s\ max} = 11.0 \text{ for } \log P \geq \log P_{s2} = 27.3$$

$$= M_{s\ max} \frac{(\log P - \log P_{s1})}{(\log P_{s2} - \log P_{s1})}$$

for $\log P_{s1} < \log P < \log P_{s2}$

$$F_s(P,z) = 0 \text{ if } z > z_c = 3.5$$

and

$$C_f = 0.035,\ C_s = 0.965$$

$$\eta_f(\alpha) = \frac{1}{\sigma_f\sqrt{2\pi}} \exp[-(\alpha-\alpha_{of})^2/2\sigma_f^2], \text{ with } \sigma_f = 0.25, \alpha_{of} = 0.25,$$

and

$$\eta_s(\alpha|P) = \frac{1}{\sigma_s\sqrt{2\pi}} \exp[-(\alpha-\alpha_{os})^2/2\sigma_s^2] \text{ where } \sigma_s = 0.20$$

and

$$\alpha_{os} = -0.14+0.037 < \log P > +0.05 .$$

2) Model B

In this model both flat- and steep-spectrum sources evolve in the same manner. The radio luminosity and spectral index are assumed to be correlated. In this case we have

$$\Psi(P,z,\alpha) = \rho(P,z=0)F(P,z)[C_f\eta_f(\alpha)+C_s\eta_s(\alpha|P)] ,$$

where

$F(P,z)$ = same as $F_s(P,z)$ of model A

$C_f = 0.015$, $C_s = 0.985$.

All the other parameters are the same as in model A.

3) Model C

In this model, flat- and steep-spectrum sources evolve in identical manner and P and α are assumed to be uncorrelated.

$$\Psi'(P,z,\alpha) = \rho(P,z=0)F(P,z)[C_f\eta_f(\alpha)+C_s\eta_s(\alpha)]$$

with $\alpha_{os} = 0.83$. All other parameters are the same as in model B above. The essential features of model C are the same as those of the model proposed by Fanaroff and Longair (1973).

The values of C_f/C_s assumed in all these models may appear rather small when one considers the fact that flat-spectrum sources constitute more than 50 per cent of the 5 GHz

count and ~ 10 per cent of the 408 MHz count. This can be easily explained in the frame work of evolutionary world models. For a given luminosity class at 408 MHz, sources with small α (flat-spectrum) can be observed to larger redshifts (at a given flux density) than those with large α. Since in the above models the comoving space density of radio sources increases rapidly with redshift, the fraction of flat-spectrum sources in the 408 MHz sample increases to ~ 10 per cent. In the high frequency sample (5000 MHz), this fraction is further enhanced by the induced strong correlation between small α (flat-spectrum) and high radio power. This is one of the many interesting results of the investigations of Fanaroff and Longair (1973).

4.4 The Results

For each of the models considered above, the values of the free parameters were obtained by trial and error by requiring that the calculated source counts and spectral index distributions at 408 MHz be consistent with the observations. The values of the free parameters and the results presented here are slightly different from those presented by us earlier (Kulkarni 1978). For example, the present calculations give a value of 0.035 for the fraction of flat-spectrum sources C_f compared to 0.05 obtained in our earlier computations. However, the earlier analysis was based on a rough approximation to local luminosity function, while the present calculations use

a more accurate representation of local luminosity function and hence they are more accurate.

In the following pages we compare the predictions of different models with the observational data at different frequencies and see which of the models gives the best agreement with the observations.

4.4.1. The Source Counts and Spectral Index Distribution at 408 MHz

As discussed in Chapter 3, the observational situation regarding the nature of spectral index distributions for sources selected at 408 MHz is not yet clear. However, since some trends are indicated, we have compared the predicted distributions with the observed (Pauliny-Toth and Kellermann 1972a) ones in Table 4.2. For each model we have calculated the fraction of flat-spectrum sources F(408,5000) and the median spectral index $\alpha_{med}(408,5000)$ in different flux density ranges. Considering the uncertainties in the observational data, all the three models can be said to give fairly good agreement with the observational results. However, there are two differences in the predictions by different models. Firstly, model A predicts an increase in the fraction of flat-spectrum sources with decreasing flux density at flux density level of $S(408) \sim 0.05$ Jy. Also, according to model A, the median spectral index for flat-spectrum sources ($\alpha < 0.5$) should decrease from ~ 0.37 at $S(408) \sim 11$ Jy to ~ 0.27 at $S(408) \sim 0.04$ Jy. It is interesting to note that from a study of

TABLE 4.2 : Comparison of Predicted and Observed (Pauliny-Toth and Kellermann (1972a) Spectral Index Distribution at 408 MHz.

Flux density S at 408 MHz (Jy)	Frequencies (MHz)	Median Spectral index α_{med}				Fraction of flat-spectrum sources			
		Observed	Model A	Model B	Model C	Observed	Model A	Model B	Model C
S > 11.8	408-5000	0.75±0.02	0.87	0.88	0.81	0.10±0.05	0.06	0.05	0.08
11.8 > S > 8.7	"	0.80±0.03	0.87	0.88	0.80	0.06±0.03	0.06	0.05	0.09
8.7 > S > 6.9	"	0.83±0.03	0.87	0.88	0.79	0.10±0.05	0.06	0.06	0.09
6.8 > S > 4.1	"	0.83±0.03	0.87	0.88	0.79	0.06±0.03	0.06	0.06	0.10
4.0 > S > 2.21	"	0.82±0.03	0.87	0.87	0.78	0.15±0.06	0.06	0.06	0.10
2.19 > S > 0.89	"	0.83±0.02	0.87	0.87	0.78	0.10±0.05	0.07	0.06	0.11
0.86 > S > 0.48	"	0.78±0.03	0.86	0.87	0.78	0.13±0.05	0.07	0.06	0.10
0.4 > S > 0.2	"		0.86	0.87	0.79		0.08	0.06	0.09
0.1 > S > 0.05	"		0.84	0.86	0.81		0.12	0.06	0.07
0.05 > S > 0.02	"		0.81	0.84	0.82		0.15	0.06	0.07

spectral indices between 408 MHz and 1400 MHz, Katgert (1976) has reported (i) a marginally significant increase in the fraction of flat-spectrum sources below about 0.06 Jy at 408 MHz and (ii) a widening in spectral index distribution at flux density level of S(408) ~ 0.06 Jy. A quantitative comparison is not very meaningful because of the different types of spectral indices involved and different ways of classifying sources as having flat- and steep-spectra. For instance, in the models we have used the two-point spectral indices $\alpha(408,5000)$ whereas Katgert's results refer to $\alpha(408,1400)$.

Secondly, the values of median spectral index predicted by models A and B are larger than those predicted by model C. This is expected, because in models A and B we have considered the correlation between P and α. The increase in α with decreasing flux density observed by Murdoch (1976) at 408 MHz is not predicted by any of these models. However, again, these predictions cannot be directly compared with Murdoch's result since the observations refer to two-point spectral indices between 408 MHz and 2700 MHz, whereas in models A, B and C two-point spectral indices between 408 MHz and 5000 MHz are used. Moreover, the steepening of spectrum at low flux densities for sources selected in a low frequency survey needs to be confirmed.

We started with model 4b of Wall et al. (1977). This model predicts source counts that are in very good agreement with the observed counts. The model was derived by assuming

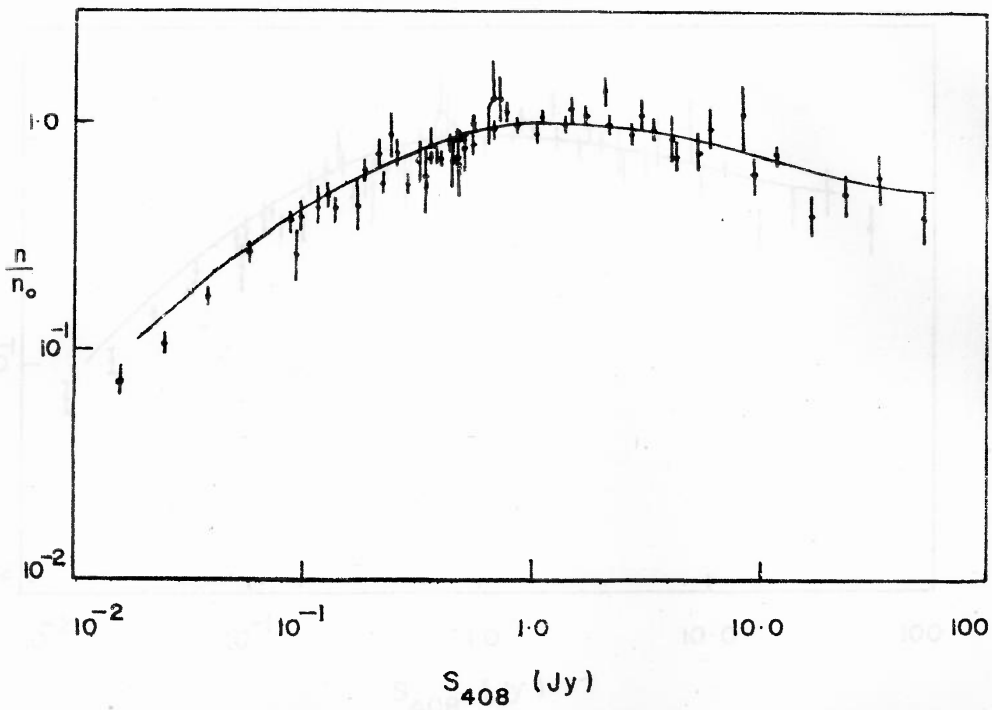

FIG. 4·2 (a) COMPARISON OF THE OBSERVED (FOR REFERENCES SEE TEXT) AND THE PREDICTED (MODEL A) NORMALIZED DIFFERENTIAL COUNTS AT 408 MHz.

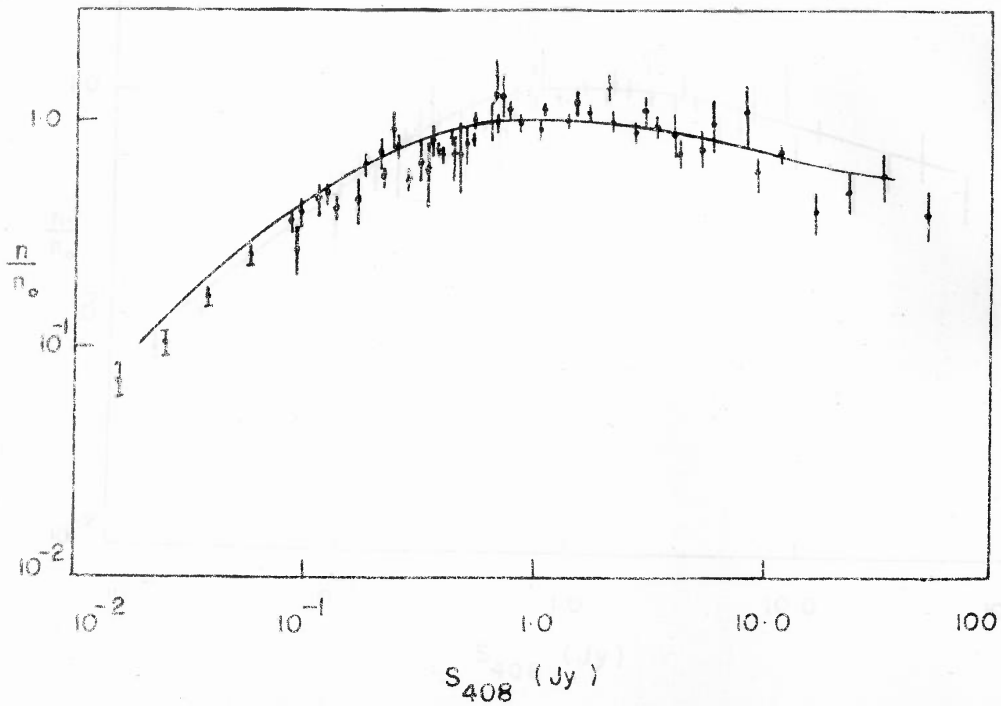

FIG. 4·2 (b) COMPARISON OF THE OBSERVED (FOR REFERENCES SEE TEXT) AND THE PREDICTED (MODEL B) NORMALIZED DIFFERENTIAL COUNTS AT 408 MHz

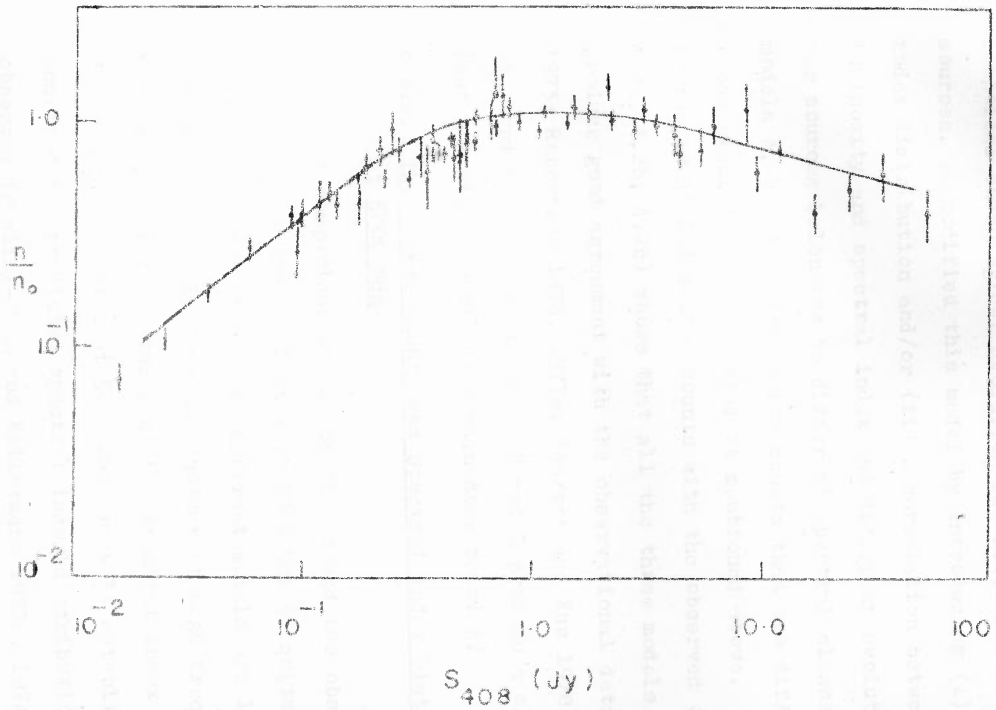

FIG. 4·2 (c) COMPARISON OF THE OBSERVED (FOR REFERENCES SEE TEXT) AND THE PREDICTED (MODEL C) NORMALIZED DIFFERENTIAL COUNTS AT 408 MHz.

(i) a spectral index of 0.75 for all the sources (ii) an identical cosmological evolution for flat- and steep-spectrum sources. We modified this model by introducing (i) a spectral index distribution and/or (ii) a correlation between radio luminosity and spectral index and different evolution function for sources belonging to different spectral classes. Hence models A, B and C give source counts that are different from those predicted by the model 4b mentioned above. A comparison of the predicted source counts with the observed ones (Figs. 4.2a, 4.2b, 4.2c) shows that all the three models A,B and C produce good agreement with the observational data(Colla et al. 1973; Robertson 1973, 1977c; Pearson and Kus 1978). However, it might be added that models B and C produce a slightly better (but not significantly)fit than does model A.

4.4.2. The Source Counts and Spectral Index Distribution at 5000 MHz

A comparison of the predicted and the observed distributions for sources selected at 5000 MHz is quite important because the predictions of different models are likely to differ considerably from one another at high frequencies. Moreover, certain features of the spectral index distributions for sources selected at 5000 MHz are well established. We have compared the predicted spectral index distributions with those observed (Pauliny-Toth and Kellermann 1972b, 1974; Condon and Jauncey 1974b; Davis 1977; Willis and Miley 1979) in Tables 4.3(a), 4.3(b) and 4.3(c). In these tables we have listed

TABLE 4.3(a) : Comparison of Predicted and Observed Values of Median Spectral Index α_{med} at 5000 MHz for all Sources

Reference for Observations	Flux density S at 5000 MHz (Jy)	Frequencies (MHz)	Median spectral index α_{med}			
			Observed	Model A	Model B	Model C
Pauliny-Toth and Kellermann (1972b, 1974)	$S \geq 1.5$	408-5000	0.30±0.06	0.46	0.45	0.47
	$1.5 > S \geq 1.0$	"	0.35±0.05	0.46	0.50	0.50
	$1.0 > S \geq 0.8$	"	0.54±0.06	0.47	0.54	0.52
	$0.8 > S \geq 0.6$	"	0.55±0.05	0.49	0.57	0.54
	$0.6 > S \geq 0.1$	"	0.60±0.07	0.57	0.68	0.62
	$0.1 > S \geq 0.067$	"	0.63±0.04	0.61	0.72	0.66
Condon and Jauncey (1974b)	$S > 1.15$	318-5000	0.34±0.15	0.46	0.47	0.48
	$1.15 > S \geq 0.8$	"	0.43±0.07	0.47	0.53	0.52
	$0.8 > S \geq 0.6$	"	$0.55^{+0.04}_{-0.11}$	0.49	0.57	0.54
	$0.6 > S \geq 0.25$	"	$0.49^{+0.10}_{-0.15}$	0.53	0.63	0.58
	$0.25 > S \geq 0.067$	"	$0.57^{+0.02}_{-0.03}$	0.60	0.70	0.64
Davis (1977)	$S > 0.02$	1400-5000	0.60	0.63	0.74	0.68
	$S > 0.009$	"		0.64	0.75	0.71

TABLE 4.3(b) : Comparison of Predicted and Observed Values of $\alpha_{n\,med}$ at 5000 MHz for Sources with $\alpha \geq 0.5$

References for Observations	Flux density S at 5000 MHz (Jy)	Frequencies (MHz)	Median spectral index $\alpha_{n\,med}$			
			Observed	Model A	Model B	Model C
Condon and Jauncey (1974b)	S > 1.15	318-5000	0.66±0.027	0.70	0.70	0.61
	1.15 > S ≥ 0.8	"	0.73±0.03	0.70	0.70	0.60
	0.8 > S ≥ 0.6	"	0.70±0.024	0.70	0.70	0.60
	0.6 > S ≥ 0.25	"	0.79±0.05	0.71	0.71	0.62
	0.25 > S ≥ 0.067	"	0.76±0.021	0.73	0.73	0.66
	S > 0.02			0.76	0.76	0.70
	S > 0.009			0.77	0.77	0.72

TABLE 4.3(c) : Comparison of Predicted and Observed Values of the Fraction of Flat-Spectrum Sources at 5000 MHz

References for Observations	Flux Density S at 5000 MHz (Jy)	Frequencies (MHz)	Fraction of 'Flat Spectrum Sources'			
			Observed	Model A	Model B	Model C
Pauliny-Toth and Kellermann (1972b, 1974)	$S \geq 1.5$	408-5000	0.57±0.10	0.53	0.53	0.53
	$1.5 > S \geq 1.0$	"	0.60±0.09	0.53	0.50	0.50
	$1.0 > S \geq 0.8$	"	0.47±0.09	0.52	0.47	0.47
	$0.8 > S \geq 0.6$	"	0.45±0.07	0.51	0.44	0.45
	$0.6 > S \geq 0.1$	"	0.43±0.10	0.44	0.27	0.30
	$0.1 > S \geq 0.067$	"	0.40±0.09	0.43	0.19	0.23
Condon and Jauncey (1974b)	$S \geq 1.15$	318-5000	0.56±0.05	0.53	0.52	0.52
	$1.15 > S \geq 0.8$	"	0.57±0.05	0.52	0.47	0.48
	$0.8 > S \geq 0.6$	"	0.48±0.05	0.51	0.44	0.45
	$0.6 > S \geq 0.25$	"	0.52±0.08	0.48	0.35	0.38
	$0.25 > S \geq 0.067$	"	0.43±0.04	0.41	0.22	0.26
Davis (1977)	$S > 0.02$	1400-5000	0.36	0.39	0.17	0.20
	$S > 0.009$	"	0.34	0.39	0.16	0.17
Willis and Miley (1979)	$S \geq 0.005$	1400-5000	0.35±0.13	0.40	0.16	0.17

for each model and in different flux density intervals, (i) the median value (α_{med}) of the spectral index for the whole distribution, (ii) the median spectral index ($\alpha_{n\ med}$) for the steep-spectrum sources and (iii) the fraction of sources with $\alpha \leq 0.5$. The values of the median spectral index $\alpha_{n\ med}$ were estimated by following a procedure similar to that of Condon and Jauncey (1974a). This procedure involves passing the distributions through a mathematical window of width ~ 0.4 and choosing the median value in such a way that it coincides with the window centre. Also note that in our comparison we have assumed that

$$f^{5000}_{S(5000)}\,[\alpha(5000,408)] \simeq f^{5000}_{S(5000)}\,[\alpha(5000,318)] \simeq f^{5000}_{S(5000)}\,[\alpha(5000,1400)]$$

In the high and intermediate flux density ranges all the three models A, B and C are in good agreement with the observations, but at low flux density levels of below ~ 0.1 Jy models B and C predict too low a value for the fraction of flat-spectrum sources. The discrepancy between the predictions can also be seen from a comparison of the observed and predicted values of α_{med}. Thus at flux density levels below ~ 0.1 Jy at 5000 MHz, only model A is in agreement with the observational data.

A comparison of predicted and observed $\alpha_{n\ med}$ shows that models A, B and C are in qualitative agreement with the

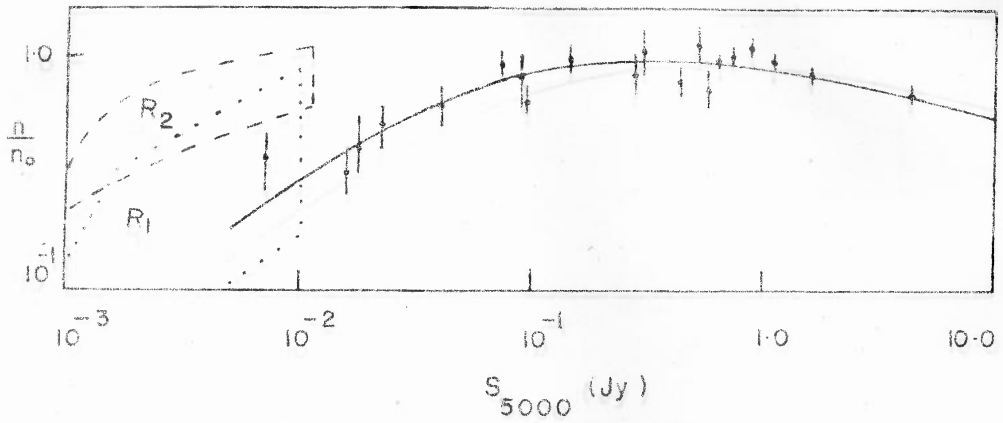

FIG. 4·3 (a) COMPARISON OF THE OBSERVED (FOR REFERENCES SEE TEXT) AND THE PREDICTED (MODEL A) NORMALIZED DIFFERENTIAL COUNTS AT 5000 MHz. THE AREAS R_1 & R_2 BOUNDED RESPECTIVELY BY DOTTED & DASHED CURVES REPRESENT THE RESULTS FROM BACKGROUND DEFLECTION OR P(D) ANALYSIS (SEE PAULINY – TOTH 1977; WALL 1978).

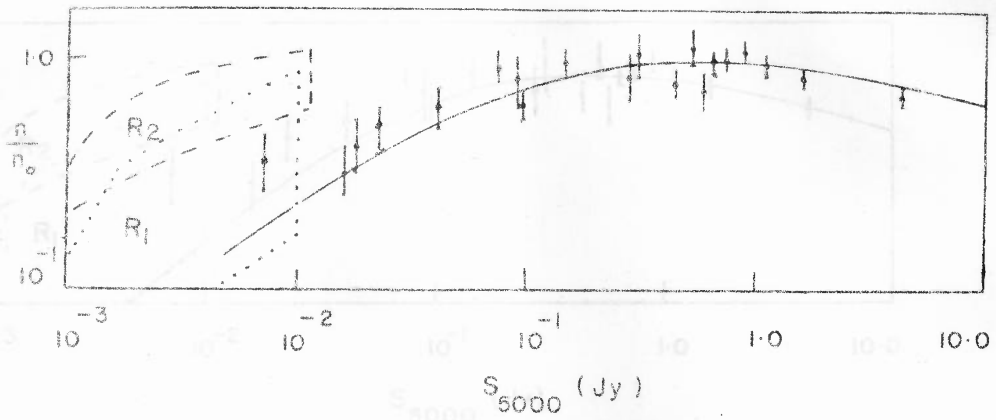

FIG. 4·3 (b) COMPARISON OF THE OBSERVED (FOR REFERENCES SEE TEXT) AND THE PREDICTED (MODEL B) NORMALIZED DIFFERENTIAL COUNTS AT 5000 MHz. THE AREAS R_1 & R_2 BOUNDED RESPECTIVELY BY DOTTED & DASHED CURVES REPRESENT THE RESULTS FROM BACKGROUND DEFLECTION OR P(D) ANALYSIS (SEE PAULINY-TOTH 1977; WALL 1978).

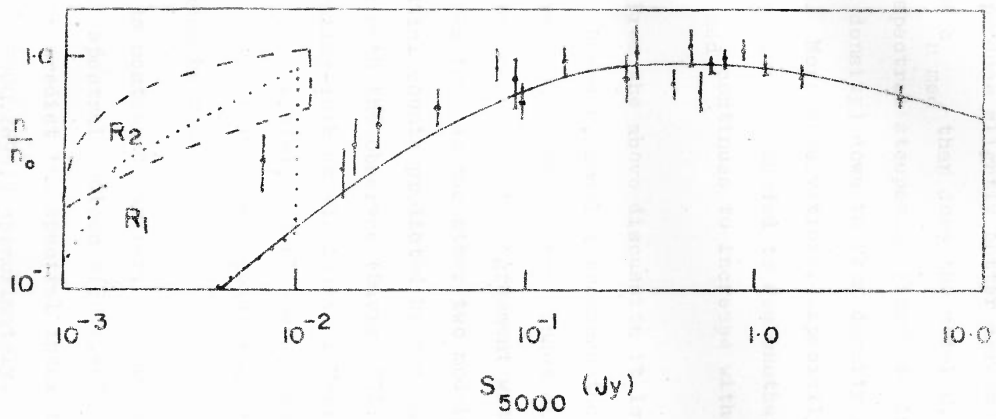

FIG. 4·3(c) COMPARISON OF THE OBSERVED (FOR REFERENCES SEE TEXT) AND THE PREDICTED (MODEL C) NORMALIZED DIFFERENTIAL COUNTS AT 5000 MHz. THE AREAS R_1 & R_2 BOUNDED RESPECTIVELY, BY THE DOTTED & DASHED CURVES REPRESENT • THE RESULTS FROM BACKGROUND DEFLECTION OR P(D) ANALYSIS (SEE PAULINY-TOTH 1977; WALL 1978).

data in the sense that all of them predict an increase (steepening) in $\alpha_{n\ med}$ with decreasing flux density. However, models A and B produce slightly better agreement with the observed values of $\alpha_{n\ med}$ than does the model C. All these models predict spectral steepening (increase in $\alpha_{n\ med}$ with decreasing flux density) down to flux density level of $\sim$ 0.01 Jy at 5000 MHz. More observations, especially in the low flux density region are needed to see whether median spectral index $\alpha_{n\ med}$ continues to increase with decreasing flux density.

From the above discussion it is clear that among models A, B and C, model A produces the best agreement with the observed 5000 MHz spectral index distribution. Moreover, model A produces a better agreement with the observed counts at 5000 MHz than do the other two models. The normalized differential counts predicted by models A, B and C are compared with the observed (Davis 1971; Pauliny-Toth et al. 1972; Pauliny-Toth et al. 1978a, 1978b; Willis and Miley 1979) ones in Figs. 4.3(a), 4.3(b) and 4.3(c) respectively. The best agreement between the predicted counts and those observed is produced by model A.

As mentioned earlier, the model calculations refer to two-point spectral indices $\alpha(5000,408)$. Nevertheless, it can be used to predict the spectral index distribution $f_{S(5000)}^{5000}[\alpha(5000,2695)]$ approximately. In Table 4.4, we have compared the predictions of models A, B and C with those

TABLE 4.4 : Comparison of Predicted and Observed Distributions $f_{S(5000)}^{5000}$ [$\alpha(5000,2695)$]

References for Observations	Flux density S at 5000 MHz (Jy)	Frequencies (MHz)	Median Spectral Index α_{med}				Fraction of Flat-Spectrum Sources			
			Observed	Model A	Model B	Model C	Observed	Model A	Model B	Model C
Pauliny-Toth and Kellermann (1974) and Pauliny-Toth et al. (1978a)	$S \geq 2.1$	2695-5000	0.43±0.09	0.46	0.44	0.47	0.54±0.07	0.52	0.54	0.53
	$2.1 > S \geq 1.3$	"	0.30±0.11	0.45	0.47	0.49	0.58±0.06	0.53	0.52	0.52
	$1.3 > S \geq 0.96$	"	0.36±0.10	0.46	0.51	0.51	0.56±0.05	0.52	0.49	0.49
	$0.96 > S \geq 0.8$	"	0.54±0.08	0.47	0.54	0.52	0.48±0.06	0.52	0.47	0.47
	$0.8 > S \geq 0.6$	"	0.47±0.05	0.49	0.57	0.54	0.50±0.04	0.51	0.44	0.45
	$0.6 > S \geq 0.5$	"	0.52±0.11	0.50	0.59	0.55	0.48±0.09	0.50	0.41	0.43
	$0.6 > S \geq 0.067$	"	0.45±0.04	0.59	0.70	0.64	0.49±0.06	0.42	0.23	0.27

observed (Pauliny-Toth and Kellermann 1974; Pauliny-Toth et al. 1978a). It is clear from Table 4.4 that there is a general agreement between model predictions and the observational data at least at high flux densities. In the flux density interval 0.07 to 0.6 Jy, all these models give a larger value for α_{med} and a smaller value for the fraction of flat-spectrum sources than the corresponding observed values. However, the discrepancy between model predictions and observational results is smallest in the case of model A.

From the above discussion it is clear that on the whole model A produces the best agreement with the experimental data. Hence in what follows we consider only model A and refer to it as 'the present model' or simply 'the model'.

4.4.3. The Source Counts and Spectral Index Distributions at 1400 MHz and 2700 MHz.

The model parameters were derived by considering the spectral index function $n[\alpha(408,5000)]$. Also in deriving a relation between $< \alpha >$ and luminosity P(408) we used two-point spectral indices $\alpha(408,5000)$. Hence, strictly speaking, the model should be used to predict source counts and spectral index distributions for sources selected either at 408 MHz or at 5000 MHz only. To predict source counts either at 1400 MHz or 2700 MHz, in deriving the model parameters we should use the appropriate two-point spectral indices i.e. $\alpha(408,1400)$ and $\alpha(408,2700)$ respectively. However, the results of the present model can still be compared with the observed spectral

index distributions at 1400 MHz and at 2700 MHz if we assume that

$$f^{408}_{S(408)}[\alpha(408,1400)] \simeq f^{408}_{S(408)}[\alpha(408,5000)] \text{ and } f^{408}_{S(408)}[\alpha(408,2700)] = f^{408}_{S(408)}[\alpha(408,5000)]$$

This appears to be a reasonable assumption because the model is based on the 408 MHz luminosity function and a majority of the sources selected at 408 MHz have straight spectra. In any case it is interesting to compare the predicted and observed spectral index distributions and source counts at 1400 MHz and 2700 MHz. This is done in the following pages.

The observational aspects of spectral index distributions for sources selected at 1400 MHz were summarized in Chapter 3. The spectral index distributions estimated on the basis of the model are compared with the observed ones (Pearson and Kus 1978) in Table 4.5(c). Considering the uncertainties in the measurements, the agreement between the predicted and observed values of spectral parameters is quite good. At the flux density level of ~2 mJy, the model seems to predict a slightly larger value for the fraction of flat-spectrum sources and the discrepancy between model predictions and observations seems to become just significant .

A comparison of the predicted spectral index distributions with those observed (Maslowski 1977) for the sources from the GB2 and GB surveys [Tables 4.5(b), 4.5(c)] tells a somewhat different story. The values of the fraction of flat-spectrum sources predicted by the model are in good agreement with the observed ones. But, the model seems to run

TABLE 4.5(a) : Comparison of Observed and Predicted Spectral Index Distributions $f^{1400}_{S(1400)}[\alpha(1400, \nu_2)]$

Sample	ν_2 (MHz)	No. of sources	Mean spectral index $\bar{\alpha}$ (1400, ν_2)		Median spectral index α_{med} (1400, ν_2)		Fraction of flat-spectrum sources F(1400, ν_2)		Mean spectral index for sources with $\alpha \geq 0.3$. $\bar{\alpha}_n$(140), ν_2)	
			Observed	Predicted	Observed	Predicted	Observed	Predicted	Observed	Predicted
5C5: All sources detected at 1407 MHz S(1407)> 1.8 mJy	408	47	0.67±0.07	0.64	0.79	0.70	0.21±0.06	0.27	0.85±0.03	0.77
5C6: All sources detected at 1407 MHz S(1407)> 1.5 mJy	408	48	0.69±0.04	0.64	0.74	0.69	0.25±0.06	0.28	0.76±0.03	0.76
5C7: All sources detected at 1407 MHz S(1407)> 1.5 mJy	408	44	0.75±0.05	0.64	0.80	0.69	0.18±0.06	0.28	0.83±0.04	0.76
Samples with 10 < S(1400) < 200 mJy 5C2, 3 and 4 (Willson 1972a)	408	38	0.72±0.06	0.69	0.77	0.76	0.26±0.07	0.23	0.83±0.04	0.31
5C5, 6 and 7	408	60	0.66±0.06	0.69	0.77	0.76	0.23±0.05	0.23	0.84±0.03	0.31
5C2 - 7	408	98	0.67±0.04	0.69	0.77	0.76	0.24±0.04	0.23	0.84±0.03	0.31
Comparison Samples:										
Westerbork S(1400) 20 mJy (Katgert et al. 1977)	610	174*	0.64±0.03	0.70		0.77	0.25±0.04	0.21		0.32
Half-mile S(1400) 10 mJy (Gillespie 1975)	408	140	0.71±0.03	0.69	0.80	0.76	0.21±0.04	0.23	0.81±0.03	0.81
BDFL/B2(2Jy) (Katgert et al. 1977)	408	50	0.61±0.05	0.70		0.76	0.25±0.07	0.19		0.80

* The Westerbork sample contains a further 9 sources for which S(610) is not available. The statistics have been calculated by including both upper limits and true estimates with equal weight (for details see Pearson and Kus 1978).

TABLE 4.5(b) : Comparison of Model Predictions with the Spectral Parameters of the Sources in the GB2 Survey

Flux density S at 1400 MHz (Jy)	Median Spectral index: Observed $\alpha_{med}(1400, \nu_2)$		Pred	Median Spectral index $\alpha_{n\,med}$ for the steep-spectrum sources: Observed $\alpha_{n\,med}(1400, \nu_2)$		Pred	Fraction of flat-spectrum sources: Observed $F(1400, \nu_2)$		Pred
	ν_2 = 408	ν_2 = 5000		ν_2 = 408	ν_2 = 5000		ν_2 = 408	ν_2 = 5000	
0.70 - 2.0	0.74±0.028	0.82±0.031	0.76	0.75±0.017	0.89±0.019	0.80	0.20±0.044	0.17±0.042	0.19
0.50 - 0.69	0.80±0.028	0.84±0.025	0.76	0.85±0.014	0.86±0.019	0.80	0.21±0.045	0.12±0.035	0.19
0.1 - 0.2			0.78			0.82			0.19
0.05 - 0.1			0.78			0.82			0.20

NOTE: The observed values are taken from Maslowski (1977).

TABLE 4.5(c) : Comparison of Model Predictions with the Spectral Parameters of the GB Sources

References for Observations	Flux density S at 1400 MHz (Jy)	Median spectral index α_{med} (1400, 2695)		Median spectral index for the steep-spectrum sources $\alpha_{n\ med}$ (1400, 2695)		Fraction of flat-spectrum sources F(1400, 2695)	
		Observed	Predicted	Observed	Predicted	Observed	Predicted
Maslowski (1977)	0.50- ∞	0.89±0.036	0.76	0.92±0.022	0.80	0.21±0.039	0.19
	0.33-0.49	0.79±0.035	0.76	0.81±0.017	0.80	0.20±0.039	0.19
	0.24-0.32	0.89±0.025	0.77	0.94±0.016	0.80	0.11±0.030	0.19
	0.20-0.23	0.85±0.036	0.77	0.92±0.020	0.81	0.20±0.038	0.19

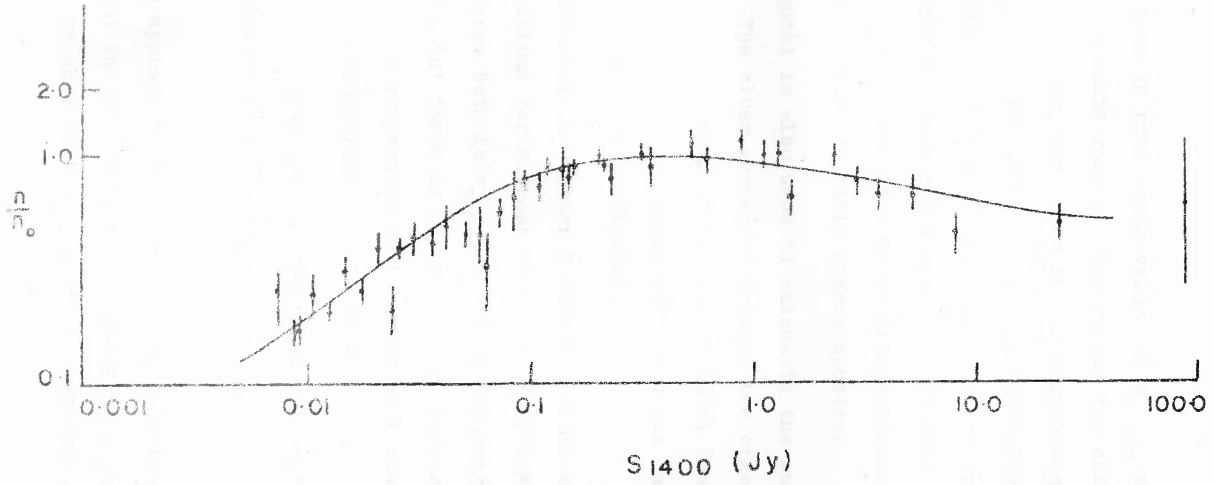

FIG. 4·4 COMPARISON OF THE OBSERVED (FOR REFERENCES SEE TEXT) AND THE PREDICTED (MODEL A) NORMALIZED DIFFERENTIAL COUNTS AT 1400 MHz.

into difficulties in predicting values of $\alpha_{n\ med}$ and α_{med} in different flux density ranges. The reason for this discrepancy is not clear. However, note that in our comparison we have assumed $f^{1400}_{S(1400)}[\alpha(1400,408)]$, $f^{1400}_{S(1400)}[\alpha(1400,2695]$ and $f^{1400}_{S(1400)}[\alpha(1400,5000]$ to be approximately equal to one another. This is probably an oversimplification. It will be interesting to investigate whether the above discrepancies can arise from the curved nature of radio source spectra.

The model is also used to calculate the source counts at 1400 MHz. The close agreement between the observed (see Fomalont, Bridle and Davis 1974; Katgert 1976; Pearson and Kus 1978; Machalski 1978b; Oosterbaan 1978) and the calculated source counts is clear from Fig.4.4.

As discussed in Chapter 3 investigations of spectral index distributions for sources selected at 2700 MHz show that there is a change both in $\alpha_{n\ med}$ and F in the range $0.5 < S(2700) < 0.85$, but there is no evidence of further change down to 0.1 Jy. A comparison of observational results (Table 4.6) and model calculations reveals that:

i) There is a good agreement between the predicted and the observed values of $F(2700,\nu_2)$.

ii) There appears to be some discrepancy between the model predictions and the observations regarding $\alpha_{n\ med}(2700,\nu_2)$. The observations show that $\alpha_{n\ med}$ starts decreasing at a flux

TABLE 4.6 : Comparison of Predicted and Observed Spectral Index Distributions at 2700 MHz

References for Observations	Flux density S at 2700 MHz (Jy)	ν_2 (MHz)	Median Spectral Index $\alpha_{n\ med}$ (2700, ν_2)		Fraction of flat-spectrum sources F (2700, ν_2)	
			Observed	Predicted	Observed	Predicted
Condon and Jauncey (1974a)	$S \geq 0.80$	318	0.698±0.017	0.74	0.38±0.05	0.34
	$0.80 > S \geq 0.51$	318	0.813±0.016	0.75	0.35±0.05	0.33
	$0.51 > S \geq 0.35$	318	0.802±0.016	0.75	0.26±0.05	0.32
Balonek et al. (1975)	$0.35 > S \geq 0.10$	430	0.76 ±0.02	0.77	0.27±0.05	0.29
	$0.1 > S \geq 0.05$			0.79		0.28
	$0.05 > S \geq 0.02$			0.80		0.29

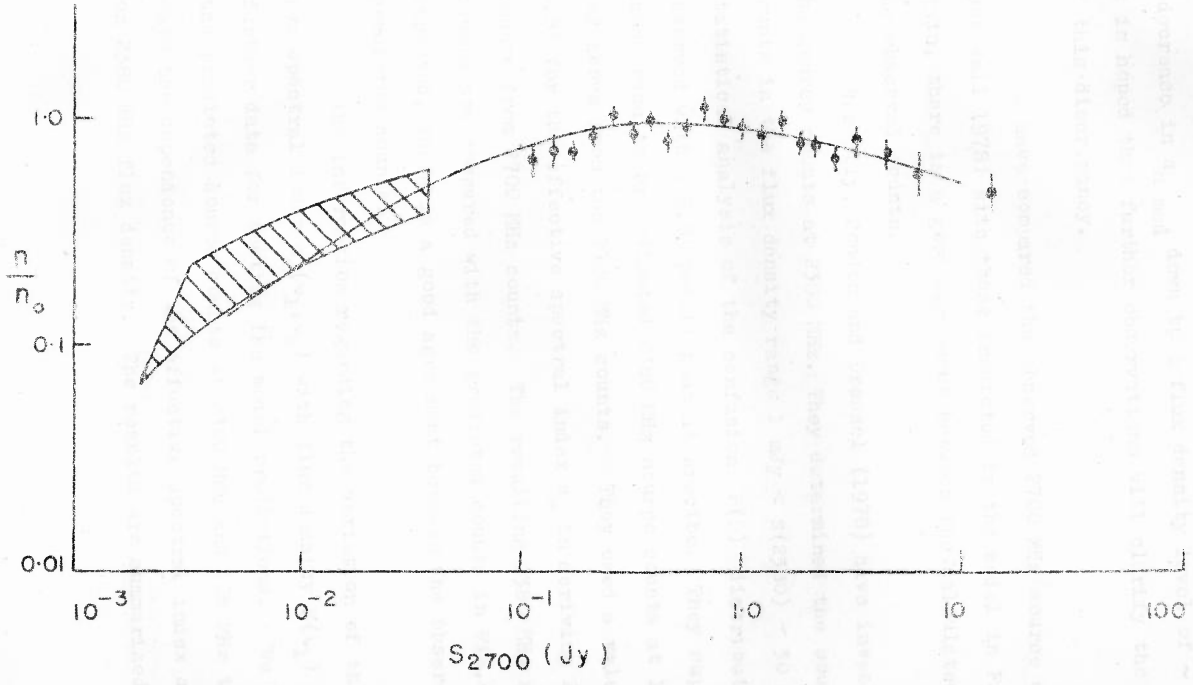

FIG. 4·5 COMPARISON OF THE OBSERVED (WALL 1978) AND THE PREDICTED (MODEL A) NORMALIZED DIFFERENTIAL COUNTS AT 2700MHz. THE HATCHED AREA IS THE REGION DEFINED BY P(D) ANALYSIS OF PARKES DATA (WALL AND COOKE 1975).

density level of $\sim$ 0.2 Jy. But the model fails to predict such a decrease in $\alpha_{n\ mod}$ down to a flux density level of $\sim$ 0.02 Jy. It is hoped that further observations will clarify the nature of this discrepancy.

We have compared the observed 2700 MHz source counts (see Wall 1978) with those predicted by the model in Fig.4.5. Again, there is a good agreement between the calculated and the observed counts.

Recently, Condon and Dressel (1978) have investigated the source counts at 2380 MHz. They determined the source counts in the flux density range 1 mJy $\lesssim$ S(2380) $\lesssim$ 30 mJy by a statistical analysis of the confusion P(D) distribution observed with a 2.8' pencil beam at Arecibo. They supplemented these results by estimated 2380 MHz source counts at 100 mJy and above from the 2700 MHz counts. They used a value of 0.83 for the effective spectral index α_e in deriving 2380 MHz counts from 2700 MHz counts. The resulting 2380 MHz source counts are compared with the predicted counts in Fig.4.6. As expected, there is a good agreement between the observed and predicted counts.

The information regarding the variation of the effective spectral index $\alpha_e(\nu_1, \nu_2)$ with flux density $S(\nu_1)$ provide further data for testing the model predictions. We have used the predicted source counts at 2380 MHz and 408 MHz to investigate the dependence of the effective spectral index $\alpha_e(2380,408)$ on 2380 MHz flux density. The results are summarized in

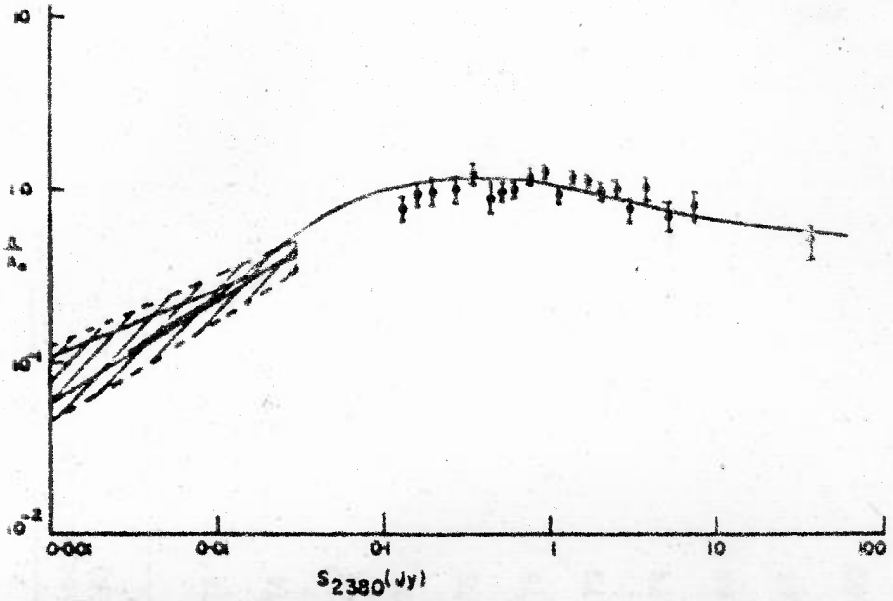

FIG. 4-6 COMPARISON OF THE OBSERVED (CONDON & DRESSEL 1978) AND THE PREDICTED (MODEL A) NORMALIZED DIFFERENTIAL COUNTS. THE SHADED REGION REPRESENTS BOUNDS DERIVED FROM P(D) ANALYSIS (FOR DETAILS SEE CONDON & DRESSEL 1978).

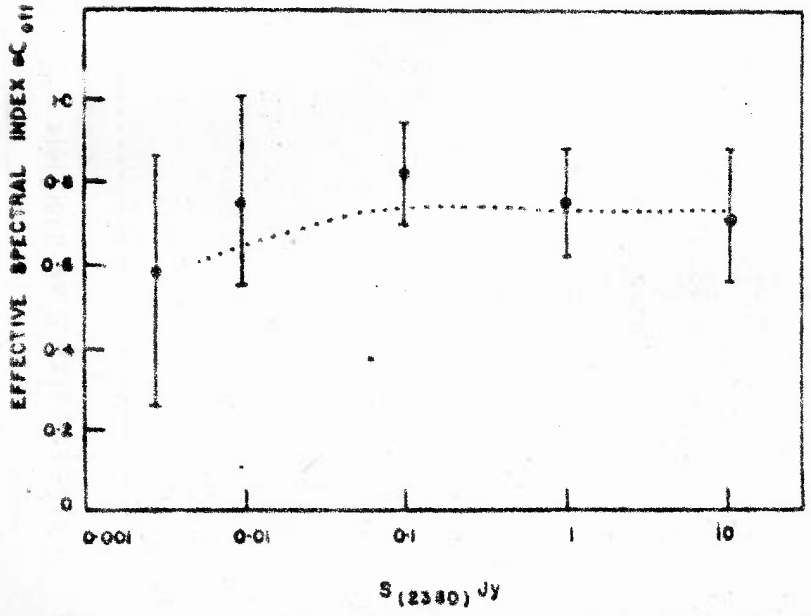

FIG. 4-7 VARIATION OF THE EFFECTIVE SPECTRAL INDEX α_{eff} (408,2380) WITH 2380 MHz FLUX DENSITY. THE OBSERVED POINTS ARE TAKEN FROM CONDON & DRESSEL (1978); THE DOTTED CURVE REPRESENTS VALUES OF α_{eff} (408, 2380) DERIVED FROM MODEL A (SEE TEXT).

TABLE 4.7 : Variation (Predicted) of Effective Spectral Index α_e (2380, 408) with S(2380)

Flux density S at 2380 MHz	Effective Spectral Index α_e (2380, 408)
10.0	0.74
5.0	0.74
2.0	0.74
1.0	0.74
0.5	0.75
0.2	0.75
0.1	0.75
0.05	0.74
0.02	0.69
0.01	0.65
0.005	0.62

TABLE 4.8 : Comparison of Predicted and Observed (Katgert 1977) Values of $\alpha_e(408, 1400)$

Flux density S at 408 MHz	Effective spectral index $\alpha_e(408, 1400)$	
	Observed	Predicted
2.8	0.8	0.78
1.1	0.8	0.78
0.39	0.7	0.78
0.12	0.5	0.74
0.032	0.2	0.66
0.02		0.64
0.01		0.64

Table 4.7. The agreement between the observed and predicted values is quite good (see Fig.4.7). Both predict a decrease (flattening of spectra) at a flux density level of ~ 0.01 Jy at 2380 MHz.

We have also used the predicted source counts at 408 MHz and 1400 MHz to calculate $\alpha_e(408,14000)$ at different 408 MHz flux densities. The predicted and the observed (Katgert 1977) values are listed in Table 4.8. There is a decrease in $\alpha_e(408,1400)$ with decreasing flux density. Since the uncertainties in the observed values of $\alpha_e(408,1400)$ are ~ 0.2, the predicted values can be said to be in agreement with the observed ones.

4.4.4. Discussion

It is clear from the preceding sections that model A gives good agreement with the observational data. This also means that the Generalized Luminosity Function derived in model A is in agreement with the observations both at low and high frequencies. However, as pointed out earlier, we have not followed any systematic optimizing procedure to obtain the optimum values of the parameters for producing the best agreement with observations. Our main aim was to see whether by modifying the conventional models it would be possible to produce a better agreement with the observed source counts and spectral index distributions. We have shown that it is possible to contrive models which are consistent with the observations.

We do not claim that the model proposed by us accounts for all the observational features and it is definitely possible to improve the model by relaxing some of the simplifying assumptions we have made in our computations. A discussion of these and the related points is given below.

1) We have assumed the same local luminosity function for both flat- and steep-spectrum sources. The results and the derived values of the parameters of the model depend on the local luminosity function used. It is very unlikely that both the flat- and steep-spectrum sources have the same local luminosity function. The effects introduced by the difference between the two LLFs might be more important than the effects of other features such as α-P correlation. This means that we must use separate local luminosity functions for flat- and steep-spectrum sources. However, since an insufficient number of identified flat-spectrum sources is present in the low frequency samples, it is not possible to determine the LLF for flat-spectrum sources separately. When more data become available, the local luminosity function can be separately determined for flat- and steep-spectrum sources. At low frequencies the effect of using a separate luminosity function for flat-spectrum sources is small because of the small fraction of flat-spectrum sources involved. The parameters of the local luminosity function for flat-spectrum sources will give additional freedom and it may be possible to get better agreement between the model predictions and observational data at high frequencies.

2) In view of the large number of parameters involved, such models are in no way unique. It is possible to rule out some models by considering redshift distributions and identifications at different flux density levels. In our investigations, we have not considered redshift distributions because we have used the same LLF for both types of sources and the predicted redshift distributions and identification content are known to depend rather sensitively on the local luminosity function employed. Also, the differences between models A, B, C and model 4b of Wall et al. (1977) are expected to be small as far as predictions at 408 MHz are concerned. Since model 4b seems to predict redshift distributions which are in agreement with the observational data it is likely that models A,B, and C also predict correct redshift distributions. It is only at high frequencies (in the present case 5000 MHz) that the differences between models become important. Hence, in order to narrow down the choice of models, it is necessary to obtain observational data giving redshift distribution of sources selected at high frequencies.

3) Strictly speaking, the present model can be used to predict source counts and spectral index distributions at 408 MHz and 5000 MHz only, because in deriving (i) a relation between α_{os} and radio luminosity P and (ii) the spectral index function we considered two point spectral indices $\alpha(408,5000)$. Application of this model to calculate the source counts and spectral index distributions at other frequencies and for

other types of spectral indices [$\alpha(\nu_1, \nu_2)$ where $\nu_1 \neq 408$ and/or $\nu_2 \neq 5000$] is equivalent to assuming straight spectra between 408 MHz and 5000 MHz, which is unlikely. In fact some observations (e.g. Maslowski 1977) indicate that a considerable fraction of the sources may have curved spectra between 408 and 5000 MHz. It is possible to improve the model by taking into account the curved nature of radio source spectra. It might also be necessary to approach the problem in a more systematic way and carry out an optimizing procedure to obtain predictions which are in agreement with the observational features at many frequencies. The following types of observations are required to test such models:

i) Redshift distributions for sources selected from low and high frequencies

ii) Generalized Source Counts at many different frequencies

iii) The spectral index distributions $f^{\nu_1}_{S(\nu_1)}[\alpha(\nu_1, \nu_2)]$ for different values of ν_1 and ν_2 and for different values of flux density $S(\nu_1)$.

4) We have assumed that the spectral index function $\eta(\alpha)$ is independent of redshift z. This implies that redshift z and spectral index α are independent of each other. It is not easy to rule out α-z correlation because α-z correlation can be mimicked by an α-P correlation. It will be interesting to include an α-z correlation in model calcutations and see in what way it affects the predicted source counts and spectral index distributions.

4.5 Summary

In this chapter we reviewed different models that have been proposed to explain source counts and spectral index distributions. Some of the assumptions made in these models and drawbacks of these models were then pointed out. From a consideration of recent observational data regarding differences between cosmological evolution of flat- and steep-spectrum sources and correlation between radio luminosity and spectral index, we argued that these models should be modified appropriately. We derived a Generalized Luminosity Function $\psi(P,z,\alpha)$ incorporating into the conventional models (i) different forms of cosmological evolution for sources belonging to different spectral classes (ii) observed correlation between radio luminosity and spectral index. We showed that by an appropriate choice of the parameters of the model, the predictions can be made to have a good agreement with the observed source counts and spectral index distributions both at 408 MHz and 5000 MHz. The predictions were also shown to be in reasonable agreement with the observations at 1400 MHz, 2380 MHz and 2700 MHz.

"Pooh-Bah: ... I am, in point of fact, a particularly haughty and exclusive person of pre-Adamite descent ... I can trace my ancestry back to a protoplasmal primordial atomic globule"

: The Mikado, W.S. Gilbert

CHAPTER 5

ANGULAR SIZE COUNTS AND COSMOLOGY

5.1 Introduction

In the preceding chapter, we derived a Generalized Luminosity Function by considering the observed spectral index distributions and source counts. This GLF describes the comoving space density of radio sources as a function of radio luminosity (P) spectral index (α) and redshift (z). However, it does not give any information regarding the linear size distribution of radio sources. This is because so far we have not made use of observational data on angular sizes of radio sources. In this chapter we will consider angular size data and derive an Extended Luminosity Function (ELF) combining GLF and linear size function for radio sources. In these calculations we take into account the observed correlation between radio luminosity and linear size. These calculations also allow us to see whether the generalized luminosity function is consistent with angular size data and to find out as to what extent the results regarding the cosmological implications of observed angular size are influenced by the inclusion of spectral index distribution and power-size correlation for radio sources.

5.2 Earlier Investigations

Several authors have investigated the cosmological implications of the observed angular sizes of extragalactic radio sources (Swarup 1975; Kapahi 1975a; 1975b; Katgert 1977).

Kapahi calculated the expected θ_{med} vs. flux density S relation for a uniform distribution of sources in space and compared it with the observed θ_{med} vs. S relation derived (Swarup 1975) from the 3CR, the All-sky and the Ooty occultation surveys. In these investigations, Kapahi considered the log N-log θ relations also. On the basis of these studies he concluded that (i) both density (or/and luminosity) evolution and linear size evolution are required to explain the observed angular size counts and θ_{med} vs. flux density relation and that (ii) the angular size data cannot be explained in the Steady State model. However, later Narlikar and Chitre (1977) claimed that a model with a luminosity-dependent linear size can be devised to explain the observational data and there is no need to introduce any evolution. Recently, Subrahmanya(1977) has critically examined the model proposed by Narlikar and Chitre using the latest angular size data available for 3CR sources, sources from the All-sky catalogue and 283 sources from the Ooty occultation survey. Subrahmanya calculated the expected angular size distributions in different models in one of which (referred to as model B by him) he used the luminosity function of model 4b of Wall et al. (1977). This luminosity function is known to reproduce correctly the 408 MHz source

counts. Subrahmanya followed a procedure (χ^2-test) similar to that employed by Narlikar and Chitre and compared the observed and predicted angular size distributions. He grouped the data into bins of angular size and flux density and performed the chi-square test. The results led him to conclude that (i) the angular size data imply an evolving luminosity function and (ii) the overall linear sizes of radio sources evolve as $(1+z)^{-n}$ with the optimum value of 1.4 ± 0.2 for n. He further pointed out that it is necessary to introduce some dependence of linear size on radio luminosity to explain both source counts and angular size counts.

In all the investigations discussed above, the fact that different sources may have different spectral indices was not considered. All the radio sources were assumed to have the same spectral index $\alpha=0.75$. However, we know that the spectral indices of radio sources span a range of ~ -0.5 to ~ 1.2. Since in a flux density limited sample, the redshift upto which a source of given luminosity can be detected depends on the spectral index α of the source, the finite width of the spectral index distribution is likely to influence the observed angular size distributions. Hence it will be interesting to include spectral index in estimating the angular size distributions. Moreover, in the investigations discussed above, the likely dependence of linear size on radio luminosity is either ignored or introduced in some arbitrary manner. A more satisfactory approach would be to derive a

relation between ℓ and P from observations and then use it in estimating angular size counts. A discussion of such an analysis and the results obtained is given in the following sections.

5.3. The Extended Luminosity Function and N(> S, > θ) Distributions

In this section, we will outline the procedure followed by us to estimate angular size distributions from the Extended Luminosity Function. We will also discuss the choice of world model, the observed correlation between radio-luminosity and linear-size and the radio size function (RSF).

5.3.1 General Formalism for Calculating N(> S, > θ)

The Extended Luminosity Function (ELF) $\Psi_E(P, z, \alpha, \ell_a)$ describes the comoving space density of radio sources as a function of (i) radio luminosity P, (ii) redshift z, (iii) spectral index α and (iv) actual linear size ℓ_a. Note that the actual linear size is represented by ℓ_a and the projected linear size by ℓ. The Extended Luminosity Function can be factorized in the following manner,

$$\Psi_E(P,z,\alpha,\ell_a) = \Psi(P,z,\alpha)\ \varphi_a(\ell_a|P,z) \qquad (5.1)$$

where $\Psi(P,z,\alpha)$ is the Generalized Luminosity Function and $\varphi_a(\ell_a|P,z)$ is the radio size function for a given P and redshift z. In order to calculate the expected angular size distributions N(> S, > θ) what we need to know is the Extended

Luminosity Function in terms of projected linear size (ℓ) rather than the actual linear size (ℓ_a). In this case we can write

$$\psi_E(P,z,\alpha,\ell) = \psi(P,z,\alpha)\ \varphi(\ell|P,z) \qquad (5.2)$$

where the distribution function for the projected linear sizes $\varphi(\ell|P,z)$ is related to the actual linear size distribution $\varphi_a(\ell_a|P,z)$ by the relation

$$\varphi(\ell|P,z) = \ell\int_{\ell}^{\ell_{max}} \frac{\varphi_a(\ell_a|P,z)d\ell_a}{\ell_a\sqrt{\ell_a^2-\ell^2}} \qquad (5.3)$$

where ℓ_{max} is the maximum linear (actual) size that radio sources can reach. Note that ℓ_{max} might be epoch dependent. The angular size counts are given by the relation,

$$N(>S,>\theta) = \int_{-\infty}^{\infty} d\alpha \int_{o}^{z_c} dV(z) \int_{P=f(z)S}^{P_u} \psi(P,z,\alpha)dP \int_{\ell=\theta/\mu(z)}^{\ell_{max}} \varphi(\ell|P,z)\,d\ell \qquad (5.4)$$

$$= \int_{-\infty}^{\infty} d\alpha \int_{o}^{z_c} dV(z) \int_{P=f(z)S}^{P_u} \psi(P,z,\alpha)dP\ \zeta(P,z,\theta) \qquad (5.5)$$

where

$dV(z)$ = volume element, depends on the cosmological model

$P=Sf(z)=Sf(z,\alpha)$; $f(z,\alpha)$ depends on the cosmological model

$\ell=\theta/\mu(z)$; $\mu(z)$ depends on the cosmological model

z_c = cut-off redshift such that $\psi(P,z,\alpha)=0$ for $z > z_c$

and

$$Q(P,z,\theta) = \int_{\ell=\theta/\mu(z)}^{\ell_{max}} \varphi(\ell|P,z)\, d\ell \qquad (5.6)$$

Thus the problem reduces to one of choosing an appropriate world model, generalized luminosity function and radio size function $\varphi_a(\ell_a|P,z)$. This is considered in the next section.

5.3.2 The Choice of World Model and GLF

As already mentioned many times, the geometric differences between the various world models are small compared to the gross effects of evolution. We have, therefore, considered only the Einstein-de Sitter world model in our calculations. We have used the GLF derived in Chapter 4 because it predicts source counts and spectral index distributions that are in good agreement with the observational data both at low and high frequencies.

5.3.3 The Size Function $\varphi_a(\ell_a|P,z)$

The choice of radio size function $\varphi_a(\ell_a|P,z)$ poses some difficulty because, as the origin and evolution of radio sources is not yet well understood, it is not possible to determine the radio size function $\varphi_a(\ell_a|P,z)$ on the basis of models of extragalactic radio sources. This situation arises because, to understand the origin and evolution of radio sources we need to know the properties of the medium surrounding them. However, to study the properties of the medium we have to use radio sources as probes, the properties of which

we are trying to determine ! Hence it is necessary to follow a model-fitting procedure and derive $\varphi_a(\ell_a|P,z)$. Further, what can be observed is $\varphi(\ell|P,z)$ and not $\varphi_a(\ell_a|P,z)$. For the sake of simplicity, in what follows, we have assumed $\varphi(\ell|P,z)$ and $\varphi_a(\ell_a|P,z)$ to be approximately the same. This is not an unreasonable assumption because, on the average, the effects of projection are expected to be small.

Let us now consider the choice of $\varphi(\ell|P,z)$. This can be factorized as

$$\varphi(\ell|P,z) = \varphi(\ell|P,z=0)\ \gamma(P,z) \qquad (5.7)$$

where $\varphi(\ell|P,z=0)$ = local size function for a given P

and $\int\varphi(\ell|P,z=0)dP$ = local size function = $\varphi_o(\ell,z=0)$

$\gamma(P,z)$ = size evolution function

Kapahi (1977) has determined the local size function from the observed distribution of projected linear sizes of nearby radio sources. Note that $\varphi_o(\ell,z=0)$ thus derived is strictly valid for low luminosity sources only, because high luminosity sources are rare and to observe a large number of them one has to sample a large enough volume of the universe (to high redshifts) where the effects of evolution and the geometric differences between the various world models are expected to become significant. However, since one is trying to determine evolution function and world model, it is not

possible to derive $\varphi_o(\ell, z=0)$ directly and again it is necessary to follow a parameter fitting procedure and estimate $\varphi_o(\ell, z=0)$ empirically. This is an involved procedure and not very meaningful one to use in view of the insufficient observational data currently available. For this reason, we use the local size function that has been approximately inferred (Kapahi 1977) from the limited sample of nearby sources. Another complication arises because the effects of radio luminosity-size correlation and that of linear size evolution cannot be decoupled from each other in a simple manner. An anti-correlation between P and ℓ (more luminous sources have smaller sizes) can in principle mimic linear size evolution i.e. a decrease in the overall linear sizes of radio sources with redshift. Hence it is necessary to use only nearby (z=0) sources in investigating possible correlation between radio luminosity and linear size.

Several authors have investigated the possible correlation between radio power and linear size of radio sources. From a study of the projected linear size versus radio luminosity (at 178 MHz) diagram for the complete sample of 3CR radio sources, Longair and Macdonald (1969) suggested that there is only a slight tendency for sources with small physical sizes to have high luminosities. A similar plot for an approximately complete subset of 64 sources (which are either known or estimated to have $z < 0.3$) shows a similar spread in the values at different luminosities implying little or no correlation between radio luminosity and linear size(Mackay 1973).

However, a correlation between radio luminosity and linear size has recently been reported (Gavazzi and Perola 1978). They used the maximum size of the galaxies in two radio-optically complete samples of sources from the 3C and B2 catalogues and derived the Bivariate Size-Luminosity Function (BSLF) $\rho_B(P,\ell)$ for radio galaxies (at $z < 0.1$) over the range $10^{22.6} < P(1415) < 10^{26.2}$ W Hz^{-1}. They found that the function $\rho_B(P,\ell)$ cannot be factorized as $\rho_1(P)\ \rho_2(\ell)$ and that the average size increases with power. They carried out these investigations by grouping sources into many different morphological classes. Two important morphological classes considered were:

i) DII sources: these are doubles with bright extremeties and sharp outer boundary (33 sources were grouped in this class).

ii) DI sources : doubles with relatively low brightness features smoothly extending beyond the outermost peak are classified in this group. There are ~ 15 such sources in the sample.

The above authors found that:

a) For DII sources

$$<\ell> = \ell_0 = 180 \text{ kpc if } P(1415) > 10^{25} \text{ W Hz}^{-1}$$

$$= 50 \text{ kpc if } P(1415) < 10^{25} \text{ W Hz}^{-1}$$

b) For DI sources

$$<\ell> = \ell_0 = 80 \text{ kpc}$$

In the following discussion, we assume that there are only two types of sources, with, ~ 65 % sources being in class DII and remaining in class DI. It might also be pointed out here that the above quantities were calculated assuming a value of 100 km/(s Mpc) for the Hubble constant H_o and since we are using a value of 50 km/(s Mpc) for H_o, we will scale the above numbers (ℓ_o and P) appropriately.

5.4 Model Calculations and Comparison with Observations

As discussed in the previous section, we can assume $\varphi_a(\ell_a|P,z)$ and $\varphi(\ell|P,z)$ to be approximately same. This allows us to write,

$$\psi_E(P,z,\alpha,\ell_a) \simeq \psi'_E(P,z,\alpha,\ell)$$

Thus the problem reduces to one of determining $\psi'_E(P,z,\alpha,\ell)$. This can be done in the following manner. We have,

$$Q(P,z,\theta) = \int_{\ell=\theta/\mu(z)}^{\ell_{max}} \varphi(\ell|P,z)\, d\ell \qquad (5.8)$$

We first evaluate $Q(P,z,\theta)$ and use it in eq.(5.6) to calculate the expected $N(>S,>\theta)$ distributions. In our analysis, we have considered three models X,Y and Z. All these models incorporate strong evolution of source properties with cosmic epoch. In model X, all the sources are assumed to have a spectral index of $\alpha = 0.75$. In model Y, spectral index distribution is introduced and flat- and steep-spectrum sources are allowed to evolve (cosmologically) in different ways , but possible

correlation between spectral index and radio luminosity is not taken into account. The generalized luminosity function which was derived in Chapter 4 and which incorporates (a) different cosmological evolution for flat- and steep-spectrum sources and (b) correlation between spectral index and luminosity is employed in model Z. The main features of these models are given in Tables 5.1,5.2 and 5.3. The angular size distributions $N(>S,>\theta)$ predicted by these models are shown in Figs. 5.1, 5.2 and 5.3 along with the observed numbers as given by Subrahmanya (1977). The crosses indicate the number of sources for which definite values of θ were available and the vertical bars indicate the numbers for which only upper limits were given. The agreement between the predicted (solid curves) and observed distributions is seen to be quite reasonable.

For a more quantitative assessment of the agreement between the predictions of different models and observations, we used a chi-square analysis similar to that employed by Narlikar and Chitre (1977), Swarup and Subrahmanya (1977) and Subrahmanya (1977). In the application of this test to the present problem the following procedure is adopted. Let us suppose that the relevant flux density range is divided into I intervals and that the ith flux density interval is further subdivided into J_i subintervals of θ. In all there will be,

$$\sum_{i=1}^{I} J_i = K$$

Table 5.1 : The Parameters of Model X

1) Generalized Luminosity Function $\Psi(P,z,\alpha)$:

$$\Psi(P,z,\alpha) = \rho(P,z=0)F(P,z)\eta(\alpha)$$

where

$\rho(P,z=0)$ = local luminosity function determined from the 408 MHz luminosity distribution given by Wall et al. (1977)

$$F(P,z) = \begin{cases} \exp[m(P)(1-t/t_o)], & z<z_c \\ 0, & z>z_c \end{cases}$$

$$m(P) = \begin{cases} 0, & P \leq P_1 \\ M\ (\log P - \log P_1)/(\log P_2 - \log P_1), & P_1 < P \leq P_2 \\ M, & P > P_2 \end{cases}$$

and t is the 'cosmic time' given by

$t/t_o = (1+z)^{-1.5}$ for the Einstein-de Sitter geometry.

The optimum values of parameters are:

$$\left.\begin{array}{l} P_1 = 10^{25}\ \text{W Hz}^{-1}\ \text{sr}^{-1} \\ P_2 = 10^{27.3}\ \text{W Hz}^{-1}\text{sr}^{-1} \end{array}\right\} \text{at 408 MHz}$$

$M = 11.0$; $z_c = 3.5$

and the spectral index function $\eta(\alpha)$ is

$$\eta(\alpha) = \delta(\alpha-0.75)$$

...2

2) Radio Size Function:

$$\varphi(\ell | P,z) = (1/\ell_o)\ \exp(-\ell/\ell_o),$$

where

$$\ell_o(z) = \ell_o(z=0)\ (1+z)^{-n}$$

with $\ell_o(z=0)$ = 360 kpc if $P(408) \gtrsim 10^{26}$ W Hz^{-1} sr^{-1}

= 100 kpc for DII type sources } $P(408) \lesssim 10^{26}$ W Hz^{-1} sr^{-1}

= 160 kpc for DI type sources }

Table 5.2 : The Parameters of Model Y

1) Generalized Luminosity Function $\Psi(P,z,\alpha)$:

$$\Psi(P,z,\alpha) = \rho(P,z=0)[C_s F_s(P,z)\eta_s(\alpha)+C_f F_f(P,z)\eta_f(\alpha)]$$

where

$\rho(P,z=0)$ = local luminosity function (same as that in model X)

C_f = fraction of flat-spectrum sources = 0.035

C_s = fraction of steep-spectrum sources=0.965

The evolution function for stee-spectrum sources is $F_s(P,z)$ same as $F(P,z)$ in model X. The evolution function for flat-spectrum sources is:

$$F_f(P,z) = \begin{cases} \exp[m'(P)(1-t/t_o)] & , z \leq z_c \\ 0 & , z > z_c \end{cases}$$

where,

$$m'(P) = \begin{cases} 0 & , P < P'_1 \\ M(\log P-\log P'_1)/(\log P'_2-\log P'_1) & , P'_1<P\leq P'_2 \\ M & , P > P'_2 \end{cases}$$

and $t/t_o = (1+z)^{-1.5}$

The optimum values are:

$P'_1=10^{22.5}$ W $Hz^{-1}sr^{-1}$

$P'_2 = 10^{28}$ W Hz^{-1} sr^{-1} } at 408 MHz

$M = 8.0$; $z_c = 3.5$

...2

The spectral index functions for steep-spectrum and flat-spectrum sources are given by

$$\eta_s(\alpha) = \frac{1}{\sigma_s\sqrt{2\pi}} \exp[-(\alpha-\alpha_{os})^2/2\sigma_s^2] \text{ where } \sigma_s=0.20, \alpha_{os}=0.83$$

$$\eta_f(\alpha) = \frac{1}{\sigma_f\sqrt{2\pi}} \exp[-(\alpha-\alpha_{of})^2/2\sigma_f^2] \text{ where } \sigma_f=0.25, \alpha_{of}=0.25$$

2) Radio Size Function: Same as in model X

Table 5.3 : The Parameters of Model Z

These are the same as for model Y, except that instead of $\alpha_{os} = 0.83$ we set $\alpha_{os} = -0.09+0.038 < \log P >$ to take into account the observed α-P correlation.

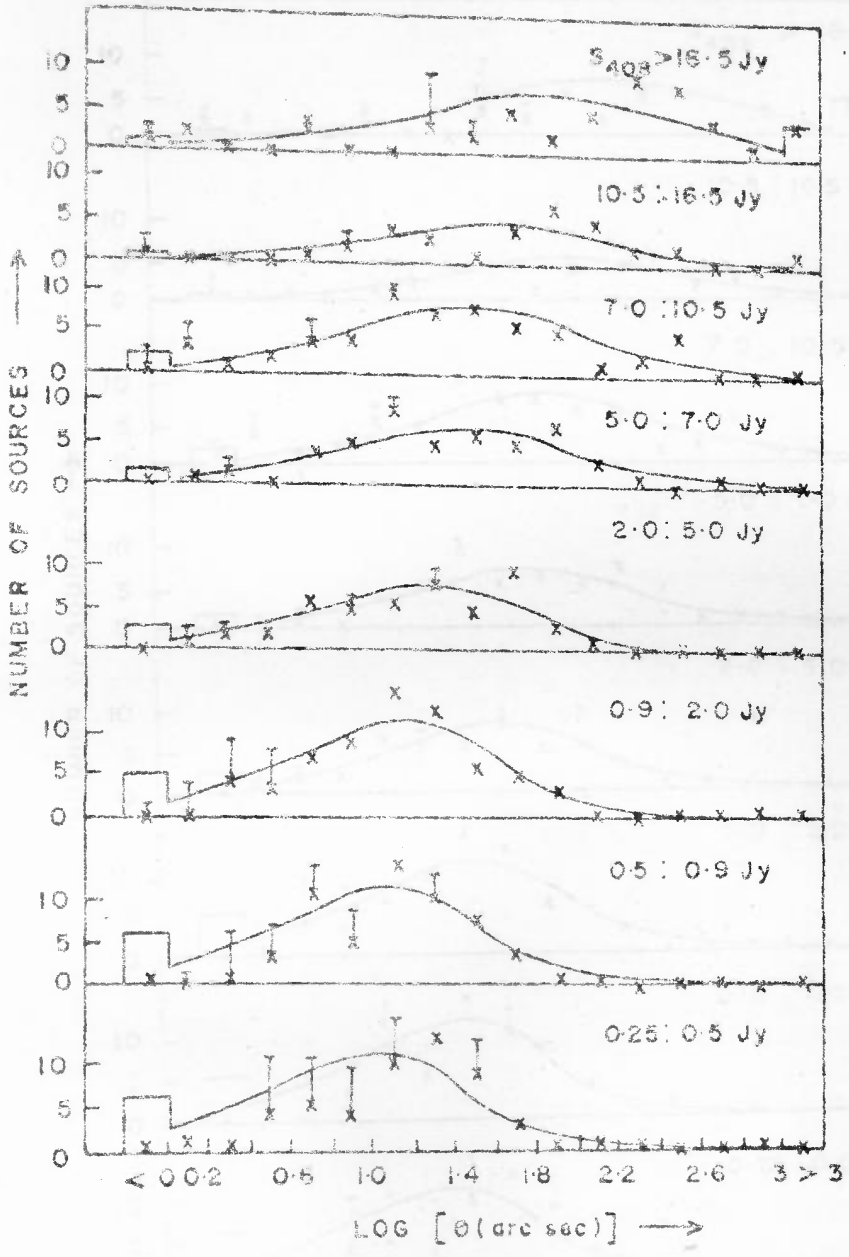

FIG. 5·1 COMPARISON OF PREDICTED (MODEL X) AND OBSERVED ANGULAR SIZE DISTRIBUTION IN DIFFERENT RANGES OF FLUX DENSITY S. THE OBSERVED NUMBER OF SOURCES INDICATED BY CROSSES REFER TO SOURCES FOR WHICH DEFINITE VALUES OF θ WERE AVAILABLE AND THE VERTICAL LINES REFER TO SOURCES FOR WHICH ONLY UPPER LIMITS WERE AVAILABLE.

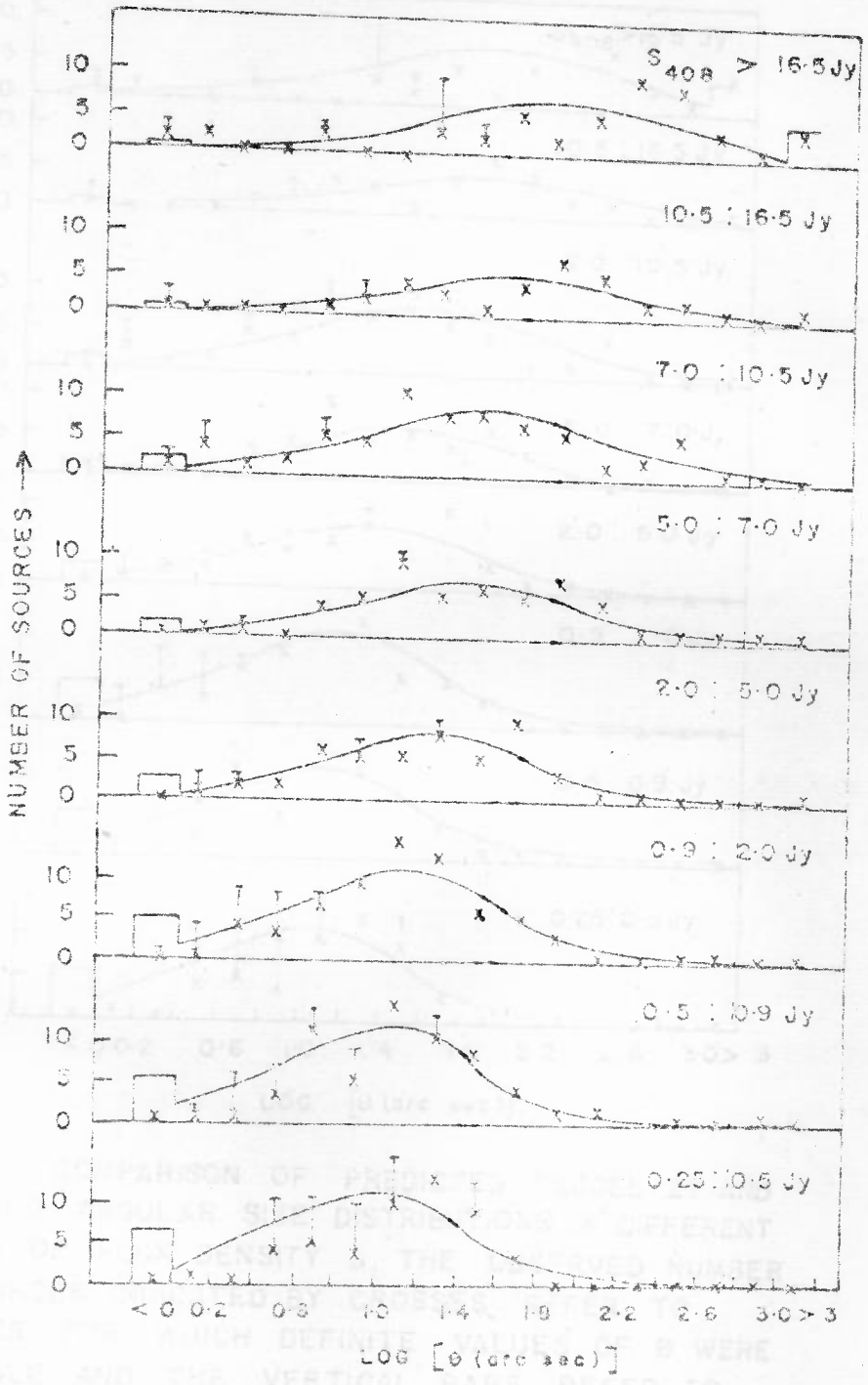

FIG. 5·2 COMPARISON OF PREDICTED (MODEL Y) AND OBSERVED ANGULAR SIZE DISTRIBUTION IN DIFFERENT RANGES OF FLUX DENSITY S. THE OBSERVED NUMBER OF SOURCES INDICATED BY CROSSES REFER TO SOURCES FOR WHICH DEFINITE VALUES OF θ WERE AVAILABLE AND THE VERTICAL BARS REFER TO SOURCES FOR WHICH ONLY UPPER LIMITS WERE AVAILABLE.

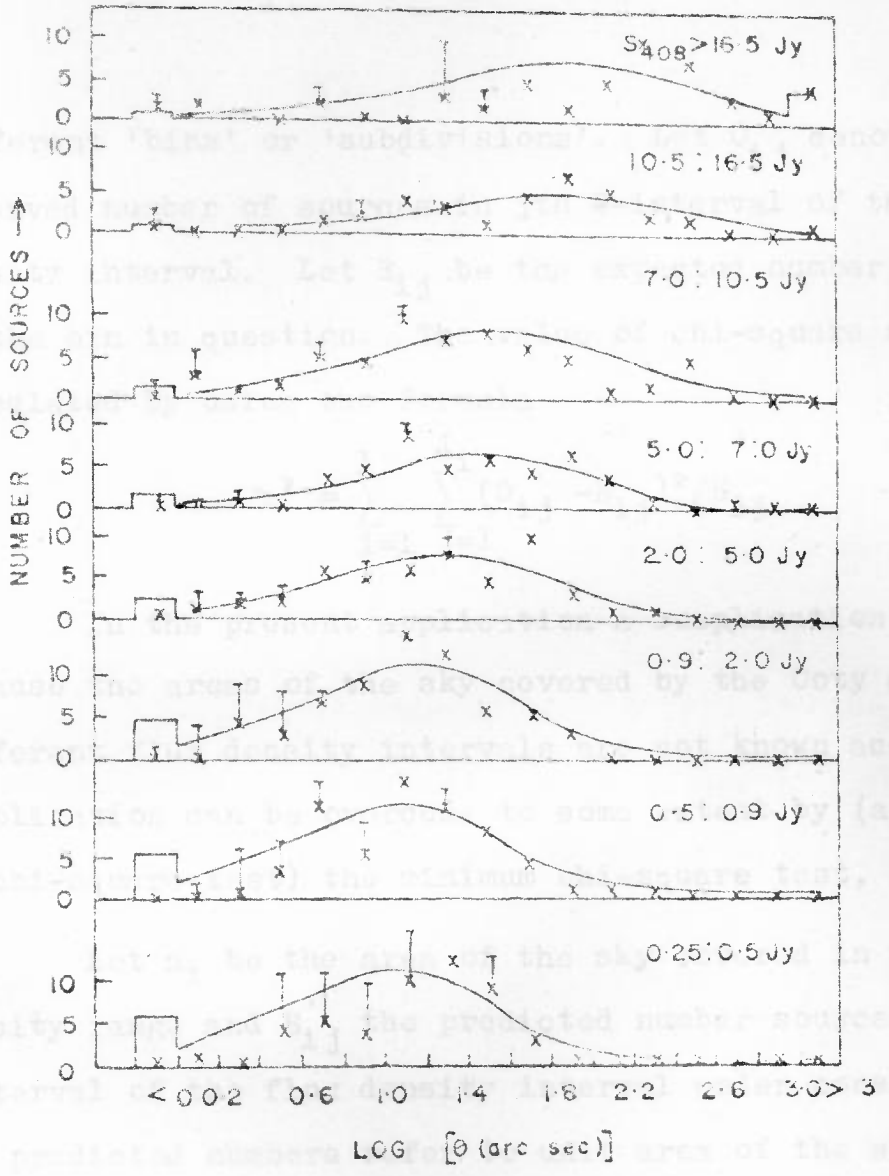

FIG. 5·3 COMPARISON OF PREDICTED (MODEL Z) AND OBSERVED ANGULAR SIZE DISTRIBUTIONS IN DIFFERENT RANGES OF FLUX DENSITY S. THE OBSERVED NUMBER OF SOURCES INDICATED BY CROSSES REFER TO SOURCES FOR WHICH DEFINITE VALUES OF θ WERE AVAILABLE AND THE VERTICAL BARS REFER TO SOURCES FOR WHICH ONLY UPPER LIMITS WERE AVAILABLE

different 'bins' or 'subdivisions'. Let O_{ij} denote the observed number of sources in jth Θ-interval of the ith flux density interval. Let E_{ij} be the expected number of sources in the bin in question. The value of chi-square can then be calculated by using the formula

$$\chi^2 = \sum_{i=1}^{I} \sum_{j=1}^{J_i} (O_{ij} - E_{ij})^2 / E_{ij} \qquad (5.9)$$

In the present application a complication arises because the areas of the sky covered by the Ooty survey in different flux density intervals are not known accurately. This complication can be overcome to some extent by (a modified form of chi-square test) the minimum chi-square test, outlined below.

Let a_i be the area of the sky covered in the ith flux density range and E'_{ij} the predicted number sources in the jth -interval of the flux density interval under consideration. If the predicted numbers refer to unit area of the sky, then the number to be compared with O_{ij} is $a_i E'_{ij} = E_{ij}$. The χ^2 is given by

$$\chi^2 = \sum_{i=1}^{I} \sum_{j=1}^{J_i} (O_{ij} - E_{ij})^2 / E_{ij} \qquad (5.10)$$

With $E_{ij} = a_i E'_{ij}$, this reduces to

$$\chi^2 = \sum_{i=1}^{I} \sum_{j=1}^{J_i} (O_{ij} - E'_{ij} a_i)^2 / a_i E'_{ij} \qquad (5.11)$$

The best possible agreement between theory and observations is obtained for the minimum value of χ^2 . This can be achieved by minimizing χ^2 with respect to all a_i. However, since the total number of sources expected should be equal to the total number of sources observed, it is necessary to minimize χ^2 subject to the following equality constraint,

$$\sum_{i=1}^{I} \sum_{j=1}^{J_i} E_{ij} = \text{Total number of sources observed} = N.$$

In the present case we have N=513, I=8 and J=17.

An application of Lagrange's method of undetermined multipliers shows that the minimum value of χ^2 is given by

$$\chi^2 = \frac{1}{N}\left[\sum_{i=1}^{I} \frac{1}{\left(\sum_{j=1}^{J_i} O_{ij}/E_{ij}\right)} \left(\sum_{j=1}^{J_i} E_{ij}\right)^2\right] - N \qquad (5.12)$$

The necessary condition for stable statistic is that $E_{ij} \geq 5$ for all (i,j) pairs. For this reason whenever $E_{ij} < 5$ for any pair (i,j) we merged the adjacent bins and obtained four groupings of bins (q=1,2,3, and 4) so that for the qth group $E_{ij} > 5q$ for all (i,j) pairs. The total number of bins contained in groups 1,2,3 and 4 were 65,40,27 and 21 respectively. The merging was done uniformly starting from the largest angular size until for the qth group $\min(E_{ij})=5q$. However, the bins with the lowest values of θ (< 4 arc sec) in the Ooty sample

which had a large fraction of unresolved sources were merged even if original number $E_{ij} \geq 5q$ for qth group.

The results of the chi-square test for the models X,Y and Z are summarized in Table 5.4, which gives χ^2 values for different groupings of bins. The χ^2values corresponding to significance levels 0.001, 0.01, 0.05, 0.10 and 0.20 are listed in Table 5.5 so that the goodness offit can be readily judged.

5.5. Discussion of Results

The results summarized in Table 5.4 provide some evidence for the presence of linear size evolution. The overall linear sizes of radio sources thus tend to decrease with redshift. The optimum value of n, where $\ell(z) = \ell(z=0)(1+z)^{-n}$, is 1.4 ± 0.2. This holds true for all the three models considered. Since all these models incorporate strong density (or luminosity) evolution of radio source population without recourse to which it is not possible to explain the source counts, it can be reasonably inferred that both density (and/or luminosity) evolution and linear size evolution are required to interpret source counts and angular size counts at the same time. The type of size evolution indicated by the present investigations is also similar to what has been inferred from the observed θ-z relation for QSOs. In our models we have taken into account: the observed correlation between radio luminosity and linear size of extragalactic radio sources. The optimum value of n obtained in each of these models is ~ 1.4 and is in close agreement with the value 1.4 ± 0.2 reported by

Table 5.4 : Chi-square Values for the Three Models X,Y and Z

No. of bins	Model X			Model Y			Model Z		
	n=1.2	n=1.4	n=1.6	n=1.2	n=1.4	n=1.6	n=1.2	n=1.4	n=1.6
65	85	87	99	88	88	98	94	92	97
40	60	58	64	63	60	64	71	65	66
27	35	33	38	37	34	38	44	38	40
21	29	26	30	32	27	30	37	31	31

Table 5.5 : χ^2 versus K,Q; K=no. of bins, Q=significance level

No.of bins K	Significance level Q				
	0.20	0.10	0.05	0.01	0.001
65	73.3	78.9	83.7	93.2	104.7
40	46.2	50.7	54.6	62.4	72.1
27	31.8	35.6	38.9	45.6	54.1
21	25.0	28.4	31.4	37.6	45.3

Subrahmanya (1977). However, these models give slightly but not significantly higher values of χ^2 than the corresponding values given by Subrahmanya (1977).

In model X we have assumed that all the sources have the same spectral index $\alpha=0.75$; the dispersion in spectral indices is ignored. On the other hand in models Y and Z the finite width of the spectral index distribution is taken into account by using the generalized luminosity function derived earlier. The χ^2 values obtained for models X,Y and Z are, however, not significantly different from one another. It follows, therefore, that the introduction of spectral index distribution does not significantly influence the results of investigations of cosmological implications of observed angular size counts. The effects of using different form of cosmological evolution for flat- and steep-spectrum sources are also small. This is hardly surprising because the investigations of angular size counts were carried out for sources selected at low frequencies where the fraction of flat-spectrum sources observed is quite small.

Models Y and Z differ from each other only in one respect, in model Z possible α-P correlation is taken into account whereas in model Y, α and P are assumed to be independent. From the roughly equal values of χ^2 obtained for these models it can be inferred that the effects of spectral index-luminosity correlation are small.

5.6 Summary

In this chapter, we have derived an extended luminosity function by combining the generalized luminosity function derived earlier and available information regarding radio size function. For this we used the structural data available for a sample containing ~ 500 sources. The expected angular size distributions were calculated employing the GLF and radio size function. In these calculations possible correlation between radio luminosity and linear size was taken into account. The predicted angular size distributions were compared with the observed ones by applying the minimum chi-square test. The results seem to imply the presence of both density (and/or luminosity) and linear size evolution effects in radio source populations as has been concluded by previous workers. Our investigations further show that the results regarding the evolutionary effects are not affected in any significant manner by the inclusion of (i) α-P correlation, (ii) different forms of cosmological evolution for flat- and steep-spectrum sources, (iii) spectral index distribution and (iv) a possible correlation between radio power and linear size. The generalized luminosity function (derived in Chapter 4) in conjunction with the size distribution function employed here gives Extended Luminosity Function $\Psi_E(P,z,\alpha,\ell)$ which is reasonably consistent with the observed (a) source counts, (b) spectral index distributions and (c) angular size counts of extragalactic radio sources.

... *"I have known the dreadful*
dissolution of the universe, I have seen all perish,
again and again, at every cycle. At that terrible time,
every single atom dissolves into the primal, pure
waters of eternity, whence all originally arose"

Ancient Indian myth quoted in 'Myths & Symbols in Indian Art & Civilization' by H. Zimmer.

CHAPTER 6

SUMMARY AND COMMENTS

In this chapter, we summarize the principal results from our analysis of the cosmological implications of the observed source counts, spectral index distributions and angular size counts of extragalactic radio sources. We also point out some limitations of the present study and comment on the possibilities for further lines of investigations.

In the present study, we have discussed many topics that are related to the study of distribution of radio sources in space. First we considered the interpretation of source counts and derivation of local luminosity function and evolution function for sources selected at a single frequency. In this connection we presented an analysis of absolute magnitude-redshift diagram and Hubble plot for QSOs. We have also proposed an extension of the Free-Form Analysis Scheme (Robertson 1978) for deriving evolution function. Secondly, we have derived a Generalized Luminosity Function for extragalactic radio sources by considering in detail radio source counts and spectral index distributions both at low and high frequencies. Lastly, we have combined the generalized luminosity function with radio size function (or linear size function) to predict angular size distributions and have compared them with the observed ones.

6.1 Absolute Magnitudes and Hubble Diagram for QSOs

As discussed in Chapter 2, interpretation of source counts in terms of evolving world models, derivation of local luminosity function and evolution function all involve the assumption that a majority of radio sources including quasars are at cosmological distances implied by their redshifts. In this connection we presented our analysis of the observed magnitude-redshift relation for quasars (Kembhavi and Kulkarni 1977). From a sample of 570 QSOs with redshifts ranging from 0.2 to more than 3, we selected in different redshift ranges, the optically most luminous QSOs and obtained a plot of absolute magnitude versus redshift. The absolute magnitudes were calculated on the assumption that the QSOs are at the cosmological distances indicated by their redshifts. These investigations, in which we have taken into account the selection effects introduced by a sharp detection cut-off for QSO samples, show that for redshift $z > 1$ the absolute magnitudes of the brightest QSOs remain nearly constant. Further, log z-apparent magnitude plot for the brightest QSO at each redshift is obtained. The slope of the least-squares fit line is shown to be consistent with the value of 0.2 expected from the cosmological hypothesis.

6.2 An Extended Free-Form Analysis Scheme for Investigating the Cosmological Evolution of Radio Sources

In the conventional method of deriving evolution function from the observed source counts and luminosity

distribution, an analytic form for evolution function is assumed and the parameters of this function are estimated through an iterative procedure. This requires us to assume a functional form for the evolution function. Sometimes it may be desirable and convenient to use a scheme which does not require such an assumption. Such a scheme of solving for the evolution function has been given by Robertson (1978). This scheme though simple, assumes that the local luminosity function is known. We presented an extension of this scheme that starts from the observed luminosity distribution rather than the derived local luminosity function. The resulting local luminosity function and evolution function display features very similar to those that follow from the conventional analysis of source counts. However, the estimated evolution function $E(z)$ does not vary smoothly with redshift but shows some unphysical oscillations. It is suggested that incorporation of some smoothness constraint(s) into Free-Form Analysis might make the method more suitable for practical applications.

6.3 Generalized Luminosity Function, Source Counts, Spectral Index Distributions and Angular Size Counts

Our investigations show that the observed radio source counts at different frequencies and also the expected variation in spectral index distributions with flux density can be explained in terms of world models which include a strong evolution of the radio source populations. We have derived a Generalized Luminosity Function (GLF) for extragalactic radio

sources by following a model-fitting procedure. This GLF describes the comoving space density of extragalactic radio sources as a function of radio luminosity, redshift and spectral index. In deriving it we have considered the observed correlation between radio luminosity and spectral index as well as different forms of cosmological evolution for flat- and steep-spectrum sources.

The observational status of source counts and spectral index distributions at different frequencies is reviewed briefly in Chapter 3. In particular, the variations in spectral index distributions with flux density and frequency dependence of source counts and spectral index distributions are discussed and the principal observational features that have to be accounted for by any successful model are pointed out.

In Chapter 4, the earlier models are reviewed pointing out the inconsistency of some of their assumptions with recent observational data and a new model is proposed. In particular the model proposed by Fanaroff and Longair (1973) is examined in some detail and some of the difficulties that this model encounters in view of recent observational data are noted. A discussion of the assumptions made in the model of Fanaroff and Longair is also given with particular reference to the following ones: (1) radio-luminosity and spectral index are not correlated (2) the cosmological evolution is identical for flat- and steep-spectrum sources. The above two assumptions

are not consistent with recent observational data and it seems necessary to take into account the α - P correlation and the difference between cosmological evolution of sources belonging to different spectral classes. A generalized model which incorporates these two features is then proposed and used for calculating the expected variations in spectral index distributions with flux density and also for studying the dependence of source counts and spectral index distributions on frequency. The free parameters of this generalized model were determined by comparing model predictions with the observed source counts and spectral index distributions at 408 MHz. It is shown that the predictions of the proposed model are in good agreement with the observed source counts and spectral index distributions at 5000 MHz. The predictions are also found to be in reasonable agreement with the observations at 1400, 2380 and 2700 MHz.

The effects of α - P correlation and of spectral index dependent evolution function are also investigated. Our investigations show that a major part of the improvement over earlier models can be attributed to the inclusion of spectral index dependent evolution function. This produces significant changes both in predicted spectral index distributions and source counts especially at low flux densities. This is also the main reason for the agreement between the observed and predicted spectral index distribution for sources selected at 5000 MHz (where observational features of spectral index distributions are well established). The cosmological evolution is

strong for the steep-spectrum sources but is confined only to the powerful sources with $P(408) \gtrsim 10^{26}$ W $Hz^{-1}sr^{-1}$. For the flat-spectrum sources, the cosmological evolution seems to be required for all the sources with $P(408) \gtrsim 10^{24}$ W $Hz^{-1}sr^{-1}$ but the evolution is not as strong as for the steep-spectrum sources.

On the other hand the overall effects of inclusion of α--P correlation are comparatively small. It has the effect of broadening source counts (expressed in the form n/n_o, i.e. normalized differential form) to some extent. Also, no significant changes are apparent in the predicted spectral index distributions.

In Chapter 5, the Generalized Luminosity Function is used along with the radio size function to derive an Extended Luminosity Function, which describes space density of radio sources as a function of P, α, z and ℓ. This ELF is used in investigating the cosmological implications of the observed angular sizes of radio sources. These investigations form an extension of the recent works (Swarup 1975; Kapahi 1975b; Swarup and Subrahmanya 1977; Subrahmanya 1977) and include the luminosity-size correlation (for radio sources) that has been inferred from recent observational data (Gavazzi and Perola 1978). A comparison of the predicted angular size distributions with the observed ones indicates the presence of both density (or luminosity) and linear size evolution effects. The results also show that the effects of the inclusion of spectral

index distribution and luminosity-linear size correlation are small.

In deriving the GLF, we have made some assumptions for simplicity and ease of computation. For example, the fact that the radio source spectra may be curved is not taken into account; also, the spectral index function is assumed to be independent of epoch. Another important assumption we have made in our investigations is related to the local luminosity function. We have assumed the local luminosity function to be the same for flat- and steep-spectrum sources, because at present sufficient data are not available to derive the local luminosity functions for flat- and steep-spectrum sources separately. Since predicted redshift distributions and identification content at different flux density levels depend on the local luminosity function and also since not much is known about the local luminosity function for flat-spectrum sources, we have not attempted any comparison of predicted and observed redshift distributions and identification content. More observations at different frequencies and at low flux density levels, especially for flat-spectrum sources, are needed for a systematic and detailed comparison of model predictions with the observational data. On the basis of future observations it should be possible to determine the generalized luminosity function more accurately. A knowledge of GLF is of considerable importance since it gives directly the relative populations of different types of sources at different epochs and can possibly give information about the epoch of quasar and galaxy formation.

REFERENCES

Baade,W. and Minkowski,R., 1954, Astrophys. J., 119, 206.

Bahcall,J.N. and Hills,R.E., 1973, Astrophys. J., 179, 699.

Balonek,T.J., Broderick,J.J., Condon,J.J., Crawford,D.F. and Jauncey,D.L., 1975, Astrophys. J., 201, 20.

Blake,G.M., 1978, Mon. Not. R. astr. Soc., 183, 21p.

Brecher,K., Burbidge,G.R. and Strittmatter,P.A., 1971, Comm. Astrophys. Sp. Phys., 3, 99.

Bridle,A.H., 1967, Mon. Not. R. astr. Soc., 136, 219.

Bridle,A.H., Davis,M.M., Fomalont,E.B. and Lequeux,J., 1972, Astr. J., 77, 405.

Bridle,A.H., Kesteven,M.J.L. and Guindon,B., 1972, Astrophys. Lett., 11, 27.

Burbidge,G.R., 1973, Nature, Phys. Sci., 246, 17.

Burbidge,G.R. and O'Dell,S.L., 1973, Astrophys.J., 183, 759.

Burbidge,G.R., Crowne,A.H. and Smith,H.E., 1977, Astrophys.J. Suppl., 33, 113.

Carswell,R. and Weymann,M.N., 1971, Mon. Not. R. astr. Soc., 156, 19p.

Colla,G., Fanti,C., Fanti,R., Ficarra,A., Formiggini,L., Gandolfi,E., Grueff,G., Lari,C., Padrielli,L., Roffi,G., Tomasi,P. and Vigotti,M., 1970, Astr. Astrophys.Suppl., 1, 281.

Colla,G., Fanti,C., Fanti,R., Ficarra,A., Formiggini,L., Gandolfi,E., Lari,C., Marano,B., Padrielli,L. and Tomasi, P., 1972, Astr. Astrophys. Suppl., 7, 1.

Colla,G., Fanti,C., Fanti,R., Ficarra,A., Formiggini,L., Gandolfi,E., Gioia,I., Lari,C., Marano,B., Padrielli,L. and Tomasi,P., 1973, Astr. Astrophys. Suppl., 11, 291.

Condon,J.J. and Jauncey,D.L., 1974a, Astr. J., 79, 437.

Condon,J.J. and Jauncey,D.L., 1974b, Astr. J., 79, 1220.

Condon,J.J. and Dressel,L.L., 1978, Astrophys. J., 222, 745.

Davies,I.M., Little,A.G. and Mills,B.Y., 1973, Aust. J. Phys. Astrophys. Suppl., 28, 1.

Davis,M.M., 1971, Astr. J., 76, 980.

Davis,M.M. and Taubes,C., 1974, Bull. Am. astr. Soc., 6, 486.

Davis,M.M., 1977, In IAU Symp. 74, 'Radio Astronomy and Cosmology', ed. Jauncey,D.L., D.Reidel, Dordrecht,Holland.

de Ruiter,H.R., 1978, Ph.D. thesis, University of Leiden.

Doroshkevich,A.G., Longair,M.S. and Zeldovich,Ya.B., 1970, Mon. Not. R. astr. Soc., 147, 139.

Fanaroff,B.L. and Longair,M.S., 1972, Mon. Not. R. astr. Soc., 159, 119.

Fanaroff,B.L. and Longair,M.S., 1973, Mon. Not. R. astr. Soc., 161, 393.

Fanti,R., Formiggini,M., Lari,C., Padrielli,L., Katgert-Merkelijn,J.K. and Katgert,P., 1973, Astr. Astrophys., 23, 161.

Fanti,C., Fanti,R., Ficarra,A., Formiggini,L., Giovannini,G., Lari,C. and Padrielli,L., 1975, Astr. Astrophys., 42, 365.

Fanti,C., Fanti,R., Lari,C., Padrielli,L., van der Laan,H. and de Ruiter,H., 1977, Astr. Astrophys., 61, 487.

Fanti,R. and Perola,G.C., 1977, In IAU Symp. 74, 'Radio Astronomy and Cosmology', ed. Jauncey,D.L., D.Reidel, Dordrecht, Holland.

Field,G.B., Arp.H. and Bahcall,J.N., 1973, 'The Redshift Controversy', W.A.Benjamin Inc.

Fomalont,E.B., 1969, Astrophys.J., 157, 1027.

Fomalont,E.B., Bridle,A.H. and Davis,M.M., 1974, Astr. Astrophys., 36, 273.

Gavazzi,G. and Perola,G.C., 1978, Astr. Astrophys., 66, 407.

Gillespie,A.R., 1975, Mon. Not. R. astr. Soc., 170, 541.

Grueff,G. and Vigotti,M., 1977, Astr. Astrophys., 54, 475.

Hazard,C., Mackay,M.B. and Shimmins,A.J., 1963, Nature,197,1037.

Hoyle,F. and Burbidge,G.R., 1966, Nature, 210, 1346.

Hoyle,F., 1968, Proc. Roy. Soc. London, A 308, 1.

Jackson,J.C., 1973, Mon. Not. R. astr. Soc., 162, 11p.

Jauncey,D.L., 1975, Ann. Rev. Astr. Astrophys., 13, 23.

Kapahi,V.K., 1975a, Ph.D. Thesis, University of Bombay.

Kapahi,V.K., 1975b, Mon. Not. R. astr. Soc., 172, 513.

Kapahi,V.K., 1977, In IAU Symp. 74, 'Radio Astronomy and Cosmology', ed. Jauncey,D.L., D.Reidel, Dordrecht,Holland.

Katgert,P., 1975, Astr. Astrophys., 38, 87.

Katgert,P., 1976, Astr. Astrophys., 49, 221.

Katgert,P., 1977, Ph.D. Thesis, University of Leiden.

Katgert,P., Padrielli,L., Katgert,J.K. and Willis,A.G., 1977, IAU Symp. 74, 'Radio Astronomy and Cosmology', ed. Jauncey,D.L., D.Reidel, Dordrecht, Holland.

Kellermann,K.I., Pauliny-Toth, I.I.K. and Davis,M.M., 1968, Astrophys. Lett., 2, 105.

Kellermann,K.I., Pauliny-Toth,I.I.K. and Williams,P.J.S., 1969, Astrophys. J., 157, 1.

Kellermann,K.I., 1972, Astron. J., 77, 531.

Kembhavi,A.K. and Kulkarni,V.K., 1977, Mon. Not. R. astr. Soc., 181, 19p.

Kulkarni,V.K., 1978, Mon. Not. R. astr. Soc., 185, 123.

Legg,T.H., 1970, Nature, 226, 65.

Longair,M.S., 1966, Mon. Not. R. astr. Soc., 133, 421.

Longair,M.S. and Scheuer,P.A.G., 1967, Nature, 215, 919.

Longair,M.S. and Macdonald,G.H., 1969, Mon. Not. R. astr. Soc., 145, 309.

Longair,M.S. and Pooley,G.G., 1969, Mon. Not. R. astr. Soc., 145, 121.

Longair,M.S. and Scheuer,P.A.G., 1970, Mon. Not. R. astr. Soc., 151, 45.

Longair,M.S., 1971, Rep. Prog. Phys., 34, 1125.

Longair,M.S. and Rees,M.J., 1972, Comm. Astrophys. Sp.Phys., 4, 79.

Longair,M.S., 1974, In IAU Symp. 63, 'Confrontration of cosmological theories with observational data', ed. Longair,M.S. D.Reidel, Dordrecht, Holland.

Lynden-Bell,D., 1971, Mon. Not. R. astr. Soc., 155, 95.

Lynds,R. and Petrosian,V., 1972, Astrophys. J., 175, 591.

Machalski,J.,1978a, Acta Astronomica, 28, 367.

Machalski,J.,1978b, Astr. Astrophys., 65, 157.

Mackay,C.D., 1971, Mon. Not. R. astr. Soc., 154, 209.

Mackay,C.D., 1973, Mon. Not. R. astr. Soc., 162, 1.

Macleod,J.M. and Doherty,L.H., 1972, Nature, 238, 88.

Maslowski,J., 1972, Acta Astronomica, 22, 227.

Maslowski,J., 1977, In IAU Symp. 74, 'Radio Astronomy and Cosmology', ed. Jauncey, D.L., D.Reidel, Dordrecht, Holland.

Masson,C.R. and Wall,J.V., 1977, Mon. Not. R. astr. Soc., 180, 193.

McCrea,W.H., 1972, In IAU Symp. 44, 'External galaxies and quasi stellar objects', D.Reidel, Dordrecht, Holland.

Miley,G.K., 1971, Mon. Not. R. astr. Soc., 152, 477.

Murdoch,H.S., 1976, Mon. Not. R. astr. Soc., 177, 441.

Narlikar,J.V. and Chitre,S.M., 1977, Mon. Not. R. astr. Soc., 180, 525.

Oosterbaan,C.E., 1978, Astr. Astrophys., 69, 235.

Pauliny-Toth,I.I.K., Kellermann,K.I., Davis,M.M., Fomalont,E.B. and Shaffer,D.B., 1972, Astr. J., 77, 265.

Pauliny-Toth,I.I.K. and Kellermann,K.I., 1972a, Astr. J., 77, 560.

Pauliny-Toth,I.I.K. and Kellermann,K.I., 1972b, Astr. J., 77, 797.

Pauliny-Toth,I.I.K. and Kellermann,K.I., 1974, In IAU Symp.63, 'Confrontation of cosmological theories with observational data', e.d. Longair, M.S., D.Reidel,Dordrecht, Holland.

Pauliny-Toth,I.I.K., 1977, In IAU Symp. 74, 'Radio Astronomy and Cosmology', ed. Jauncey,D.L., D.Reidel, Dordrecht, Holland.

Pauliny-Toth,I.I.K., Witzel,A., Preuss,E., Kühr,H., Kellermann, K.I., Fomalont,E.B. and Davis,M.M., 1978a, Astr. J., 83, 451.

Pauliny-Toth,I.I.K., Witzel,A., Preuss,E., Baldwin,J.E. and Hills,R.E., 1978b, Astr.Astrophys. Suppl. 34, 253.

Pearson,T.J. and Kus,A.J., 1978, Mon. Not. R. astr. Soc.,182, 273.

Penzias,A.A. and Wilson,R.W., 1965, Astrophys.J., 142, 419.

Petrosian,V., 1969, Astrophys. J., 155, 1029.

Petrosian,V. and Dickey,J., 1973, Astrophys.J., 186, 403.

Phillips,D.L., 1962, J. Assoc. Comp. Mach., 9, 84.

Pooley,G.G. and Ryle,M., 1968, Mon. Not. R. astr. Soc., 139, 515.

Rees,M.J. and Schmidt,M., 1971, Mon. Not. R. astr. Soc.,154,1.

Rees,M.J., 1972, In IAU Symposium No.44, 'External galaxies and quasi-stellar objects', ed. Evans,D.S., p407, D.Reidel, Dordrecht, Holland.

Reinhardt,M., 1972, Astrophys.Lett., 12, 135.

Richter,G.M., 1973, Astrophys.Lett., 13, 63.

Ringenberg,R. and McVittie, G.C., 1970, Mon. Not. R. astr. Soc., 149, 341.

Robertson,J.G., 1973, Aust.J. Phys., 26, 403.

Robertson,J.G., 1977a, Aust.J. Phys., 30, 209.

Robertson,J.G., 1977b, Aust.J. Phys., 30, 231.

Robertson,J.G., 1977c, Aust.J. Phys., 30, 241.

Robertson,J.G., 1978, Mon. Not. R. astr. Soc., 182, 617.

Rowan-Robinson,M., 1968a, Mon. Not. R. astr. Soc., 138, 445.

Rowan-Robinson,M., 1968b, Mon. Not. R. astr. Soc., 141, 445.

Rowan-Robinson,M., 1971, Nature, 229, 388.

Rowan-Robinson,M., 1972, Nature, 236, 112.

Rowan-Robinson,M., 1976, Nature, 262, 97.

Sandage,A.R., 1965, Astrophys. J., 141, 1560.

Sandage,A.R., 1968, Astrophys. J., 152, L149.

Scheuer,P.A.G., 1975, In 'Galaxies and the Universe' eds. A.Sandage et al., University of Chicago Press.

Schmidt,M., 1963, Nature, 197, 1040.

Schmidt,M., 1968, Astrophys.J., 151, 393.

Schmidt,M., 1970, Astrophys. J., 162, 371.

Schmidt,M., 1972a, Astrophys. J., 176, 273.

Schmidt,M., 1972b, Astrophys. J., 176, 289.

Schmidt,M., 1972c, Astrophys. J., 176, 303.

Schmidt,M., 1975, In 'Galaxies and the Universe', eds. Sandage, A. et al., University of Chicago Press.

Schmidt,M., 1976, Astrophys. J. Lett., 209, L55.

Schmidt,M., 1977, In IAU Symp. 74, 'Radio Astronomy and Cosmology', ed. Jauncey,D.L., D.Reidel, Dordrecht,Holland.

Setti,G. and Woltjer,L., 1973, Ann. N. Y. Acad. Sci., 224, 8.

Shimmins,A.J., Bolton,J.G. and Wall,J.V., 1968,Nature,217,818.

Subrahmanya,C.R., 1977, Ph.D.thesis, University of Bombay.

Sutton,J.M., Davies,I.M., Little,A.G. and Murdoch,H.S.,1974, Aust. J. Phys. Astrophys. Suppl., No. 33, 1.

Swarup,G., 1975, Mon. Not. R. astr. Soc., 172, 501.

Swarup,G. and Subrahmanya,C.R., 1977, In IAU Symp. 74, 'Radio Astronomy and Cosmology', ed. Jauncey,D.L., D.Reidel, Dordrecht,Holland.

van der Laan,H., 1969, Bull. astr. Inst. Netherl., 20, 171.

Véron,M.P., Véron,P. and Witzel,A., 1972, Astr. Astrophys., 18, 82.

von Hoerner,S., 1973, Astrophys. J., 186, 741.

Wall,J.V., 1972, Aust. J. Phys. Astrophys. Suppl., 24, 49.

Wall,J.V. and Cooke,D.J., 1975, Mon. Not. R. astr. Soc., 171,9.

Wall,J.V., 1977, In IAU Symp. 74. 'Radio Astronomy and Cosmology', ed. Jauncey,D.L., D.Reidel, Dordrecht,Holland.

Wall,J.V., Pearson,T.J. and Longair,M.S., 1977, In IAU Symp.74, 'Radio Astronomy and Cosmology', ed. Jauncey,D.L., p269, D.Reidel, Dordrecht, Holland.

Wall,J.V., 1978, Mon. Not. R. astr. Soc., 182, 381.

Wardle,J.F.C. and Miley,G.K., 1974, Astron. Astrophys., 30,305.

Webster,A., 1976, Mon. Not. R. astr. Soc., 175, 71.

Webster,A., 1977, In IAU Symp. 74, 'Radio Astronomy and Cosmology', ed. Jauncey,D.L., D.Reidel, Dordrecht,Holland.

Weedman,D.W., 1976, Astrophys. J., 208, 30.

Willis,A.G., Oosterbaan,C.E. and de Ruiter,H.R., 1976, Astr. Astrophys. Suppl. 25, 453.

Willis,A.G., Oosterbaan,C.E., Le Poole,R.S., de Ruiter,H.R., Strom,R.G., Valentijn,E.A., Katgert,P. and Katgert-Merkelijn,J.K., 1977, In IAU Symp. 74, 'Radio Astronomy and Cosmology' ed. Jauncey,D.L., D.Reidel, Dordrecht,Holland.

Willis,A.G. and Miley,G.K., 1979, Astr. Astrophys.,

Wills,D. and Lynds,R., 1978, Astrophys. J. Suppl., 36, 317.

Willson,M.A.G., 1972a, Mon. Not. R. astr. Soc., 155, 385.

Willson,M.A.G., 1972b, Mon. Not. R. astr. Soc., 156, 7.